Radio Resource Management in Wireless Networks with Multicast Transmissions

RADIO RESOURCE MANAGEMENT IN WIRELESS NETWORKS WITH MULTICAST TRANSMISSIONS

BY

HADI MESHGI, M.Sc.

A THESIS

SUBMITTED TO THE DEPARTMENT OF ELECTRICAL & COMPUTER ENGINEERING

AND THE SCHOOL OF GRADUATE STUDIES

OF MCMASTER UNIVERSITY

IN PARTIAL FULFILMENT OF THE REQUIREMENTS

FOR THE DEGREE OF

DOCTOR OF PHILOSOPHY

Doctor of Philosophy (2015) McMaster University

(Electrical & Computer Engineering) Hamilton, Ontario, Canada

TITLE:	Radio Resource Management in Wireless Networks with Multicast Transmissions
AUTHOR:	Hadi Meshgi M.Sc., (Electrical Engineering) Iran University of Science and Technology, Tehran, Iran
SUPERVISOR:	Dr. Dongmei Zhao
CO-SUPERVISOR:	Dr. Rong Zheng
NUMBER OF PAGES:	xvi, 159

To my beloved parents for their unlimited love and support

Abstract

With the increasing demand for wireless communications, radio resource management (RRM) plays an important role in future wireless networks in order to provide higher data rates and better quality of services, given the limited amount of available radio resources. Although some specific features of wireless communication networks cause challenges to effective and efficient RRM, they bring opportunities that help improving network performance and resource utilization. In this thesis, we focus on RRM issues related to the broadcast/multicast nature in wireless communication networks. The work is divided into two parts.

In the first part, we exploit how to take advantage of the broadcast nature of wireless transmissions in RRM by opportunistically applying two-way relaying (or network coding) and traditional one-way relaying. Different objectives are considered, including maximizing total packet transmission throughput (Chapter 2), minimizing costs related to transmission power and delay (Chapter 3), and minimizing packet transmission delay subject to maximum and average transmission power limits (Chapter 4). While designing these scheduling schemes, the random traffic and channel conditions are also taken into consideration. Our results show that the proposed opportunistic scheduling schemes can indeed take good advantage of the broadcast feature at the relay nodes and achieve much higher throughput and, in some scenarios, provide

close-to-optimum QoS performance.

The second part (Chapter 5) of the thesis deals with the issue of efficient resource management in multicast communications, where we study channel sharing and power allocations for multicast device-to-divice (D2D) communication groups underlaying a cellular network. In such a scenario, D2D multicasting together with the mutual interference between cellular and D2D communications, makes the interference conditions and power allocations a very complicated issue. Different approaches are proposed that allow each D2D group to share the cellular channels and allocate transmission power to each D2D and cellular transmitter, so that the sum throughput of D2D and cellular users is maximized. Our results indicate that it is possible to achieve close-to-optimum throughput performance in such a network.

Acknowledgements

This thesis marks the end of a journey! I would like to express my gratitude to all who have supported me throughout this journey, and have taken parts in all unforgettable memories during the course of my studies at McMaster university.

First, I would like to express my deepest gratitude to my supervisor, Prof. Dongmei Zhao, for her thoughtful advice, insightful criticism, and wise guidance through the duration of my studies. She provided me with motivation and inspiration and I do appreciate her for her consistent help and support. I would also like to thank Prof. Rong Zheng as my co-supervisor. Her insight and critical thinking had a huge influence on my chain of thoughts and have greatly motivated me to serve as a better scholar.

I extend my warm thanks to the members of my Ph.D. supervisory committee Prof. Terence D. Todd and Prof. Ted Szymanski for providing suggestions, comments and questions that greatly helped in improving the quality of the work. I would like to thank Prof. Ben Liang for serving as the external committee member and for his valuable suggestions and comments. I am also thankful to the administrative and technical staff of the ECE department at McMaster university for much efficient assistance throughout these years.

Finally, my foremost gratitude and recognition goes to my family for their unwavering love and support. My deepest appreciation goes to my parents for their unconditional and insatiable dedication and love and for teaching me the significant values of life. Thanks to my one and only sister, Mojdeh, for being unconditionally understanding and encouraging. My Fiance, Sahar, deserves a great deal of thanks for her everlasting support which has made this work possible. I was continually amazed by her willingness to proof read countless pages of bore-some mathematics.

Abbreviations

AADTR	average absolute deviation of transmission rate
AWGN	additive white Gaussian noise
BER	bit error rate
BIA	backward induction algorithm
BS	base station
CDMA	code division multiple access
CMDP	constrained Markov decision process
CSI	channel state information
CU	cellular user
D2D	device-to-device
EDF	earliest deadline first
FSMC	finite-state Markov channel
GBD	generalized bender decomposition
HOL	head-of-line
HSDPA	high-speed downlink packet access
IPTV	internet protocol television
LTE-A	long term evolution advanced

MAC	media access control
MDP	Markov decision process
MINLP	mixed integer nonlinear programming
NC	network coding
OFDMA	orthogonal frequency-division multiple access
ONC	opportunistic network coding
PIA	policy iteration algorithm
QoS	quality of service
RRM	radio resource management
SDP	simulation based dynamic programming
SINR	signal-to-interference-plus-noise-ratio
UL	uplink
VIA	value iteration algorithm
WFQ	weighted fair queueing
WiMAX	worldwide interoperability for microwave access
XOR	exclusive or

Contents

List of Figures

Chapter 1

Introduction

For most wireless communication networks, effectiveness and efficiency are two basic requirements for data transmissions. Effectiveness is to reliably deliver messages to their destinations with required quality of service (QoS), and efficiency is to minimize the total costs or amount of required resources, e.g., bandwidth and transmission power. Next generation wireless networks are expected to provide significantly higher data rates, reliability, and energy efficiency than the current systems. In recent years, significant effort has been put into developing new techniques that improve the performance of wireless networks to meet these requirements.

Depending on the applications of wireless networks, different types of QoS objectives need to be satisfied. Real-time applications, such as streaming audio or video, typically, have a strict rate requirement [1]. Moreover, they also have an upper bound on the packet loss rate for satisfactory user experience. On the other hand, data applications, such as file downloading, are not time critical and do not have strict rate requirements. However, they require very low packet loss rates. Other QoS requirements may also be considered such as minimum and average rate guarantees,

maximum and average packet transmission delay, maximum jitter between packets, etc.

In order to enhance performance for wireless networks and satisfy QoS requirements for wireless users, it is of great importance to design effective and efficient radio resource management (RRM) frameworks based on specific network applications.

1.1 Radio Resource Management in Wireless Networks

The notion of radio resource management is concerned with the distribution of different types of radio resources in wireless networks among mobile users or transmission links. Given the scarcity of radio resources, RRM frameworks are designed to efficiently utilize the radio resources while satisfying the QoS requirements of the users. Some special features of wireless networks, such as the time-varying channel conditions, user mobility, and broadcast nature of wireless transmissions can make the resource management problem a challenging task, especially for emerging high data rates wireless applications. Traditionally, these features are considered to be negative towards effective QoS provisioning and efficient resource utilization. However, some of these features have been exploited for improving the network performance.

First of all, the time variation of the wireless channel due to fading can cause higher data loss rate and low bandwidth efficiency in static resource allocations. In order to overcome this effect, the amount of resources allocated to each user should be strongly dependent on the users channel conditions. For example, users in deeper fading require higher transmission power to satisfy their QoS requirements. On the

other hand, the random fading also provides opportunities for improving resource allocation efficiency. If users can delay their transmissions and wait until their channel conditions become good, the network resources can be efficiently utilized, and the system capacity can be improved. This leads to opportunistic scheduling in wireless networks [2].

Second, due to the broadcast nature of the wireless channel, transmission by any user can cause interference to all the other users nearby, if they happen to operate at the same frequency channel at the same time. Such co-channel interference reduces the QoS perceived by the users. On the other hand, since one transmission can simultaneously reach multiple receivers, the broadcast feature can be used to improve the network performance. Using network coding in wireless networks is one good example of taking advantage of the broadcast feature of wireless transmissions, and can offer benefits in terms of energy efficiency, transmission delay, spectral efficiency and interference management [3].

Overall, the special characteristics of wireless networks make RRM a very challenging task, and at the same time provide opportunities for improving the network performance. Radio resources are managed using various resource allocation and control schemes. In the following, we briefly describe power allocation and scheduling schemes that are the main topics in this thesis and review related works.

1.1.1 Power allocation and interference management

Transmission power control is important for interference management, energy saving, and connectivity control in wireless communication networks. Higher transmission power typically translates into higher signal-to-noise ratio (SNR) at the receiver,

which reduces the bit error rate (BER) of a communication link if there is no interference. Higher SNR also allows a system that uses link adaptation to transmit at a higher data rate, resulting in greater spectral efficiency. On the other hand, when co-channel interference exists, increasing transmission power increases co-channel interference and results in reduced signal-to-interference-plus-noise ratio (SINR), which increases the BER of data transmissions. Power control in such a scenario is interference control and helps ensure efficient spatial reuse and desirable user experience. Power control and interference management techniques for conventional cellular communication systems have been a focus of intensive studies (see [4–6] and references therein).

In addition, increasing transmission power increases the overall energy consumption, which is a very important issue in mobile devices with the limited battery life. Wireless communication networks are often deployed in places where wired power supplies are not available, and both the infrastructure and the end equipment have to be powered by batteries or solar/wind-powered storage [7]. In such cases, efficient power allocation or power control is important to extend the battery lifetime and minimize the overall energy consumption of a network. There have been various techniques in physical and media access control (MAC) layers for energy efficient resource allocation [8, 9]. A comprehensive survey of energy efficiency in code-division multiple access (CDMA) networks is presented in [10], and in [11, 12] the design of energy-efficient orthogonal frequency-division multiple access (OFDMA) systems is considered.

Often times the term of *power control* is used interchangeably in the literature with *power distribution* and *power allocation*. The main purpose of power control is

to find out the relationship between the target transmission or receive power levels as a function of channel allocations, propagation conditions, traffic loads, and other network conditions. Power allocation schemes often involve an optimization formulation with two types of terms in the objective function: QoS-based utility and network resource cost [6]. A cost function for resource usage can be relatively simple, for example it can be a linear function of transmit power. A utility function is generally a function of QoS metrics such as throughput or delay. These metrics are in turn functions of transmit power and other optimization variables, such as time schedules and bandwidth allocation in a power control problem.

1.1.2 Scheduling

Wireless technology advancements make scheduling a popular topic nowadays. The work of scheduling is to decide which nodes in a network should transmit at what time and be allocated to how much network resources. The overall objective is to meet the wide-ranging QoS requirements of different applications, while efficiently utilizing the available network resources. Three well-known classic scheduling policies are: 1) round-robin, that serves users in a circular manner without any other consideration, 2) earliest deadline first (EDF), that schedules the packet that will be expired the soonest, and 3) weighted fair queueing (WFQ), that allocates the resources considering the weights associated with every user [13].

Most of the traditional implementations of schedulers do not utilize the advanced features of the physical layer, and users are often scheduled regardless of their channel conditions [14]. It has been well established now that network performance can be substantially improved by designing channel aware scheduling algorithms [15]. This

leads to the concept of cross-layer design, the idea of allowing layers to cooperate more closely and exchange information. This form of cooperation can be achieved through cross-layer optimization (see [16] for an overview).

In recent years, different scheduling methods have been proposed that opportunistically take advantage of physical layer information. With this type of opportunistic scheduling in delay-tolerant applications like data downloading, packets can be buffered for favorable transmission opportunities, such as good channel conditions or low interference level. The notion of opportunistic scheduling was first introduced in [17], which shows that using the multiuser diversity in scheduling process can significantly improve the capacity. Opportunistic scheduling can also take into account QoS metrics like throughput and delay that allow the scheduler to find the proper transmission resources for each user. In a pure opportunistic approach, the scheduler always chooses the user in the best channel condition to use the channel. This approach is referred to as MaxRate scheduling.

Opportunistic scheduling algorithms can be more effective than non-opportunistic ones for wireless networks [14]. Initial proposals employing heuristic opportunistic algorithms to design a scheduler show a considerable improvement in comparison to non-opportunistic ones [18], [19]. In [18] authors present a joint scheduling and resource allocation framework for WiMAX that operates based on a heuristic credit-based scheduler. Later, mathematical models for wireless channels were used to study different aspects of the system such as delay and throughput, and were incorporated in the design of optimal schedulers. Some of these works assume full channel state information (CSI) availability (i.e., base stations have instantaneous knowledge of all users CSI) [20–23]. Other works consider that base stations do not have access to

CSI, but can periodically acquire CSI from mobile users [24, 25].

In the literature, opportunistic scheduling is used to improve QoS of the networks. The proposed opportunistic scheduling in [26] is designed in a way that QoS flows receive a fixed average throughput per slot. The authors argue that providing an average throughput to QoS flows in every slot decreases the probability of starvation in the long run. The works in [25] and [27] are dedicated to delay improvement. The work in [27] focuses on the performance and robustness of packet schedulers in which a Markov chain is used to obtain the queue state transition probabilities and minimize the average queue length of users. In [28], a throughput-optimal scheduler is proposed which guarantees the worst-case delay without any prior knowledge of channel conditions. The opportunistic scheduling algorithm proposed in [29] targets OFDMA wireless networks in which the system throughput is maximized, and the required average transmission rate and the average absolute deviation of transmission rate (AADTR) are satisfied. AADTR is a metric to control the transmission rate fluctuations to avoid larger queues and longer delays. In [30], throughput, delay and packet loss are the QoS objectives of the scheduler. Based on these three aspects of QoS, the authors establish a three-dimensional space with specific basis vectors for QoS and find the efficient point of the system performance in that space.

Scheduling decisions in wireless networks are not only affected by random channel conditions but also random traffic changes. Because of all the randomness, exact scheduling policies cannot be determined using static optimization techniques. Since the packet scheduling problem is inherently dynamic, stochastic dynamic programming algorithms [31] are employed to determine the optimal scheduling schemes. One

such example is the optimal scheduling scheme designed in [23] for high-speed downlink packet access (HSDPA) networks.

1.2 Multicast Transmission

Multicast transmission is becoming increasingly important in today's wireless networks. When the same information content should be transmitted from one transmitter to multiple receivers, instead of sending data via multiple unicasts, multicasting may maximize spectral efficiency and minimize transmission power consumption.

Many services require transmission to selected groups of users through multicasting [32–34]. One of the main multicast services is audio /video streaming, which covers a large range of applications such as IPTV, mobile TV, video or audio conference call, and web radio. The resource management of multicast audio/video is challenging since these services characterized by strict QoS constraints. Another important multicast application is file downloading. Multicast file downloading is used for off-line applications such as software update transmission, image and text transmission, and multimedia content delivery. In terms of QoS requirement, these multicast services do not pose strict constraints in delay and guaranteed bit rate, but they have strict requirements in packet loss ratio. Recently, the transmission of geographic information updates such as traffic reports, local news, weather forecast, stock prices, and location-based advertisements is growing in the mobile market. In these applications, data must be delivered to users in a given area. The QoS requirements of these services are similar to the multicast file downloading.

1.3 Contributions and Overview of the Thesis

In this thesis, we design different RRM techniques to leverage the broadcast feature of wireless transmissions in order to control the amount of the assigned resources to each user. In chapters 2–4, we study how the broadcast nature of the wireless channel can be used to improve the network performance using network coding and opportunistic scheduling schemes. In chapter 5, we study resource allocations for multicast communication groups that experience relatively complicated co-channel interference. In the following, we outline the main contributions of the thesis.

In Chapter 2, we design an opportunistic scheduling scheme for a bidirectional communication link with relaying using network coding. We consider the scheduling of both the relay node and the end nodes, and the objective is to maximize the transmission throughput over a long term. An optimization problem is formulated and solved to find the optimum scheduling by considering the link conditions, maximum buffer sizes at the relay node, and maximum transmission power of each node. A heuristic scheduling scheme is then proposed to opportunistically take advantages of the channel conditions between the two end nodes. The proposed heuristic algorithm has less complexity compared to the optimal solution and achieves close-to-optimal throughput.

In Chapter 3, we consider a network with multiple bidirectional links that share a common relay node, and study the delay and power performance of opportunistic network coding. We formulate a stochastic dynamic program with the objective of minimizing the long-run cost, defined as a function of both the transmission power and data transmission delay. An unconstrained Markov decision process (MDP) model is developed and solved for the average and discounted cost problems. The optimal

solution requires high computational and modeling complexity when the state space is large. For this reason, we develop heuristic solutions with lower complexity. For the discounted cost problem, a simulation-based dynamic programming (SDP) algorithm is proposed that not only simplifies the modeling process and reduces the computational complexity, but also achieves close-to-optimum cost. for the average cost problem, a heuristic scheduling scheme is proposed, which makes transmission decisions based on estimated costs in the current and next time slots. The heuristic scheme achieves close-to-optimum cost performance while greatly reducing the computational complexity.

In Chapter 4, the system studied in Chapter 3is extended so that nodes are allowed to overhear transmissions of each other. A constrained Markov decision process (CMDP) is first formulated with an objective to minimize the average delay of packet transmissions, subject to the maximum and average transmission power limits of the relay node. For a special case, when there is no overhearing of transmissions between different end nodes, we formulate another CMDP with less complexity. Two heuristic schemes are then proposed, the first one applies to the general case, and the second applies to only the no-overhearing case. Numerical results demonstrate that the heuristic schemes can achieve close-to-optimul average packet transmission delay. Furthermore, the second scheme achieves lower maximum delay while keeping the same average packet transmission delay and relay node power consumption as the first scheme.

In Chapter 5, we study resource management for multicast device-to-device (D2D) communications underlaying a cellular network. Because of the broadcast feature of wireless transmissions, D2D communications and existing cellular users may cause

strong interference to each other if not designed properly. We design a resource allocation scheme to maximize the overall network throughput while guaranteeing the QoS requirements for both D2D users and regular cellular users (CUs). The problem of power and channel allocation is formulated as a mixed integer nonlinear programming (MINLP) problem, where one D2D group can reuse the channels of multiple CUs and the channel of each CU can be reused by multiple D2D groups. Distinct from existing approaches in the literature, our formulation and solution methods provide an effective and flexible means to utilize radio resources in cellular networks and share them with multicast groups without causing harmful interference to each other. A variant of the generalized bender decomposition (GBD) is applied to optimally solve the MINLP problem. A greedy algorithm and a low-complexity heuristic solution are also devised.

Chapter 2

Resource Management in a Bidirectional Communication Link

Starting from this chapter, we study radio resource management and traffic scheduling in bidirectional relaying links using network coding. The basic idea is to explore the benefits brought by the multicast feature of using NC at the relay node. The issue is first studied for a three-node bidirectional link in Chapter 2, and extended to multiple bidirectional links sharing the same frequency channel in Chapters 3 and 4, where different objectives are focused on resource allocations. This chapter starts with a brief literature survey on NC and related work on RRM, followed by our proposed opportunistic scheduling scheme that maximizes the throughput of a bidirectional communication link.

The remainder of the chapter is organized as follows. In Section 2.1 after introducing the basic concept of network coding, related works in opportunistic network coding are presented. In Section 2.2, we describe the bidirectional communication channel with relaying and formulate an optimization problem for scheduling transmissions of

the nodes. A heuristic scheme is proposed in Section 2.3 that opportunistically takes advantages of the channel condition variations and different relaying options at the relay node. Numerical results are shown in Section 2.4 to demonstrate the performance of the proposed scheduling scheme. Finally, we summarize our main results and give concluding remarks in Section 2.5.

2.1 Background and Related Works

2.1.1 Network coding

Network coding [35] was first proposed for wired networks by allowing intermediate nodes in a network to perform both data processing and forwarding. Each message sent on a node's output link can be a function or mixture of the messages that arrived earlier on the node's input links. Using network coding can reduce the number of transmissions and improve the network resource utilization.

Performing two-way relaying is a simple use of network coding in wireless networks. When two nodes should communicate with each other and there is no direct link between them, a relay node can be used to forward the data between them. When each of the nodes is equipped with a single transceiver, traditional one-way relaying for the bidirectional communication takes four time slots in order to transmit one packet in each direction. Alternatively, the relay node can combine the data from the two end nodes and broadcast to both using network coding, and this is referred to as two-way relaying.

Based on whether the incoming traffic is decoded at the relay nodes, wireless network coding can be implemented in two ways: physical and digital network coding.

When using physical network coding, it takes two time slots for the two end nodes to exchange one packet in each direction – one time slot is required for the two end nodes to transmit simultaneously to the relay node, and another time slot is for the relay node to multicast an amplified version of the mixed signal to the two end nodes (using the amplify-and-forward technique) [36]. In digital network coding, the two end nodes transmit to the relay node at different time slots so that the relay node can decode the received data packets before combining them and broadcasting to the end nodes, i.e., using decode-and-forward technique.

Different works have been done to exploit potential benefits for using NC, which include increasing the overall network throughput [37–43], saving transmission power [44], improving network reliability, achieving better fairness, and enhancing routing efficiency [45–47]. On the other hand, the throughput improvement of using NC may depend on various network and traffic conditions, such as overflowed or possibly emptying queues, scheduled or random access MAC layer, multicast or broadcast communications [42], and latency requirements of the traffic [48].

Among different works on transmission scheduling using network coding, two network coding approaches can be distinguished in the literature, namely full [49, 50] and opportunistic [51, 52] network coding. In the full NC approach, all packets from different end nodes are combined into one packet using NC and then the relay node transmits the packet to all receivers. In [53], full NC has been proved to achieve optimal throughput in broadcast scenarios. However, this optimality is achieved at the cost of large delays in packet decoding, since the receivers need to collect a large number of coded packets before being able to decode all of them simultaneously. This may be proper for delay tolerant applications but is not suitable for applications that

do not tolerate such packet delays, such as real-time applications. Moreover, full NC is not efficient in multicast scenarios in terms of throughput since it must deliver all the packets to all receivers, including the non-requested ones, which usually requires more transmissions than delivering the requested packets only.

On the other hand, in the opportunistic network coding (ONC) approach whether a packet is transmitted with or without network coding is determined by the buffer's queue state at a given node and channel conditions. This network coding approach is much more suitable for ensuring the quality of real-time applications since packets do not have to wait to be network-coded. In the following, we review the related work in ONC.

2.1.2 Opportunistic network coding

Using NC in wireless networks complicates efficient resource allocations and effective quality of service (QoS) provisioning. First, when a node transmits a network coded packet, it must transmit at the rate or power supported by the receiver with the worst link conditions; otherwise, some of the receivers will not be able to correctly receive the packet. As a result, the transmission efficiency of using NC may be significantly reduced, especially when the link conditions of the multiple receiving nodes to the relay node are significantly different. This leads to opportunistic scheduling, such as in [54], where the scheduling takes advantage of the random fading channels to maximize the end-to-end transport-layer rates. The opportunistic scheduling in [52] tries to find an optimum number of users for the NC operation that results in a maximum throughput at each instant. In [55] a heuristic scheme is designed to select which node should transmit network coded packets, and show that the opportunistic

scheduling can maximize the average capacity by choosing the appropriate set of network-coded nodes according to the instantaneous link conditions. In [56] and [57] the performance of opportunistic wireless network coding in [52] is evaluated assuming that the relay node always has an infinite amount of data to transmit to both end nodes. In [56] users have the same average SNRs while in [57] users are at different distances from relay station and hence have different average SNRs.

Second, packets that arrive at the relay node earlier should wait for other packets in order to be network coded, and therefore may experience longer delay and higher loss probability. A cross-layer design is proposed in [58], referred to as buffer-aware NC, where a certain probability is allowed to transmit uncoded packets in order to reduce the delay introduced by NC in bidirectional relaying topology and X-topology networks. The work in [59] considers a butterfly network that supports real-time traffic, where a queueing model is developed by assuming a fixed transmission power and path loss channel gains, and the results show that significant gain can be achieved by using NC under the conditions of additive white Gaussian noise (AWGN) and identical link capacities. Although an optimum trade-off should exist between transmission power and packet transmission delay in a network using NC, this issue has not been thoroughly studied, possibly due to the fact that such trade-off is dependent on various network conditions such as network topology and routing protocols, and can be very complicated. Some works consider transmission power allocations, e.g., [60, 61], and other works study packet transmission delay, e.g., [62, 63], but little work considers both transmission power and delay when NC is used.

2.1.3 Bidirectional relaying link

Because of the complexity to study resource management in a network using NC, a lot of works has been focusing on networks with special topologies, such as the X-topology, e.g., [58], bufferfly topology, e.g., [59, 64], and bidirectional topology, e.g., [58, 65]. The work in [65] first demonstrates the application of NC in bidirectional relaying, where the relay node combines packets from the two end nodes using binary XOR operation and broadcasts the XORed packet to the end nodes. Each of the end nodes then decodes the packet from the other end by simply XORing the received packet from the relay node with its own packet.

The two-way relaying channel has attracted much research attention because of its simplicity while still keeping the major benefits of NC such as throughput improvement. In particular, a bidirectional relaying network with two end nodes and one relay node is studied in [56, 64, 66–68], where the main objective is to maximize the instantaneous throughput [56], maximize the long-term average throughput [68], or minimize the total time span for sending a certain amount of data [67]. In these works, the relay node is assumed to always have an infinite amount of data [56]. In [56, 64, 67], the relay node always uses NC; and in [66, 68], the relay node can choose either to transmit to a single end node using traditional relaying mode or to both end nodes simultaneously using NC. Link conditions are important for efficient data transmission scheduling as in [66**?**]. The works in [69, 70] consider more complicated two-way relaying links. In [69], a network with a set of nodes that communicate through a relay node is studied, where NC is used at the relay node, and transmission power and rate are jointly controlled based on current channel conditions. The work in [70] considers how to select the best relay node based on link gain information to

improve data transmission efficiency. The works in [71, 72] study traffic scheduling in two-way relaying links using analog or physical NC, where [71] focuses more on the gain of using multiple antennas while [72] focuses more on signal constellation. Although either transmission power or data transmission delay is considered in some of the existing works, only [58] studies the trade-off between transmission power and data transmission delay for a butterfly network. Overall, jointly considering transmission power and data transmission delay with NC still requires more in-depth research work.

In the remaining part of this chapter, we will study transmission scheduling for a bidirectional communication link with relaying by taking advantage of the link conditions and opportunistically using one-way or two-way relaying. We consider the scheduling of both the relay node and the end nodes, and the objective is to maximize the transmission throughput over a long term.

2.2 System Description and Problem Formulation

We consider two nodes S and D communicating with each other via a relay node R, as shown in Fig. 2.1. Each node is equipped with one transceiver, and all transmissions share a common frequency channel. At most one node is allowed to transmit at a given time. When node S transmits a packet, node R receives it, decodes and stores it in buffer 1 of size $B_{\max,1}$. Similarly, when node D transmits a packet, node R receives it, decodes it and stores in buffer 2 of size $B_{\max,2}$. There are different transmission options for node R: it can transmit the data in buffer 2 to node S, or the data in buffer 1 to node D. In addition, node R can combine an equal amount of data from both buffers, do bit-wise XOR, and multicast to both nodes S and D. Channel time

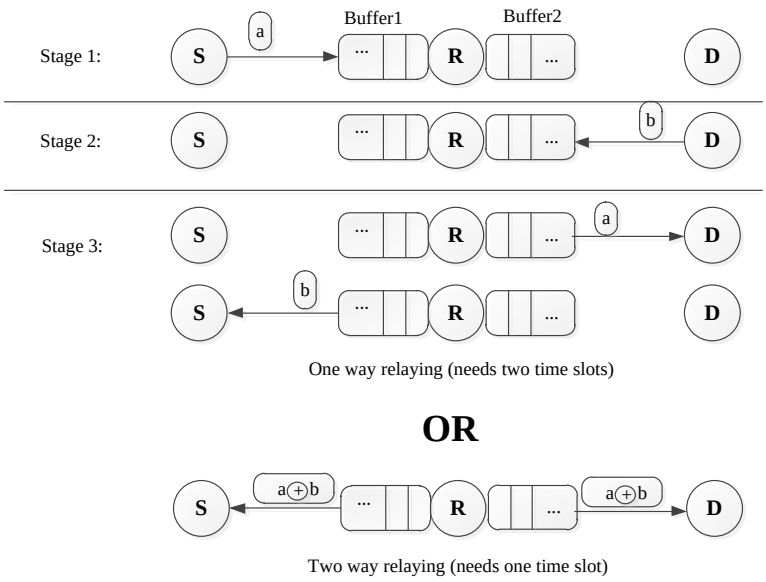

Figure 2.1: Network coding and traditional schemes

is divided into equal length time slots, and each transmission takes one time slot, whose duration is normalized to 1.

Note that the transmission rate of each node depends on several aspects. First, each node has a maximum transmission power limit, $P_{\max}$, which limits the achievable transmission rate of the node. Second, the buffer occupancy and available buffer space also limit the transmission rates. For nodes S and D, their transmissions are limited by the available (or empty) spaces in buffers 1 and 2, respectively, in order to prevent buffer overflow. For node R, the transmission rate is limited by the amount of available data in the buffers. Our objective is to find the best transmission scheduling by taking advantage of both the high efficiency of network coding and channel condition variations, so that to optimize the overall transmission throughput.

Define binary variables $X_{sr,t}$, $X_{dr,t}$, $X_{rs,t}$, and $X_{rd,t}$ at time slot t, where the subscripts s, r and d represent nodes S, R, and D, respectively. Each of these variables is equal to 1 only when the node represented by the first subscript transmits

to the node represented by the second subscript at time slot t. For example, $X_{sr,t} = 1$ if node S transmits to node R at time slot t, and $X_{sr,t} = 0$ otherwise. In addition, we define $X_{r2,t}$, which is equal to 1 if node R transmits to both nodes S and D at time slot t, and equal to 0 otherwise. At any given time, at most one of the five binary variables should be one. That is,

$$X_{sr,t} + X_{dr,t} + X_{rs,t} + X_{rd,t} + X_{r2,t} \leq 1. \tag{2.1}$$

The transmission rates depend on the transmission power and link conditions. Define $P_{sr,t}$, $P_{dr,t}$, $P_{rs,t}$, and $P_{rd,t}$ as the transmission power from the node represented by the first subscript to the node represented by the second subscript of each variable at time slot t, and $P_{r2,t}$ as the transmission power when node R transmits to both nodes S and D at time slot t. We further define the transmission rates corresponding the the above transmission power as $C_{sr,t}$, $C_{dr,t}$, $C_{rs,t}$, $C_{rd,t}$, and $C_{r2,t}$, respectively. Let g_{sr} and g_{dr} be the link gains between nodes S and R and that between nodes D and R, respectively, where we assume that the link gains are reciprocal (i.e., $g_{sr} = g_{rs}$ and $g_{dr} = g_{rd}$). Then

$$C_{sr,t} \leq X_{sr,t} \log_2 \left(1 + \tfrac{P_{sr,t} g_{sr}}{P_{n,r}}\right), \tag{2.2}$$

$$C_{dr,t} \leq X_{dr,t} \log_2 \left(1 + \tfrac{P_{dr,t} g_{dr}}{P_{n,r}}\right), \tag{2.3}$$

$$C_{rs,t} \leq X_{rs,t} \log_2 \left(1 + \tfrac{P_{rs,t} g_{rs}}{P_{n,s}}\right), \tag{2.4}$$

$$C_{rd,t} \leq X_{rd,t} \log_2 \left(1 + \tfrac{P_{rd,t} g_{rd}}{P_{n,d}}\right), \tag{2.5}$$

$$C_{r2,t} \leq X_{r2,t} \log_2 \left(1 + \min\left\{\tfrac{P_{r2,t} g_{rs}}{P_{n,s}}, \tfrac{P_{r2,t} g_{rd}}{P_{n,d}}\right\}\right), \tag{2.6}$$

where $P_{n,\cdot}$ is the power of the background additive white Gaussian noise at the receiver

of the node specified by the second subscript.

Note that the transmission rate of node R is limited by the amount of data that node R has received from the other two nodes. At time slot τ, the cumulative amount of data that node S has transmitted to node R since time slot 1 is no less than the cumulative amount of data that node R has transmitted to node D. That is,

$$\sum_{t=1}^{\tau} C_{sr,t} \geq \sum_{t=1}^{\tau} (C_{rd,t} + C_{r2,t}), \tag{2.7}$$

for all $\tau > 0$, where the left-hand side of (2.7) is the total amount of data transmitted from node S to node R, and the right-hand side is the total amount of data transmitted from node R to node D through both one-way and two-way relaying. A similar condition should be satisfied for the opposite direction. That is,

$$\sum_{t=1}^{\tau} C_{dr,t} \geq \sum_{t=1}^{\tau} (C_{rs,t} + C_{r2,t}), \tag{2.8}$$

for all $\tau > 0$.

Furthermore, we notice that the difference between the left-hand side and the right-hand side of (2.7) is the amount of data in buffer 1 at time τ. Therefore,

$$\sum_{t=1}^{\tau} C_{sr,t} - \sum_{t=1}^{\tau} (C_{rd,t} + C_{r2,t}) \leq B_{\max,1}, \tag{2.9}$$

for all $\tau > 0$. Note that (2.9) also limits the transmission rate of node S. Similarly, the transmission rate of node D is also limited by the available buffer space in buffer 2. That is,

$$\sum_{t=1}^{\tau} C_{dr,t} - \sum_{t=1}^{\tau} (C_{ra,t} + C_{r2,t}) \leq B_{\max,2}, \tag{2.10}$$

for all $\tau > 0$. Note that $B_{\max,1}$ and $B_{\max,2}$ are normalized buffer sizes, each of which is equal to the respective actual buffer size in bits divided by the product of the transmission bandwidth and time slot duration.

Define the average throughput of the considered link over a duration of T time slots as $(C_{sd,T} + C_{ds,T})/T$, where $C_{sd,T}$ is the cumulative transmission rate from node S to node D up to time T, and given by

$$C_{sd,T} = \sum_{t=1}^{T} (C_{rd,t} + C_{r2,t}), \tag{2.11}$$

and $C_{ds,T}$ is the cumulative transmission rate from node D to node S up to time T, and given by

$$C_{ds,T} = \sum_{t=1}^{T} (C_{rs,t} + C_{r2,t}). \tag{2.12}$$

Define $\mathbf{P} = [P_{\cdot,t}]$, $\mathbf{C} = [C_{\cdot,t}]$, and $\mathbf{X} = [X_{\cdot,t}]$. An optimization problem can be formulated to maximize the average throughput, subject to the above constraints. That is,

$$\max_{\mathbf{P},\mathbf{C},\mathbf{X}} \frac{C_{sd,T} + C_{ds,T}}{T} \tag{2.13}$$

$$\text{s.t.}\; C_{sr,t} \le X_{sr,t} \log_2 \left(1 + \frac{P_{sr,t} g_{sr}}{P_{n,r}}\right), \tag{2.14}$$

$$C_{dr,t} \le X_{dr,t} \log_2 \left(1 + \frac{P_{dr,t} g_{dr}}{P_{n,r}}\right), \tag{2.15}$$

$$C_{rs,t} \le X_{rs,t} \log_2 \left(1 + \frac{P_{rs,t} g_{rs}}{P_{n,s}}\right), \tag{2.16}$$

$$C_{rd,t} \le X_{rd,t} \log_2 \left(1 + \frac{P_{rd,t} g_{rd}}{P_{n,d}}\right), \tag{2.17}$$

$$C_{r2,t} \leq X_{r2,t} \log_2 \left(1 + \min \left\{ \frac{P_{r2,t} g_{rs}}{P_{n,s}}, \frac{P_{r2,t} g_{rd}}{P_{n,d}} \right\} \right), \tag{2.18}$$

$$0 \leq \sum_{t=1}^{\tau} C_{sr,t} - \sum_{t=1}^{\tau} (C_{rd,t} + C_{r2,t}) \leq B_{\max,1},\ \tau > 0, \tag{2.19}$$

$$0 \leq \sum_{t=1}^{\tau} C_{dr,t} - \sum_{t=1}^{\tau} (C_{rs,t} + C_{r2,t}) \leq B_{\max,2},\ \tau > 0, \tag{2.20}$$

$$C_{sd,T} = \sum_{t=1}^{T} (C_{rd,t} + C_{r2,t}), \tag{2.21}$$

$$C_{ds,T} = \sum_{t=1}^{T} (C_{rs,t} + C_{r2,t}), \tag{2.22}$$

$$P_{sr,t}, P_{dr,t}, P_{rs,t}, P_{rd,t}, P_{r2,t} \leq P_{\max}, \tag{2.23}$$

$$X_{sr,t}, X_{dr,t}, X_{rs,t}, X_{rd,t}, X_{r2,t} \in \{0, 1\}, \tag{2.24}$$

$$X_{sr,t} + X_{dr,t} + X_{rs,t} + X_{rd,t} + X_{r2,t} \leq 1. \tag{2.25}$$

Although this is a non-linear optimization problem, each transmission rate is a non-decreasing function of the corresponding transmission power (even with limited buffer space), and therefore the transmission rate for each node is maximized if the transmission power of the node is maximized. Therefore, when solving the problem, we first assume that all the powers are equal to $P_{\max}$. In this way, the problem is reduced to a linear integer programming problem and can be solved using commercial software easily. Although the transmission power only limits the upper bound on achievable rate for each transmission, the actual transmission rates of the nodes are also limited by the buffer occupancy or free buffer space.

2.3 Heuristic Scheduling Schemes

Solving the optimization problem requires high complexity, even when the channel conditions are static and all the link gains are known. Therefore, we seek a heuristic scheduling scheme in this section so that it can be implemented with lower complexity.

2.3.1 General heuristic algorithm

The heuristic scheduling scheme is performed at the beginning of each time slot and based on the channel and buffer information at the current time slot. Therefore, below we drop the subscript t when there is no confusion. We assume that link gain information, i.e., values of g_{sr} and g_{dr}, are available at the relay node, which can make the scheduling decision based on the link gains and the current buffer occupancy. We assume that the changes of link gains between two successive time slots can be neglected. The scheduling decision for the next time slot is made and informed to the end nodes at the end of the current time slot.

Let b_1 and b_2 (which have the same units as $B_{\max,1}$ and $B_{\max,2}$) be the current buffer occupancy at buffers 1 and 2, respectively. Consider node S first. If the node is scheduled to transmit, its transmission rate is determined by the transmission power, channel condition to node R, and the available space in buffer 1. That is

$$C_{sr} = \min \left\{ \log_2 \left(1 + \frac{P_{\max} g_{sr}}{P_{n,r}} \right), B_{\max,1} - b_1 \right\}. \tag{2.26}$$

When the available space in buffer 1 is sufficiently large, C_{sr} is limited by the transmission power of node S, and therefore, $P_{sr} = P_{\max}$. Otherwise, less transmission

power is required from node S. The actual transmission power can be calculated as

$$P_{sr} = \min\left\{P_{\max}, \frac{(2^{B_{\max,1}-b_1}-1)P_{n,r}}{g_{sr}}\right\}. \tag{2.27}$$

Similarly, if node D is scheduled to transmit, its transmission rate is given by

$$C_{dr} = \min\left\{\log_2\left(1+\frac{P_{\max}g_{dr}}{P_{n,r}}\right), B_{\max,2}-b_2\right\}, \tag{2.28}$$

and the actual transmission power of node D is given by

$$P_d = \min\left\{P_{\max}, \frac{(2^{B_{\max,2}-b_2}-1)P_{n,r}}{g_{dr}}\right\}. \tag{2.29}$$

When node R is scheduled to transmit to node S only, its transmission rate is given by

$$C_{rs} = \min\left\{\log_2\left(1+\frac{P_{\max}g_{rs}}{P_{n,s}}\right), b_2\right\}, \tag{2.30}$$

and the actual transmission power is given by

$$P_{rs} = \min\left\{P_{\max}, \frac{(2^{b_2}-1)P_{n,s}}{g_{rs}}\right\}. \tag{2.31}$$

When node R is scheduled to transmit to node D only, its transmission rate is given by

$$C_{rd} = \min\left\{\log_2\left(1+\frac{P_{\max}g_{rd}}{P_{n,d}}\right), b_1\right\}, \tag{2.32}$$

and the transmission power of node R is given by

$$P_{rd} = \min\left\{P_{\max}, \frac{(2^{b_1}-1)P_{n,d}}{g_{rd}}\right\}. \tag{2.33}$$

When node R is scheduled to transmit to both nodes S and D, its transmission rate is given by

$$C_{r2} = \min\left\{\log_2\left(1+\min\left\{\frac{P_{\max}g_{rs}}{P_{n,s}}, \frac{P_{\max}g_{rd}}{P_{n,d}}\right\}\right), \min\{b_1, b_2\}\right\}, \tag{2.34}$$

and the transmission power of node R is given by

$$P_{r2} = \min\left\{P_{\max}, (2^{\min\{b_1,b_2\}}-1)\max\left\{\frac{P_{n,s}}{g_{rs}}, \frac{P_{n,d}}{g_{rd}}\right\}\right\}. \tag{2.35}$$

A heuristic scheme can be designed as in Algorithm 1. A higher priority is given to node R when $2C_{r2}$ is larger than both C_{rs} and C_{rd}. That is, the two-way relay can provide higher throughput than the one-way relay. This is shown in Lines 2-5. When $2C_{r2}$ is between C_{rs} and C_{rd}, the two-way relay cannot provide the highest throughput among all the relay options, then one-way relay is used so that node R transmits to node D if C_{rd} is the largest among the three rates (Lines 7-11) and to node S if C_{rs} is the largest (Lines 12-15). When $2C_{r2}$ is smaller than both C_{rs} and C_{rd}, either node S and node D transmits, depending on the relative values of C_{sr} and C_{dr}. Note that in this scheduling scheme, the relay node is given a higher priority to transmit than the the S and D nodes. An intuitive explanation to this is that transmissions from the relay node contribute directly to the objective throughput calculation.

Algorithm 1 Heuristic algorithm to maximize the sum throughput

for $t = 1 : T$ **do**
  if $2C_{r2} > \max\{C_{rs}, C_{rd}\}$ **then**
    Node R transmits to both nodes S and D.
    Update both buffers b_1 and b_2 as $b_1 = b_1 - C_{r2}$ and $b_2 = b_2 - C_{r2}$.
    Update $C_{sd} = C_{sd} + C_{r2}$ and $C_{ds} = C_{ds} + C_{r2}$.
  else
    if $C_{rs} < 2C_{r2} < C_{rd}$ **then**
      Node R transmits to node D only.
      Update buffer b_1 as $b_1 = b_1 - C_{rd}$.
      Update $C_{sd} = C_{sd} + C_{rd}$.
    else
      if $C_{rd} < 2C_{r2} < C_{rs}$ **then**
        Node R transmits to node S only.
        Update buffer b_2 as $b_2 = b_2 - C_{rs}$.
        Update $C_{ds} = C_{ds} + C_{rs}$.
      else
        if $C_{sr} > C_{dr}$ **then**
          Node S transmits.
          Update buffer b_1 as $b_1 = b_1 + C_{sr}$.
        else
          Node D transmits.
          Update buffer b_2 as $b_2 = b_2 - C_{dr}$.
        end if
      end if
    end if
  end if
  Find the average sum throughput $\frac{C_{sd}+C_{ds}}{T}$.
end for

2.4 Numerical Results

Consider a bidirectional communication link, where the distance between nodes S and D is d_{sd}, and node R is located somewhere along the line between S and D, i.e., $d_{sr} + d_{dr} = d_{sd}$, where d_{sr} and d_{dr} are the distances between nodes S and R and between nodes D and R, respectively. We consider the distance-based path loss and Rayleigh fading for the transmission channel. The path loss exponent is set to 4. The noise power is -126 dBm. We plot the average throughput versus different network parameters for both the optimal and heuristic scheduling solutions. For comparison, we also compare these solutions with two other solutions, one is for the relay node to always use one-way relay, and the other one is for the relay node to always use network coding to do two-way relay.

We first set the location of node R at exactly the middle point between nodes S and D. That is, $d_{sr} = d_{dr} = d_{sd}/2$. Fig. 2.2 shows the average throughput using different scheduling solutions. As we can see, the proposed heuristic scheme using Algorithm 1 has better performance than both the "one-way relay" and "two-way relay" scheduling. This indicates that the proposed opportunistic scheduling that combines both one-way relay and two-way relay can indeed make better use of the network resources and improve the throughput performance. The proposed heuristic scheduling achieves lower throughput performance than the optimal scheduling, since the former does not have future channel and buffer information, and makes the scheduling decisions on time slot basis. As shown in Algorithm 1 the heuristic scheme gives strictly higher priority to node R by always checking the rates of node R (one-way relay and two-way relay) first. When scheduling node R to transmit, the heuristic scheme is concerned about whether it should do one-way (and which way) or

two-way relay. The scheduling decisions made before line 16 are based on the relative values of the one-way and two-way relay rates. When there is only a small amount of data in the buffers, node R can only transmit at very low rate, both in one-way and two-way relay, but the node may still be scheduled to transmit. On the other hand, it may be more efficient for nodes S or D to transmit in such a case. This is the main reason causing the difference between the proposed heuristic scheduling and the optimum.

Fig. 2.3 illustrates the average sum throughput versus maximum transmission power, where we set different distance values between nodes S and D. It is seen from the figure that the throughput increases with the transmission power. However, when the transmission power is relatively large, the throughput does not increase as significantly as it does when the transmission power is low. This is because of the limited buffer space which limits the maximum rate for the nodes. The figure also shows that when the distance between nodes S and D is smaller, the throughput can be much higher due to better link transmission conditions.

In Fig. 2.4 we show the average sum throughput versus maximum buffer size. With a larger buffer size, higher throughput can be achieved. On the other hand, the throughput stops increasing as the buffer size is larger than a certain value. This is because when the buffer size is large enough, the transmission rate is limited by the maximum transmission power of the nodes. It is also interesting to see that, the difference between throughput at different maximum powers is larger when the buffer size is relatively large. This later observation can be explained by how the heuristic scheme works. When the buffer size is too small, the available buffer space limits the transmission of all the nodes and increasing the transmission power will not affect

the total throughput considerably.

Next we move the location of node R along the line connecting nodes S and D. Let $d_{sr} = r \times d_{sd}$, where $r \in (0, 1)$. We plot the average sum throughput versus different values of r in Fig. 2.5. From the figure, we can see that when node R is located in the middle of nodes D and S, i.e., $r = 0.5$, the average throughput is the maximum. This is because the link gains between node R and the two end nodes are most balanced, and the chance to use network coding (or two-way relay) is maximized. When r is increasing or decreasing from 0.5, the link gains between node R and the two end nodes become less balanced, and the chance to take advantage of the high efficiency of two-way relay becomes less. As r is much larger or smaller than 0.5, node R becomes closer to nodes S or D. In this case, the chance of using two-way relay is little because g_{sr} and g_{dr} can be significantly different in most cases, and having node R to transmit to the node that has better link gain is much more efficient than the two-way relay. For the "one-way relay" and "two-way relay" scheduling, the "two-way relay" scheme achieves higher throughput for a wider range of r than the "one-way relay" scheme, and during this range of r, the throughput performance of the "two-way relay" scheduling is closer to that of the proposed scheduling scheme. When r is very close to 0 or 1, the "one-way relay" scheme achieves better throughput, which is close to the throughput of the proposed heuristic scheduling. This is because the two-way relay has to support the weaker node and when there is a large difference between the channel conditions, the weaker one results in a very low transmission rate diminishing the advantage of two-way relay.

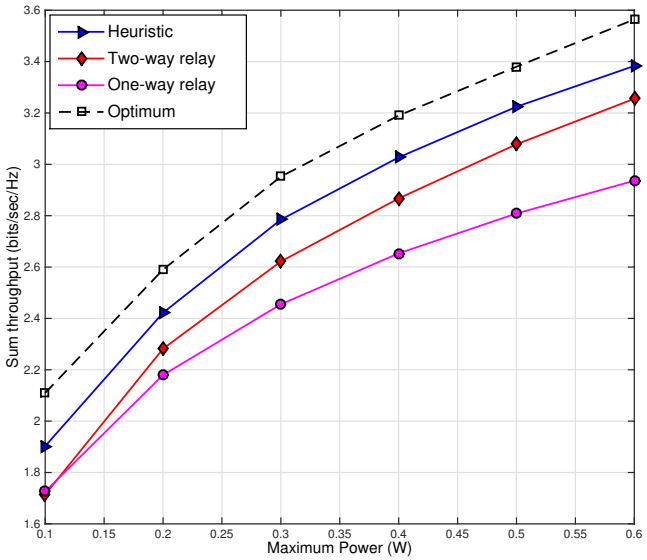

Figure 2.2: Comparison of different scheduling schemes ($d_{sr} = d_{dr} = 300$ m)

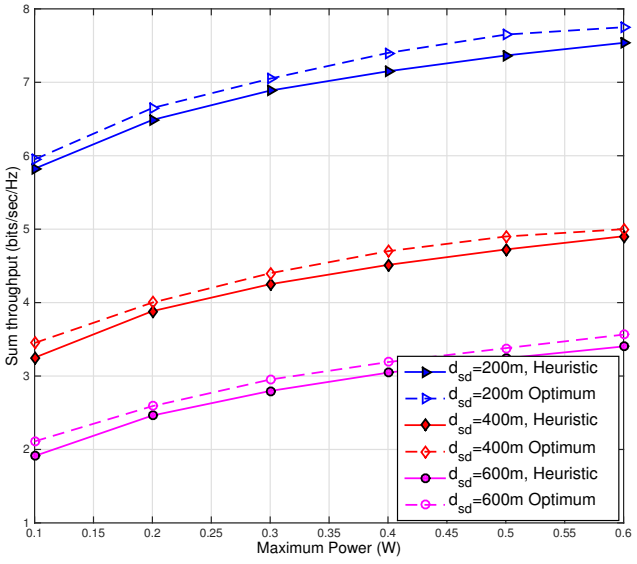

Figure 2.3: Sum throughput versus maximum transmission power

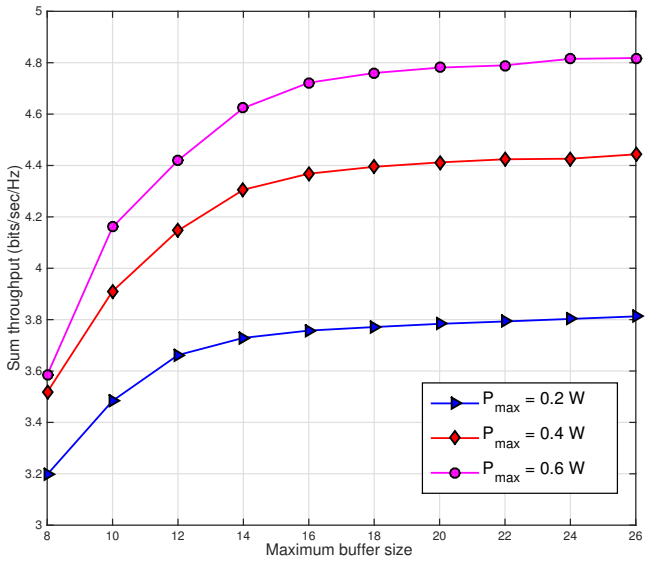

Figure 2.4: Sum throughput versus maximum buffer size ($d_{sr} = d_{dr} = 200$ m)

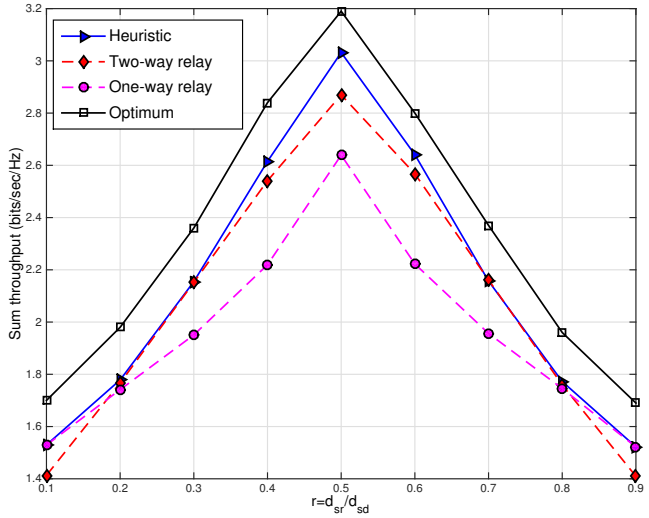

Figure 2.5: Sum throughput versus r ($d_{sd} = 600$ m, $P_{\max} = 0.4$ W)

2.5 Summary

In this chapter, we have designed an opportunistic scheduling scheme for a bidirectional communication link with relaying and investigated its performance. Our results indicate that the proposed scheduling scheme achieves higher throughput than both the scheduling using one-way relay and two-way relay only. The throughput performance of the proposed scheduling scheme is close to the optimal throughput. In the following two chapters, we will extend the work to a more complicated network, where a number of bidirectional relaying links share the same frequency channel and compete for the resources at a shared relay node.

Chapter 3

Cost-Minimization Resource Management for a Network with Bidirectional Relaying Links

In Chapter 2, we showed that significant throughput gain can be obtained by opportunistically using network coding at the relay node. In this chapter, we consider packet transmission scheduling in a network where multiple bidirectional relaying links share the resources at the relay node. The scheduling problem should resolve the resource competition among multiple links while taking into consideration the random traffic and channel conditions. We seek dynamic programming techniques to solve the scheduling problem. A Markov decision process (MDP) model is developed that incorporates both the buffer and channel states for multiple links. An optimal transmission policy is derived with an objective to minimize a certain cost, which is defined as a function of both the transmission power and data transmission delay. The optimal solution requires high computation complexity due to large state spaces

when the number of links or channel states is large. We then design heuristic scheduling schemes with lower complexity. Two types of cost functions are defined, one is discounted with time, and another is averaged over a certain period.

The remaining part of this chapter is organized as follows. In Section 3.1 we briefly introduce the Markov decision process and finite state Markov channel model. In Section 3.2 we describe the system model and formulate the basic scheduling problem. In Section 3.3 the MDP model is derived, and in Section 3.4 simulation-based dynamic programming is developed for the discounted cost problem. In Section 3.5 the MDP problem is formulated for the average cost problem and solved, and in Section 3.6 a heuristic scheduling scheme is proposed for the average cost problem. Numerical results are shown in Section 3.7, and conclusions are given in Section 3.8.

3.1 Preliminaries

In Subsection 3.1.1 we begin with a description of the MDP framework, including both the finite and infinite horizon settings and a summary of the associated optimality equations. We then present the well-known exact solution algorithms for solving MDP, value iteration and policy iteration. In Subsection 3.1.2, we describe the channel model that will be used in this chapter and Chapter 4.

3.1.1 Markov decision process (MDP)

A Markov decision process (MDP) is a discrete time stochastic control process that provides a mathematical framework for modeling decision-making in dynamic systems where outcomes of the actions decided by the decision-maker are random [31]. An

MDP can be employed if a process has the Markov property, i.e. the conditional probability distribution of future states of the process depends only on the present state and the action chosen. An MDP is generally defined by four-tuples:

1. State space $\mathcal{S}$: It represents all the possible situations the process can go through.

2. Action space $\mathcal{A}$: It represents the set of all possible actions in the different states of the process. In some processes, it is more comprehensive to define an action space $\mathcal{A}_s(s) \in \mathcal{A}$ for each state $s \in \mathcal{S}$.

3. State transition probability $P_s(s, s', a)$: Each of these probabilities represents the transition probability from state $s \in \mathcal{S}$ to state $s' \in \mathcal{S}$ when action $a \in \mathcal{A}_s(s)$ is taken.

4. State-action cost function $C(s, a)$: It represents the immediate cost endured by the process when taking action a in state s. We will assume that the cost is non-negative and bounded, i.e., $0 \leq C(s, a) \leq C_{\max}$ for all $s \in \mathcal{S}$, $a \in \mathcal{A}_s(s)$.

Let $\Pi_s = [\pi(s)]$ be the set of all Markovian policies where $\pi : \mathcal{S} \to \mathcal{A}$ is a function such that $\pi(s) \in \mathcal{A}_s(s)$ for all $s \in \mathcal{S}$. The goal is to find a policy π^* that minimizes:

- the overall expected cost over a finite horizon, when the process will stop after a finite number of steps, or

- the expected cost per unit time (or expected discounted cost) over an infinite horizon, when the process continues indefinitely.

In general, the action space, transition probabilities, and costs may be either stationary or time-varying, which leads to either stationary or non-stationary optimal policies. In this thesis, we will focus only on stationary MDPs where the state transitions and costs do not depend on time.

We define the expected total discounted cost (or cost-to-go) value for state $s \in \mathcal{S}$ by

$$V^{\pi}(s) = E\left[\sum_{t=0}^{H-1} \beta^t C(s_t, \pi(s_t))\right], \tag{3.1}$$

where $0 < \beta \leq 1$ is the discount factor. If H is finite we have a finite-horizon problem; otherwise we have an infinite horizon problem. The optimal value function is denoted by $V^* : \mathcal{S} \rightarrow \mathcal{R}^+$, where the optimal cost-to-go value for a given state $s \in \mathcal{S}$ is given by

$$V^*(s) = \min_{\pi \in \Pi} V^{\pi}(s), \tag{3.2}$$

and a corresponding policy yielding that optimal value function will be denoted by π^*, where

$$V^*(s) = V^{\pi *}(s), \tag{3.3}$$

for which the well-known Bellman optimality principle holds as follows. For all $s \in \mathcal{S}$,

$$V^*(s) = \min_{a \in A_s(s)} \left\{ c(s,a) + \beta \sum_{s' \in \mathcal{S}} P_s(s, s', a) V^*(s') \right\}, \tag{3.4}$$

where $V^*(s)$ is unique, and there exists an optimal policy $\pi^* \in \Pi$ satisfying

$$\pi^*(s) = \arg \min_{a \in A_s(s)} \left\{ C(s,a) + \beta \sum_{s' \in \mathcal{S}} P_s(s, s', a) V^*(s') \right\}, s \in \mathcal{S}. \tag{3.5}$$

The two most well-known algorithms to find the optimal policy of an MDP are the policy iteration algorithm (PIA) and the value iteration algorithm (VIA) (also known

as the backward induction algorithm (BIA)). Each step of PIA consists of two parts: policy evaluation and policy improvement. The policy evaluation step obtains V^{π} for a given $\pi \in \Pi_s$ by solving a set of $|S|$ linear equations with $|S|$ unknowns, where $|S|$ is the total number of states,

$$V^{\pi}(s) = C(s, \pi(s)) + \beta \sum_{s' \in \mathcal{S}} P_s(s, s', \pi(s)) V^{\pi}(s'). \tag{3.6}$$

The complexity of policy evaluation step is $O(|S|^3)$ [73]. In the next step, the algorithm updates the policies minimizing the new value function expressions using the following set of equations for all $s \in \mathcal{S}$,

$$\pi(s) = \arg \min_{a \in A_s(s)} \left\{ C(s, a) + \beta \sum_{s' \in \mathcal{S}} P_s(s, s', a) V^{\pi}(s') \right\}, s \in \mathcal{S}. \tag{3.7}$$

The complexity of the policy improvement step is $O(|S|^2|A|)$ [73]. These two steps are repeated until no further change in the policy is possible. The obtained value and policy vectors are thus optimal. Therefore, the overall complexity of one iteration in PIA is $O(|S|^3 + (|S|^2|A|))$.

In VIA, value functions are first initialized and then updated iteratively for all $s \in \mathcal{S}$ as follows:

$$V_i(s) = \min_{a \in A_s(s)} \left\{ C(s, a) + \beta \sum_{s' \in \mathcal{S}} P_s(s, s', a) V_{i-1}(s') \right\}, s \in \mathcal{S}. \tag{3.8}$$

The iterations of the algorithm continue until the difference between two consecutive value functions is smaller than a tolerance value. Consequently, the complexity of each iteration in the VIA is $O(|S|^2|A|)$ [73]. It has been shown that by running VIA

for a number of iterations, which is polynomial in $|S|$ and $|A|$, the convergence to the optimal policy is guaranteed [73].

3.1.2 Finite state Markov channel model

Next we describe the discrete wireless channel model. A slowly varying wireless fading channel can be modeled as an amplitude based Rayleigh fading finite state Markov channel (FSMC) [74], which is done by partitioning the received signal-to-noise ratio (SNR). The FSMC was proved to be a good model of the wireless medium and has been shown to be in good agreement with realistic cases [75]. The basic methodology in amplitude based modeling is to model the amplitude (or equivalently, SNR) process since the amplitude is what determines the packet error probabilities. The channel is generally considered constant during the packet transmission time T_p, and the FSMC state change occurs at a multiple of packet transmission time.

Assuming the transmission power and the distance from transmitter to receiver are both fixed, the FSMC model partitions the received SNR into a finite number of intervals and represents each interval as a state of the Markov process. Since the received SNR is proportional to the channel link gain, the FSMC model applies to the channel link gain too. Let $0 = g_0 < g_1 < g_2 < ... < g_K = \infty$ be link gain thresholds. The channel is in state k, $k = 0, 1, 2, \ldots, K-1$ if the link gain is in the interval $[g_k, g_{k+1})$. We allow transitions from a given state to its adjacent states only. In Fig. 3.1 one can observe a FSMC with K states. The steady state probability of being in state k is

$$\pi_k = \int_{g_k}^{g_{k+1}} f_G(x)dx = e^{-\frac{g_k}{G}} - e^{-\frac{g_{k+1}}{G}}, \tag{3.9}$$

where $f_G(x)$ is the probability density function of the channel link gains. For a Rayleigh fading channel, $f_G(x) = \frac{1}{\bar{G}} e^{-\frac{x}{\bar{G}}}$, where $\bar{G}$ is the average channel gain.

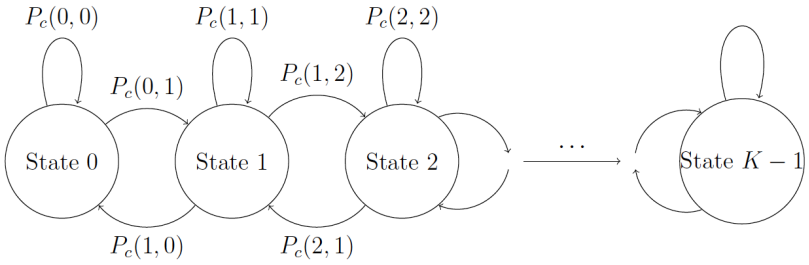

Figure 3.1: The finite state Markov channel model representation

According to [74] the equal-probability method is used so that $\pi_0 = \pi_1 = ... = \pi_{K-1} = \frac{1}{K}$, and link gain thresholds are determined by this requirement. Also, the transition probabilities can be approximated as [74]

$$P_c(k, k+1) \approx \frac{N(g_{k+1})T_p}{\pi_k}, \tag{3.10}$$

$$P_c(k, k-1) \approx \frac{N(g_k)T_p}{\pi_k}, \tag{3.11}$$

where T_p is the packet duration, $N(g_k)$ is the level crossing rate of level g_k,

$$N(g_k) = \sqrt{\frac{2\pi g_k}{\bar{G}}} f_D e^{-\frac{g}{\bar{G}}}, \tag{3.12}$$

and f_D is the maximum Doppler frequency.

With a given partition of the link gain values $g_0, ...g_K$ we can obtain the steady-state probabilities $\pi_0, ..., \pi_{K-1}$ and the transition probabilities P_c.

3.2 System Description

We consider a network with bidirectional communication links and a relay node. Each of the links has two end nodes, denoted as $A_{1,m}$ and $A_{2,m}$ for $m = 1, 2, \ldots, M$, where M is the total number of links. All the communications of a given link are through the relay node, which is shared by all the links. An end node sends data to the relay node, which then forwards the data to the other end node. The timeline of the relay node is divided into equal length time slots, each for one packet transmission. We consider that all packets are of the same size and transmitted at a fixed rate. Depending on the channel conditions, the nodes can adaptively adjust their transmission power so that the required SNR at the receiver can be satisfied in order to correctly decode the packet. We emphasize the transmissions at the relay node, and consider that a different channel is available for packet transmissions from the end nodes to the relay node.

We consider that the relay node is equipped with a single transmitter. There can be two ways for the data forwarding. When a data packet x is received from node $A_{1,m}$, the relay can forward the packet to node $A_{2,m}$ at a selected time slot using the traditional one-way relaying method. Alternatively, if it can combine another packet y received from node $A_{2,m}$, and multicast $z = x \oplus y$ to both nodes $A_{1,m}$ and $A_{2,m}$ using two-way relaying.

The link state between node $A_{h,m}$ $(h = 1, 2)$ and the relay node is denoted as $g_{h,m}$. We consider a FSMC model, which has K states, indexed as $k = 0, 1, 2, \ldots, K-1$. We assume that the channel state keeps constant during one time slot, but may change between different time slots. The transition probabilities from state k to its two neighboring channel states are denoted as $P_c(k, k-1)$ (for $0 < k \leq K-1$) and

$P_c(k, k+1)$ (for $0 \leq k < K-1$). These probabilities can be calculated based on practical fading models [74] as we described in the previous section.

Let γ_{th} be the minimum SNR in order for an end node to correctly receive a packet from the relay node, and $p(t)$ the transmission power of the relay node at time t, then $p(t)g_{h,m} \geq \gamma_{th}$ if the relay node should transmit to node $A_{h,m}$, or $g_{h,m} \geq \gamma_{th}/p_{\max} \triangleq g_{th}$, where $p_{\max}$ is the maximum allowed transmission power of the relay node, and g_{th} is the minimum link gain below which the relay node does not transmit to node $A_{h,m}$ because the required transmission power for the node to correctly receive a packet is larger than the maximum transmission power of the relay node.

We use $b_{h,m}$ $(h = 1, 2)$ to represent the number of packets buffered at the relay node from node $A_{h,m}$, and $0 \leq b_{h,m} \leq B_{\max}$, where $B_{\max}$ is the buffer size. The state of a buffer changes when there is a new packet arrival from the end node or after the relay node successfully transmits one packet from the buffer. We consider a Bernoulli process for the packet arrival process from each end node to the relay node. At each time slot, the probability of receiving one packet from node $A_{h,m}$ is $\theta_{h,m}$, and $\overline{\theta}_{h,m} = 1 - \theta_{h,m}$ is the probability of no packets received from node $A_{h,m}$.

3.3 The MDP Model

Given a network with bidirectional communication links and a relay node as described in the previous section, the objective is to schedule transmissions at the relay node so that a certain cost function is minimized. A Markov decision process (MDP) can be used to model the system. In this section we first define the state and action spaces and derive the state transition probability when a given action is taken. Next, we find the relationship between the objective cost function and the actions, and finally

solve the optimum policy in order to minimize the long-term discounted cost.

3.3.1 State and action spaces

Let $\mathcal{S}$ and $\mathcal{A}$, respectively, represent the state space and action space of the considered system. The system state is fully defined by a combination of the buffer state and the channel state. That is, $\mathcal{S} = \{b_{h,m}, g_{h,m}, h = 1, 2; m = 1, 2, \ldots, M\}$, and the total number of states is

$$|S| = (B_{\max} + 1)^{2M} K^{2M}. \tag{3.13}$$

The action space $\mathcal{A} = \{a, a = 0, 1, \ldots, 3M\}$ includes all transmission decisions at the relay node. For an action $a \in \mathcal{A}$, when $a = 0$, the action is no transmission, i.e., the relay node does not transmit; when $a = 3(m-1)+1 = 3m-2$ for a given m, the relay transmits to node $A_{1,m}$ only using traditional relay technique; when $a = 3(m-1)+2 = 3m-1$ for a given m, the relay transmits to node $A_{2,m}$ only using traditional relay technique; and when $a = 3m$ for a given m, the relay transmits to both nodes $A_{1,m}$ and $A_{2,m}$ using NC technique. We also define an action space $\mathcal{A}_s(s) \in \mathcal{A}$ for each state $s \in \mathcal{S}$ which shows feasible actions in each state based on the buffer and channel states. Action 0 is feasible in all the system states; the action of transmitting to one of the end nodes of a given link is feasible only if the corresponding data buffer is not empty and the link state is above the threshold; and the action of transmitting to both end nodes of a link is feasible only if both buffers for the link are nonempty and both the link states are above the threshold.

With the definition of $\mathcal{S}$ and $\mathcal{A}$, the system state is completely defined. That is, once an action is selected (i.e., a transmission decision is made), the system state in the next time slot is completely determined by that in the current time slot and

independent of the system states in the past. Therefore, the process is Markov.

3.3.2 State transition probability

Consider the state transition from s to $s^{'}$ when action a is taken. Since the packet arrival processes and the channel states of the two hops for the same link change independently, we can consider channel state and buffer state transitions of different links and hops separately. Therefore,

$$P_s(s, s^{'}, a) = \prod_{m=1}^{M} \prod_{h=1}^{2} P_l((b_{h,m}, g_{h,m}), (b^{'}_{h,m}, g^{'}_{h,m}), a), \tag{3.14}$$

where $P_l((b_{h,m}, g_{h,m}), (b^{'}_{h,m}, g^{'}_{h,m}), a)$ is the transition probability for the transmission hop (from the relay node to node $A_{h,m}$) to change from buffer-channel state $(b_{h,m}, g_{h,m})$ to buffer-channel state $(b^{'}_{h,m}, g^{'}_{h,m})$ when action a is taken. The remaining part of this subsection is to find this probability for different actions.

When the action is not to transmit, i.e., $a = 0$, we have

$$\begin{aligned} &P_l((b_{h,m}, g_{h,m}), (b^{'}_{h,m}, g^{'}_{h,m}), a = 0) \\ &\qquad = \begin{cases} \theta_{h,m} P_c(g_{h,m}, g^{'}_{h,m}), & b^{'}_{h,m} = b_{h,m} + 1 \leq B_{\max}, \\ P_c(g_{h,m}, g^{'}_{h,m}), & b^{'}_{h,m} = b_{h,m} = B_{\max}, \\ \overline{\theta}_{h,m} P_c(g_{h,m}, g^{'}_{h,m}), & b^{'}_{h,m} = b_{h,m} < B_{\max}, \\ 0, & \text{otherwise.} \end{cases} \end{aligned} \tag{3.15}$$

When the relay node transmits to node $A_{h,m}$ only, $a = 3(m-1) + h$, where $h = 1, 2$ and $m = 1, 2, \ldots, M$, the transition probability corresponding to the same hop is

given as

$$P_l((b_{h,m}, g_{h,m}), (b^{'}_{h,m}, g^{'}_{h,m}), a = 3(m-1)+h)$$
$$= \begin{cases} \theta_{h,m} P_c(g_{h,m}, g^{'}_{h,m}), & b^{'}_{h,m} = b_{h,m} < B_{\max}, \\ P_c(g_{h,m}, g^{'}_{h,m}), & b^{'}_{h,m} = b_{h,m} - 1, b_{h,m} = B_{\max}, \\ \overline{\theta}_{h,m} P_c(g_{h,m}, g^{'}_{h,m}), & b^{'}_{h,m} = b_{h,m} - 1, 0 < b_{h,m} < B_{\max}, \\ P_c(g_{h,m}, g^{'}_{h,m}), & b^{'}_{h,m} = b_{h,m} = 0, \\ 0, & \text{otherwise.} \end{cases} \tag{3.16}$$

With the transmission decision $a = 3(m-1)+h^{'}$, $h^{'} = 1, 2$, the transition probability corresponding to the other hop h ($h = 1, 2$ and $h \neq h^{'}$) of the same link is given as

$$P_l((b_{h,m}, g_{h,m}), (b^{'}_{h,m}, g^{'}_{h,m}), a = 3(m-1)+h^{'})$$
$$= \begin{cases} \theta_{h,m} P_c(g_{h,m}, g^{'}_{h,m}), & b^{'}_{h,m} = b_{h,m} + 1 \leq B_{\max}, \\ P_c(g_{h,m}, g^{'}_{h,m}), & b^{'}_{h,m} = b_{h,m} = B_{\max}, \\ \overline{\theta}_{h,m} P_c(g_{h,m}, g^{'}_{h,m}), & b^{'}_{h,m} = b_{h,m} < B_{\max}, \\ 0, & \text{otherwise.} \end{cases} \tag{3.17}$$

Furthermore, when $a = 3(m^{'} - 1) + h$, the transition probability corresponding to a

hop of a different link m ($m \neq m^{'}$) is given as

$$P_l((b_{h,m}, g_{h,m}), (b^{'}_{h,m}, g^{'}_{h,m}), a = 3(m^{'} - 1) + h)$$
$$= \begin{cases} \theta_{h,m} P_c(g_{h,m}, g^{'}_{h,m}), & b^{'}_{h,m} = b_{h,m} + 1 \leq B_{\max}, \\ P_c(g_{h,m}, g^{'}_{h,m}), & b^{'}_{h,m} = b_{h,m} = B_{\max}, \\ \overline{\theta}_{h,m} P_c(g_{h,m}, g^{'}_{h,m}), & b^{'}_{h,m} = b_{h,m} < B_{\max}, \\ 0 & \text{otherwise.} \end{cases} \tag{3.18}$$

When the action is to transmit simultaneously to both end nodes of link m, the transition probability for the hops of the same link is given by

$$P_l((b_{h,m}, g_{h,m}), (b^{'}_{h,m}, g^{'}_{h,m}), a = 3m)$$
$$= \begin{cases} \theta_{h,m} P_c(g_{h,m}, g^{'}_{h,m}), & b^{'}_{h,m} = b_{h,m} < B_{\max}, \\ P_c(g_{h,m}, g^{'}_{h,m}), & b^{'}_{h,m} = b_{h,m} - 1, b_{h,m} = B_{\max}, \\ \overline{\theta}_{h,m} P_c(g_{h,m}, g^{'}_{h,m}), & b^{'}_{h,m} = b_{h,m} - 1, 0 < b_{h,m} < B_{\max}, \\ P_c(g_{h,m}, g^{'}_{h,m}), & b^{'}_i = b_{h,m} = 0, \\ 0, & \text{otherwise.} \end{cases} \tag{3.19}$$

When the action is to transmit simultaneously to both end nodes of link $m^{'}$, the

transition probability for the hops of link m ($m \neq m^{'}$) is given by

$$P_l((b_{h,m}, g_{h,m}), (b^{'}_{h,m}, g^{'}_{h,m}), a = 3m^{'}) = \begin{cases} \theta_{h,m} P_c(g_{h,m}, g^{'}_{h,m}), & b^{'}_{h,m} = b_{h,m} + 1 \leq B_{\max}, \\ P_c(g_{h,m}, g^{'}_{h,m}), & b^{'}_{h,m} = b_{h,m} = B_{\max}, \\ \overline{\theta}_{h,m} P_c(g_{h,m}, g^{'}_{h,m}), & b^{'}_{h,m} = b_{h,m} < B_{\max}, \\ 0 & \text{otherwise.} \end{cases} \tag{3.20}$$

3.3.3 Unconstrained MDP for discounted cost

We consider the tradeoff between delay performance of the data transmissions and transmission power of the relay node. A cost function is defined as a combination of the transmission power from the relay node and the average number of buffered packets, and is given as

$$C(s, a) = f_c(p(s, a), Q(s, a)), \tag{3.21}$$

where $p(s, a)$ and $Q(s, a)$, respectively, are the transmission power of the relay node and the average number of buffered packets when taking action a at state s, and are defined as follows,

$$p(s, a) = \gamma_{th} \sum_{m=1}^{M} \left(\sum_{h=1}^{2} \frac{\mathbf{I}|_{a=a_{3(m-1)+h}}}{g_{h,m}} + \frac{\mathbf{I}|_{a=a_{3m}}}{\min\{g_{1,m}, g_{2,m}\}} \right), \tag{3.22}$$

and

$$Q(s,a) = \begin{cases} \frac{1}{2M}\sum_{h=1}^{2}\sum_{m=1}^{M} b_{h,m} - 1, & a = 3(m-1)+h, \\ \frac{1}{2M}\sum_{h=1}^{2}\sum_{m=1}^{M} b_{h,m} - 2, & a = 3m, \\ \frac{1}{2M}\sum_{h=1}^{2}\sum_{m=1}^{M} b_{h,m}, & \text{otherwise.} \end{cases} \tag{3.23}$$

Note that the average number of buffered packets directly corresponds to data packet transmission delay. The exact format of the function $f_c(\cdot)$ may depend on practical applications and system scenarios, but is not important to the formulation of the MDP problem.

Given the definition of the cost function in (3.21), our objective is to find the optimal stationary policy over all Markov deterministic stationary policies, so that the expected total discounted cost in (3.1) is minimized. It is proven that if the state space $\mathcal{S}$ is discrete and the action set associated with each state is finite, there exists an optimal deterministic stationary policy $\pi^* : \mathcal{S} \to \mathcal{A}$ that minimizes the discounted total expected cost per stage [31].

It is evident that the state space is finite and, therefore, the cost is bounded. Also, the system is stationary, that is, the system equation, the cost per stage and the transition probabilities do not change from one stage to the next stage. Such unconstrained MDP problem can be solved using different methodologies [31] as explained in subsection 3.1.1. In this section we use value iteration algorithm for finite horizon MDP as explained in Algorithm 1, where H is the number of horizons or stages.

Note that in this system that has limited buffer size, packet losses cannot be avoided. Let $L(s,a)$ be the probability of packet loss in state s after decision a, we

Algorithm 1 Value iteration algorithm

1: $V_0(s) = 0, \forall s \in \mathcal{S}$
2: $t = 0$
3: **while** $t < H$ **do**
4: $\quad V_{t+1}(s) = \min_{a \in A_s(s)} \left\{ c(s,a) + \beta \sum_{s' \in \mathcal{S}} P_s(s,s',a) V_t(s') \right\}, s \in \mathcal{S}$
5: $\quad t = t + 1$
6: **end while**
7: $\pi^*(s) = \arg\min_{a \in A_s(s)} \left\{ c(s,a) + \beta \sum_{s' \in \mathcal{S}} P_s(s,s',a) V_{t+1}(s') \right\}, s \in \mathcal{S}$

have

$$L(s,a) = \frac{1}{2M} \sum_{h=1}^{2} \sum_{m=1}^{M} \mathbf{I}|_{\{b_{h,m} = B_{\max}\}} \theta_{h,m}. \tag{3.24}$$

For relatively low packet arrival rate, the packet loss rate due to buffer overflow can be kept very low, and the delay performance based on the Little's Law gives very good approximation to the actual delay performance, and always provides a lower bound on the true average delay.

3.4 Approximate Dynamic Programming

Approximate dynamic programming (ADP) is a method for overcoming the classic curse of dimensionality [76] in dynamic programming that is well-known to plague the use of Bellmans equation. The computational and storage requirements of solving MDP are exponentially growing with the number of states and actions which makes it either computationally impractical or infeasible to implement the traditional techniques of policy iteration or value iteration methods. Therefore, our goal is to devise an algorithm that reduces the modeling complexity and computational complexity. In this section, we use the simulation-based dynamic programming to estimate the

optimal value function. The proposed algorithm is targeted at MDPs with large finite state spaces and relatively smaller action spaces for finite horizon model.

3.4.1 Simulation-based dynamic programming

We can describe an MDP using a simulation model the same as MDP using four-tuples $(\mathcal{S}, \mathcal{A}, f, C')$, where f is the next-state transition function such that the system dynamics are given by

$$s_{t+1} = f(s_t, a_t, w_t), \forall t = 0, 1, \ldots, H-1, \tag{3.25}$$

and $C'(s_t, a_t, w_t) \leq C_{\max}$ is the associated non-negative cost, where $s_t \in \mathcal{S}, a_t \in \mathcal{A}(s_t)$, and w_t is a random number generated using the channel and arrival rate distributions. The corresponding optimal cost-to-go value V_t^* at stage t is defined by,

$$V_t^*(s) = \min_{a \in A(s)} E\Big\{C'(s, a, w) + \beta V_{t-1}^*(f(s, a, w))\Big\}. \tag{3.26}$$

In the proposed simulation-based dynamic programming (SDP) the optimal cost-to-go function V_t^* is replaced by an approximation. In Algorithm 2, we estimate the optimal cost-to-go function defined by (3.26) for a given state s, based on N_t simulations in stage t. The approach is to minimize the discounted cost over actions, based on the recursive optimality equations given by (3.26) as depicted in Algorithm 2. At each stage t, the SDP algorithm iterates N_t times to compute the average discounted cost of each tuple (s, a). From those costs, the action that results in the minimum cost is the best action. In this algorithm, we use a random number w_j in each iteration j and the chosen action a will then be used to simulate $f(s, a, w_j)$ in order to produce

a simulated next state from s. After finding $\hat{V}_t(s,a)$ for all $a \in \mathcal{A}_s(s)$ in line 8, we update the estimate of the value function by taking the minimum of $\hat{V}_t(s,a)$ over all actions (line 12).

For the finite horizon problem, we iterate this procedure H times for all states and find the (approximate) optimal policy at the final stage. We can also use this algorithm in an on-line manner in the context of rolling horizon control [77] for solving infinite horizon problem.

Algorithm 2 SDP algorithm

1: $t = 0$
2: Set $V_0^*(s) = 0$ for all $s \in \mathcal{S}$.
3: **while** $t < H$ **do**
4: $t = t + 1$
5: **for** $s \in \mathcal{S}$ **do**
6: **for** $a \in \mathcal{A}_s(s)$ **do**
7: **for** $j = 1 : N_t(s)$ **do**
8: $\hat{V}_t(s,a) = \frac{1}{N_t(S)} \sum_{j=1}^{N_t(s)} (C'(s,a,w_j) + \beta V_{t-1}^*(f(s,a,w_j)))$
9: **end for**
10: **end for**
11: $V_t^*(s) = \min_{a \in \mathcal{A}_s(s)} \{\hat{V}_t(s,a)\}$
12: **end for**
13: **end while**

Complexity: The simulation-based algorithm, to some extent, decreases the modeling complexity in the MDP problem. Specifically, when the state space is large, it is difficult to construct the transition probability matrix. Using the SDP method, we do not need to have the transition probabilities. Second, the SDP algorithm reduces the computational complexity (the curse of dimensionality problem). It can be seen that the computational complexity for one iteration of this algorithm is $O(N_t|S||A|)$. Since N_t is normally much smaller than $|S|$, this complexity is significantly less than $O(|S|^2|A|)$ of VIA.

3.5 MDP for the Average Cost Problem

In this section, our objective is to find the optimal stationary policy over all Markov deterministic stationary policies so that the average cost per stage is minimized. It is proven [31] that if the state space $\mathcal{S}$ is discrete and the action set associated with each state is finite, there exists an optimal deterministic stationary policy $\pi^* : \mathcal{S} \rightarrow \mathcal{A}$ that minimizes the average cost per stage.

$$\lim_{T\to\infty} \sup \frac{1}{T} \sum_{t=1}^{T} E[C(s_t, \pi_t^*(s_t))], \tag{3.27}$$

where $\pi_t^*(s_t)$ is the optimal decision action taken in stage t when the system state is s_t.

This unconstrained MDP problem can be solved using equivalent LP methodology [31] as presented below. Let $x(s,a)$ represent the "steady-state" probability that the process is in state $s \in \mathcal{S}$ and action $a \in \mathcal{A}_s(s)$ is applied. The optimal solution can be obtained by solving the following linear program (LP):

$$\min \sum_{\forall s\in\mathcal{S}} \sum_{a\in\mathcal{A}_s(s)} x(s,a)C(s,a) \tag{3.28}$$

$$\text{s.t.} \sum_{a\in\mathcal{A}_s(s)} x(s',a) = \sum_{s\in\mathcal{S}} \sum_{a\in\mathcal{A}_s(s)} P_s(s,s',a)x(s,a), \forall s^{'} \in \mathcal{S}, \tag{3.29}$$

$$\sum_{s\in\mathcal{S}} \sum_{a\in\mathcal{A}_s(s)} x(s,a) = 1, \tag{3.30}$$

$$0 \leq x(s,a) \leq 1, \ \forall s \in \mathcal{S}, a \in \mathcal{A}_s(s). \tag{3.31}$$

Let x^* be the optimal solution to the LP problem. The primal policy, $\pi^*(s)$ can be

found by

$$\pi^*(s) = \frac{x^*(s,a)}{\sum_{a' \in \mathcal{A}_s(s)} x^*(s,a')}. \tag{3.32}$$

Since the problem is unconstrained, the optimal policy is deterministic rather than randomized. The corresponding average transmission power can be found as

$$P(\pi^*) = \sum_{s \in \mathcal{S}} \sum_{a \in \mathcal{A}_s(s)} x^*(s,a) p(s,a), \tag{3.33}$$

and the average buffer occupancy for link m is given by

$$D(\pi^*) = \frac{1}{2M} \sum_{s \in \mathcal{S}} \sum_{a \in \mathcal{A}_s(s)} x^*(s,a) Q(s,a). \tag{3.34}$$

The optimum overall cost of the system can be written as

$$C^* = f_c(P(\pi^*), D(\pi^*)). \tag{3.35}$$

3.6 Heuristic Scheme for Minimizing Average Cost

The computational load of optimal scheduling increases exponentially with the number of system states, and therefore, finding the optimum solution is not practical when the buffer size and the number of channel states are large. In this section, a heuristic scheme is proposed to minimize the average cost.

Algorithm 3 shows the scheme, which includes two parts. The first part (Lines 1–29) is to estimate potential costs for different actions, where $C_{t,h,m}$ represents the cost in the tth time slot for the hth hop of the link m. Q_t is the total number of packets in all the buffers in each time slot, $U_{h,m}$ is a binary variable which is equal

to 1 if $b_{h,m} > 0$ and $g_{h,m} \geq g_{th}$ (Line 6) and zero otherwise. The transmission power ($P^t_{h,m}$) of the relay node to reach node $A_{h,m}$ is calculated based on the current channel state (Line 9). Moreover, the transmission power in the next time slot in order for the relay node to reach the same end node is estimated based on the channel state transition probability (Line 10).

In Lines 12–27, the cost for transmitting the head-of-line (HOL) packet(s) is estimated for different cases. In the first case (Lines 12–18), $U_{1,m} = U_{2,m} = 1$, $C_{t,1,m}$ is the total estimated cost assuming the relay transmits to node $A_{1,m}$ in the current time slot; $C_{t,2,m}$ is the total estimated cost assuming the the relay transmits to node $A_{2,m}$ in the current time slot; and $C_{t,3,m}$ is the total estimated cost assuming the relay transmits to both nodes $A_{1,m}$ and $A_{2,m}$ in the current time slot. $C_{t+1,1,m}$, $C_{t+1,2,m}$, and $C_{t+1,3,m}$, respectively, are the total estimated cost assuming the relay transmits to node $A_{1,m}$ only, node $A_{2,m}$ only, and both nodes $A_{1,m}$ and $A_{2,m}$ in the next time slot but not in the current time slot. When $U_{1,m} = 1$ and $U_{2,m} = 0$ (Line 19), Lines 20 and 21 give the estimated costs for transmitting the head-of-line (HOL) packet to node $A_{1,m}$ in the current and the next time slots, respectively. When $U_{1,m} = 0$ and $U_{2,m} = 1$ (Line 22), Lines 23 and 24 give the estimated costs for transmitting the HOL packet to node $A_{2,m}$ in the current and the next time slots, respectively. The total buffer occupancy, Q_t, is decreased by 1 if the transmission of the current HOL is done in the current time slot and keeps unchanged if the transmission is delayed to the next time slot. After the costs are estimated, Line 29 is used to find which transmission arrangement has the minimum cost. It should be mentioned that if $U_{1,m} = U_{2,m} = 0$, the relay node does not transmit to any end nodes of link m in the current time slot (Line 26).

Algorithm 3 Heuristic algorithm for minimizing cost

$\mathbf{C} = \infty$
$Q_t = \sum_{h=1}^{2} \sum_{m=1}^{M} b_{h,m}$
$\mathbf{U} = 0$
for $m = 1 : M$ **do**
  for $h = 1 : 2$ **do**
    if $b_{h,m} > 0$ and $g_{h,m} > g_{th}$ **then**
      $U_{h,m} = 1$
    end if
    $P^t_{h,m} = f_p(g_{h,m})$
    $P^{t+1}_{h,m} = \sum_{g'_{h,m}=0}^{N-1} f_p(g'_{h,m}) P_c(g_{h,m}, g'_{h,m})$
  end for
  if $U_{1,m} = 1$ and $U_{2,m} = 1$ **then**
    $C_{t,1,m} = f_c(P^t_{1,m}, Q_t - 1)$;
    $C_{t,2,m} = f_c(P^t_{2,m}, Q_t - 1)$;
    $C_{t,3,m} = f_c(\max\{P^t_{1,m}, P^t_{2,m}\}, Q_t - 2)$;
    $C_{t+1,1,m} = f_c(P^{t+1}_{1,m}, Q_t)$;
    $C_{t+1,2,m} = f_c(P^{t+1}_{2,m}, Q_t)$;
    $C_{t+1,3,m} = f_c(\max\{P^{t+1}_{1,m}, P^{t+1}_{2,m}\}, Q_t)$;
  else if $U_{1,m} = 1$ and $U_{2,m} = 0$ **then**
    $C_{t,1,m} = f_c(P^t_{1,m}, Q_t - 1)$;
    $C_{t+1,1,m} = f_c(P^{t+1}_{1,m}, Q_t)$;
  else if $U_{1,m} = 0$ and $U_{2,m} = 1$ **then**
    $C_{t,2,m} = f_c(P^t_{2,m}, Q_t - 1)$;
    $C_{t+1,2,m} = f_c(P^{t+1}_{2,m}, Q_t)$;
  else
    Do not transmit at current time slot, $a = 0$.
  end if
end for
$[t^*, h^*, m^*] = \arg\min_{t'=t,t+1;h=1:3;m=1:M} C_{t',h,m}$
if $t^* = t$ **then**
  if $h^* = 1$ **then**
    Transmit to node $A_{1,m}$, $a = 3m - 2$.
  else if $h^* = 2$ **then**
    Transmit to node $A_{2,m}$, $a = 3m - 1$.
  else
    Transmit to both $A_{1,m}$ and $A_{2,m}$, $a = 3m$.
  end if
else
  Do not transmit at current time slot, $a = 0$.
end if

The second part (Lines 30–40) finalizes the decision for the current time slot based on the results in the first part. If $t^* = t$, the relay node transmits in the current time slot; if $h^* = 1$ or 2, the relay transmits to node A_{h^*,m^*}; and if $h^* = 3$ (only possible when $U_{1,m^*} = U_{2,m^*} = 1$), the relay transmits to both end nodes of link m^*. When $t^* = t + 1$, the relay node does not transmit in the current time slot. However, this does not necessarily mean that the relay should transmit in the next time slot. The actual decision for the next time is recalculated using the same process as above.

3.7 Numerical Results

In this section, we generate numerical results for both the discounted and average cost models. We consider the distance-based path loss and Rayleigh fading for the transmission channel. Based on this link gain distribution, the FSMC model partitions the entire range of link gain values into K intervals, each of which represents a state of the Markov process. The equal-probability method in [74] is used to find the link gain thresholds and state transition probabilities.

Default parameters are given below. The average packet arrival rate from each end node to the relay is $\theta_{h,m} = \theta = 0.1$ packets per time slot for all m and h, the maximum Doppler shift of each channel is $f_D = 100\,\text{Hz}$, the path loss exponent is 2.5, and the average distance between each end node and the relay node is $d = 200\,\text{m}$. For the cost function, we consider a linear function of the transmission power (P) and the number of buffered packets (Q), which represent the transmission delay, as $f_c(P, Q) = A \times P + B \times (Q/B_{\max})$, where A and B are parameters chosen based on the contribution of the transmission power and delay to the cost function. Similar cost functions are available in the literature, such as [78–81]. In all the results, the

packet loss rates are below 10^{-2}.

Table 3.1: Comparison between actions in the SDP algorithm for different values of N_t and optimal actions in the MDP

Index of state	**Index of action**			
	SDP, $N_t = 5$	**SDP,** $N_t = 10$	**SDP,** $N_t = 20$	**Optimal**
60	1	2	2	2
61	2	2	2	2
62	2	1	2	2
63	1	2	2	2
64	1	1	1	1
65	2	3	3	3
66	3	3	3	3
67	1	2	2	2
68	4	4	4	4
69	3	4	4	4
70	2	1	2	2
71	3	3	4	4
72	4	4	4	4
73	1	1	1	1
74	1	3	3	3
75	3	3	3	3
76	1	2	2	2
77	3	4	4	4
78	3	3	4	4
79	2	2	2	2
80	2	3	4	4
81	3	4	4	4

We first examine the convergence of the SDP algorithm (Algorithm 2). In Table 3.1 we show the transmission policy results for different number of samples (N_t) per action. In this table, we simulate the SDP algorithm for $K = 3$, $B_{\max} = 4$, $H = 100$, $M = 1$, and show the best actions for a number of states. It can be seen that when $N_t = 5$ the actions are quite different from the optimal results. As N_t increases, the resulting actions in more states are the same as the optimal ones.

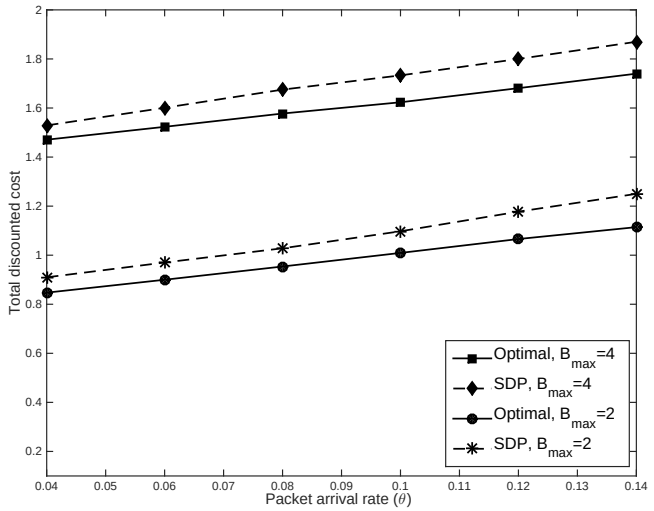

Figure 3.2: Total discounted cost versus θ for $K = 8$, $M = 1$, $f_D T_p = 0.05$, $A = 0.001$, $B = 1$, and $\gamma_{th} = 10$ dB

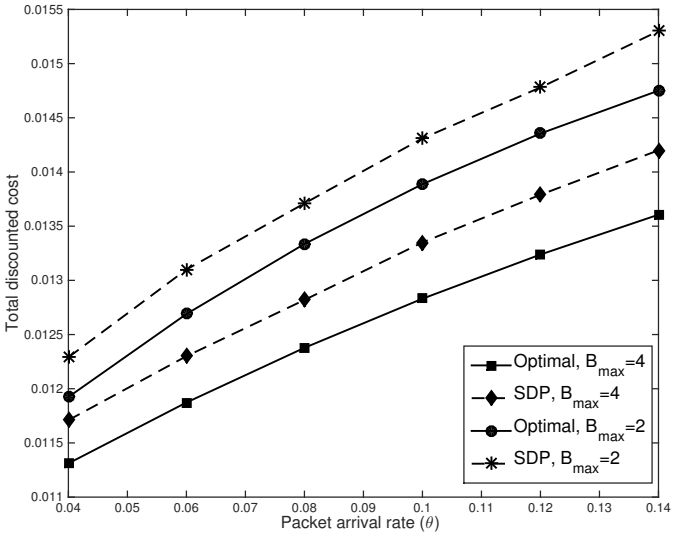

Figure 3.3: Total discounted cost versus θ for $K = 8$, $M = 1$, $f_D T_p = 0.05$, $A = 1$, $B = 0.001$, and $\gamma_{th} = 10$ dB

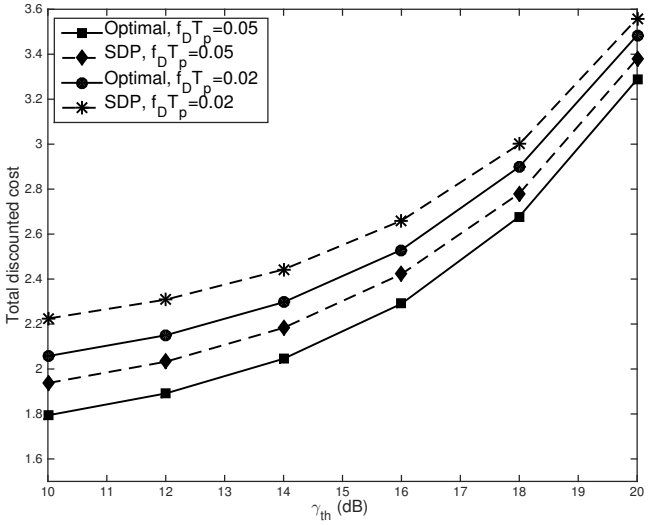

Figure 3.4: Total discounted cost versus γ_{th} for $B_{\max} = 4$, $K = 8$, and $M = 1$

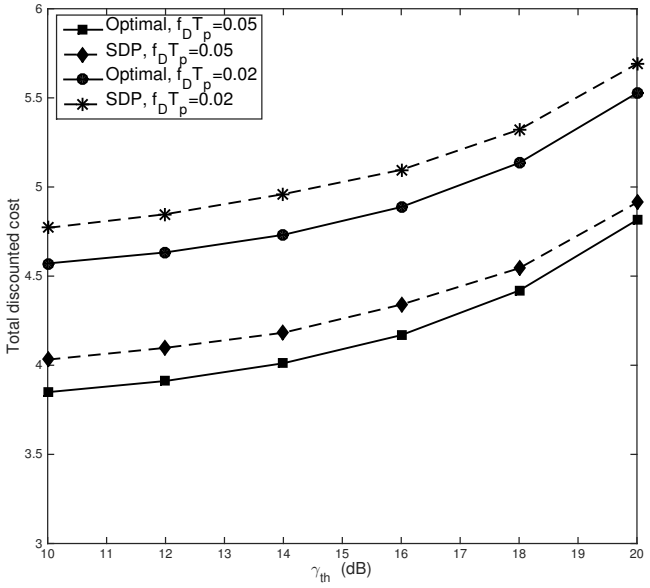

Figure 3.5: Total discounted cost versus γ_{th} for $B_{\max} = 2$, $K = 3$, and $M = 2$

Figs. 3.2-3.5 show the results based on the discounted cost, where the discount factor is $\beta = 0.9$. In Fig. 3.2, we consider $A = 0.001$ and $B = 1$ to emphasize the contribution of the delay in the cost function. On the other hand, in Fig. 3.3, we consider $A = 1$ and $B = 0.001$ to emphasize the contribution of the transmission power in the cost function. In these two figures, the optimal solution in Algorithm 1 and the solution using simulation-based dynamic programming in Algorithm 2 are compared. It is seen that increasing the arrival rate (θ) leads to more packets waiting in the buffer and eventually increases the cost. Although having larger buffer size ($B_{\max}$) allows more packets to be buffered and transmitted at better channel conditions, and results in lower transmission power, it increases packet transmission delay. Overall, the cost in Fig. 3.2 is much lager than in Fig. 3.3 due to the fact that A is much larger than B in the cost function for Fig. 3.2, or the weight for buffer occupancy is much larger than that for transmission power. As the traffic load increases, the increase of queue length is much more significant than that of the transmission power.

Next, we consider $A = 1$ and $B = 1$. In Fig. 3.4, it can be seen that the discounted cost increases with the SNR threshold. This is because higher SNR threshold delays packet transmissions as well as results higher average transmission power. Both algorithms are applied to fading channels with different fading rates, where T_p is the symbol period. It is shown that faster channel variations help reduce the discounted cost. The basic reason is that when the traffic load is relatively low (and therefore packet loss rate is low), the number of buffered packets is small. In this case, fast channel variations help to purge buffered packets as soon as possible. This may not be the case when the channel states change slower since packets may have to be buffered for a longer period when the channel is in poor states. Moreover, it is seen that the

SDP algorithm performs very good and has close-to-optimal costs.

In Fig. 3.5 we examine the performance of the optimal and SDP algorithms for two links ($M = 2$). It can be seen that the SDP algorithm performs close-to-optimal for different values of SNR threshold and fading rates. Unfortunately, the computation load prevents us from generating optimum results for larger $B_{\max}$, and therefore, in order to keep reasonably low packet loss rate, we are unable to increase $B_{\max}$ but only keep low packet arrival rate when examining performance of the optimal solutions.

Next, we demonstrate performance of the solutions based on the average cost in Figs. 3.6-3.8. Fig. 3.6 compares the average cost of the optimal solution and the proposed heuristic scheme. The results show that the performance of the proposed heuristic scheme is very close to the optimal solution, and the gap between the two is minor for a wide range of SNR thresholds. Fig. 3.7 compares the optimal solution with the proposed heuristic scheme for different d when $M = 2$. It is shown that as the distance between the relay node and the end nodes (d) increases, average channel gains decreases which increases both transmission delay and power and consequently the average cost. Moreover, for larger values of d ($d = 200$ m), the cost will increase with the SNR threshold significantly. As the distance d increases, the cost caused by transmission power gradually dominates the overall cost, and therefore, the total cost is more significantly affected by the SNR threshold changes. Also, it can be seen that the performance of the proposed heuristic scheme is very close to the optimal one.

Fig. 3.8 illustrates the performance of the proposed heuristic scheme for different number of links (M). This figure shows that the average cost is increased with M since the average delay of the system increases with the number of links.

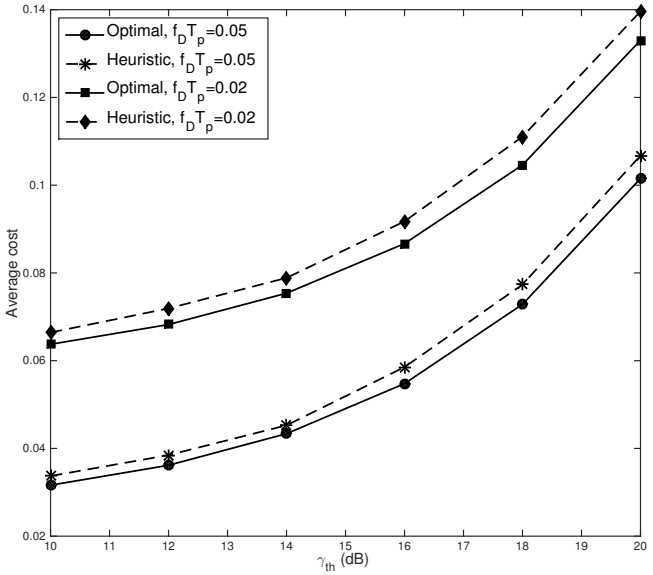

Figure 3.6: Average cost versus γ_{th} for $B_{\max} = 4$, $K = 8$, and $M = 1$

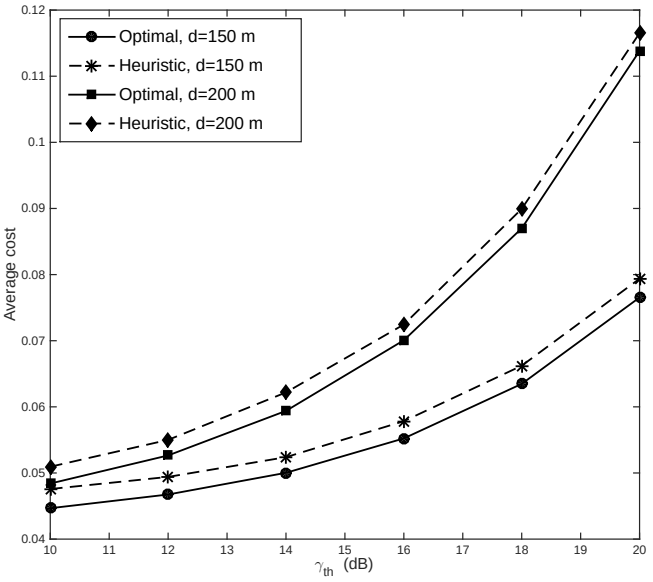

Figure 3.7: Average cost versus γ_{th} for $B_{\max} = 2$, $K = 3$, and $M = 2$

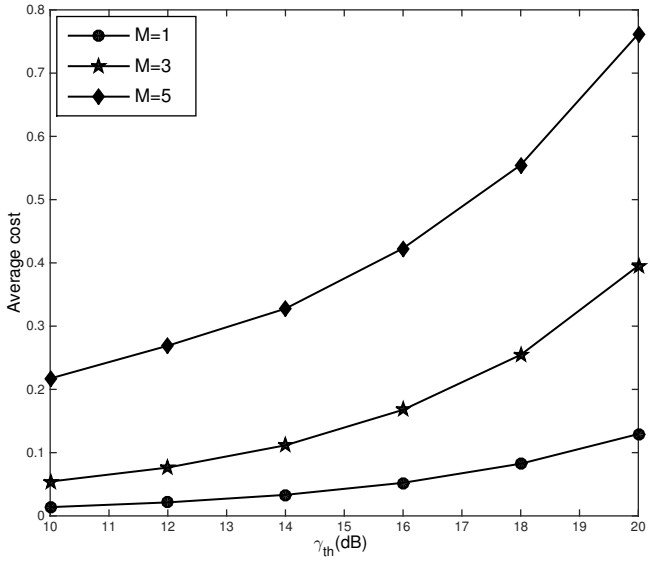

Figure 3.8: Average cost versus γ_{th} for $B_{\max} = 20$, $K = 8$, and $f_D T_p = 0.05$

3.8 Summary

We have studied the transmission scheduling in multiple bidirectional relaying links with the objective of minimizing the long-term cost in a fading channel. The optimized scheduling algorithm based on MDP minimizes the discounted and average costs in finite and infinite horizon scenarios, respectively. The simulation-based dynamic programming algorithm has three advantages: 1) simplifying the modeling process in transforming the scheduling problem to an MDP problem, 2) reducing the computational complexity, and 3) achieving close-to-optimal performance. The proposed heuristic scheme for minimizing average cost can be easily performed when the number of end nodes, buffer size, and number of channel states are large, under which conditions solving the MDP problem can be very difficult due to high computational

complexity.

In the current unconstrained MDP model as well as the SDP algorithm and the heuristic scheme, packet loss rate cannot be easily controlled. In the next chapter, a constrained MDP problem will be formulated to incorporate relay station transmission power and time as well as the data packet transmission delay and packet loss rate.

Chapter 4

Delay-Minimization Resource Management for a Network with Bidirectional Relaying Links

In this chapter, we continue our study on opportunistic scheduling and power allocation in a network with multiple bidirectional relaying links. Different from Chapter 3, where the objective was to minimize a cost that incorporates both transmission power and delay, in this chapter we consider more specific QoS objectives, including average packet loss rate, average packet transmission delay, maximum and average transmission power. A constrained Markov decision process (CMDP) model is developed, and an optimal transmission policy is derived with an objective to minimize the average packet transmission delay, subject to the maximum and average transmission power limits of the relay node. Heuristic scheduling schemes with lower complexity are then proposed, which make transmission decisions based on channel and buffer states, overhearing status, maximum and average transmission power.

The remaining part of the chapter is organized as follows. In Section 4.1 we describe the system model that this work is based on. A constrained MDP problem is formulated in Section 4.2, where a linear optimization problem is formulated to solve the steady state decisions of the relay node at different system states. In Section 4.3 heuristic scheduling schemes are proposed. Numerical results are shown in Section 4.4, and a summary is given in Section 4.5.

4.1 System Description and Problem Formulation

We consider a network with bidirectional communication links and a relay node as shown in Fig. 4.1. The two end nodes of each link communicate with each other through the relay node, which is shared by all the links. We consider that transmissions in the uplink (from the end nodes to the relay node) and the downlink (from the relay node to the end nodes) use orthogonal channels, so that there is no interference or competition between them. Our focus in this work is the power-delay relation when NC is being used, and therefore we limit the scope of the work to the transmissions at the relay node, i.e., downlink transmission scheduling only. Same as in Chapter 3, we consider that the relay node is equipped with a single transmitter, and its timeline is divided into equal length time slots, each for one packet transmission. There is one buffer for storing packets from each end node.

We consider M bidirectional links, indexed by $m = 1, 2, \ldots, M$. There are $2M$ end nodes, indexed from 1 to $2M$. For convenience, we use n and $\hat{n}$ to represent a pair of the end nodes of the same link, and define $\hat{n} = n-1$ if n is even, and $\hat{n} = n+1$ if n is odd. For example, if $n = 3$, then $\hat{n} = 4$; and if $n = 4$, $\hat{n} = 3$. These are the indexes of the two end nodes that belong to link $m = 2$. The relay node can use

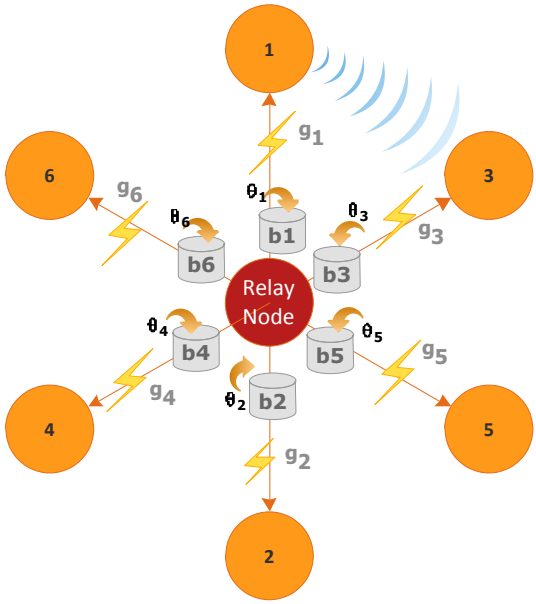

Figure 4.1: System model for $M = 3$

the traditional one-way relaying, and transmit to only one end node at a time. In addition, it can use NC to combine transmissions of multiple packets from end nodes of the same links, as in Chapter 3.

In addition, we consider that nodes near each other are allowed to overhear each other's transmissions. NC can also be performed between nodes belonging to different links, as long as the overhearing condition is satisfied. For this reason, we define an overhearing matrix $\mathbf{O}$ with $2M$ rows and $2M$ columns. The element in the n_1th row and n_2th column in the matrix is $O_{n_1 n_2}$. When $O_{n_1 n_2} = 1$, node n_1 can overhear the transmission of node n_2; otherwise, $O_{n_1 n_2} = 0$. As a special case, $O_{nn} = 1$ for all $n = 1, 2, \ldots, 2M$. In Fig. 4.1, only nodes 1 and 3 can overhear each other, and the

overhearing matrix is given by

$$\mathbf{O} = \begin{pmatrix} 1 & 0 & 1 & 0 & 0 & 0 \\ 0 & 1 & 0 & 0 & 0 & 0 \\ 1 & 0 & 1 & 0 & 0 & 0 \\ 0 & 0 & 0 & 1 & 0 & 0 \\ 0 & 0 & 0 & 0 & 1 & 0 \\ 0 & 0 & 0 & 0 & 0 & 1 \end{pmatrix}.$$

We assume that the overhearing matrix is available at the relay node and does not change during the decision-making process. Given the overhearing relation, the relay node can combine packet x_i from node n_i and packet x_j from node n_j, and transmit $x_i \oplus x_j$ to both nodes $\hat{n}_i$ and $\hat{n}_j$. In order for node $\hat{n}_i$ to recover packet x_i, it should be able to overhear x_j from node n_j; and similarly, in order for node $\hat{n}_j$ to recover packet x_j, it should be able to overhear x_i from node n_i. In general, we define two sets of end nodes, $\mathcal{N}_s$ and $\mathcal{N}_d$ so that $\hat{n} \in \mathcal{N}_d$ for each node $n \in \mathcal{N}_s$, and $\hat{n} \in \mathcal{N}_s$ for each node $n \in \mathcal{N}_d$. The relay node can combine one packet from each of the nodes in $\mathcal{N}_s$ and multicast the XORed packets to all the nodes in $\mathcal{N}_d$, only if each node $n \in \mathcal{N}_d$ can overhear transmissions of all the nodes in $\mathcal{N}_s$ except $\hat{n}$.

The channel state between node n and the relay node is represented by g_n for $n = 1, 2, \ldots, 2M$. The buffer occupancy for packets from node n at the relay node is represented by b_n for $n = 1, 2, \ldots, 2M$, where $0 \leq b_n \leq B_{\max}$, and $B_{\max}$ is the buffer size. The channel model and the distribution of the arrival process are the same as in Chapter 3. The system state is fully defined by a combination of the buffer state and the channel state. That is, $\mathcal{S} = \{b_n, g_n, n = 1, 2, \ldots, 2M\}$.

4.2 The CMDP Model

Given the system model as described in the previous section, our objective is to schedule transmissions at the relay node so that the average packet transmission delay of all buffers in the relay node is minimized, subject to the maximum and average transmission power of the relay node. A constrained Markov decision process (CMDP) can be used to model the system. In the remaining part of this section we first define the actions, then find the state transition probabilities, and finally formulate the CMDP.

4.2.1 Action set

Let $a = (a_1 a_2 \cdots a_{2M})_2$ be a binary sequence that represents the action chosen by the relay at current decision epoch, where a_n is the nth bit of the sequence and referred to as the sub-action to buffer n. When $a_n = 0$, the relay node does not transmit any packets from buffer n; and when $a_n = 1$, the relay node transmits one packet from buffer n to node $\hat{n}$. When multiple bits in a are equal to 1, the relay node uses NC, XORs the corresponding packets into one, and multicasts the NCed packet to all the receiving nodes. As mentioned earlier, the use of NC is subject to the overhearing conditions. We use $\mathcal{A} = \{a = (a_1 a_2 \cdots a_{2M})_2, a_n \in \{0, 1\},\ \forall n = 1, , 2, \ldots, 2M\}$ to represent the action space of the considered system.

Mathematically, set $\mathcal{A}$ can include 2^{2M} different actions, but transmissions based on some of them are not eligible. First, $a_n = 1$ is not eligible when either the buffer for node n is empty, i.e., $b_n = 0$, or the channel state to node $\hat{n}$ is below the threshold, i.e., $g_{\hat{n}} \leq g_{th}$. Second, the use of network coding at the relay node is restricted by the overhearing conditions among the nodes. For action $a = (a_1 a_2 \ldots a_{2M})_2$, in order

for any two bits $a_{n_1} = a_{n_2} = 1$, both $O_{n_1\hat{n}_2}$ and $O_{n_2\hat{n}_1}$ should be 1. For this reason, we define a matrix $\Delta = (\delta(s,a), \forall s, a)$ with $\delta_{s,a} = 1$ if action a is eligible for state s based on the overhearing condition, channel state, and buffer occupancy; and $\delta_{s,a} = 0$ otherwise. Let $\mathcal{N}_a = \{n | 1 \leq n \leq 2M, a_n = 1\}$. We have $\delta(s,a) = 1$ if and only if the following conditions are true: i) $b_n > 0$ for all $n \in \mathcal{N}_a$, ii) $g_{\hat{n}} \geq g_{th}$ for all $n \in \mathcal{N}_a$, and iii) $O_{\hat{n_1}n_2} = 1$ for all $n_1, n_2 \in \mathcal{N}_a$ and $n_1 \neq n_2$.

4.2.2 State transition probability

Once an action is selected (i.e., a transmission decision is made), the system state in the next time slot is completely determined by that in the current time slot and independent of the system states in the past. Therefore, the process is Markov, and the system status is completely defined by $\mathcal{S}$ and $\mathcal{A}$. When the system is at a typical state $s \in \mathcal{S}$, after an action a is taken, the probability that the system is in state $s^{'}$ is the state transition probability of the system, denoted as $P_s(s, s^{'}, a)$, and we further define $\mathbf{P}_S(a) = (P_s(s, s^{'}, a), \forall s, s^{'} \in \mathcal{S})$. This transition probability is a joint effect of the buffer and channel state changes to individual node n. Since each system state includes both the buffer and channel states of all the links, in order to find $\mathbf{P}_S(a)$, we first find the state transition probability of an individual buffer after a sub-action to this buffer is taken, and then combine it with the state transition probability of individual channels.

Let $P_{b,n}(b_n, b_n^{'}, a_n)$ be the transition probability of buffer n from b_n to $b_n^{'}$ after sub-action a_n is taken. Define two matrices of size $(B_{\max}+1) \times (B_{\max}+1)$ as follows. $\mathbf{P}_{b,n}(0) = (P_{b,n}(b_n, b_n^{'}, 0), b_n, b_{n'} = 0, 1, \ldots, B_{\max})$ and $\mathbf{P}_{b,n}(1) = (P_{b,n}(b_n, b_n^{'}, 1), b_n, b_{n'} =$

$0, 1, \ldots, B_{\max}$), which are the transition probability matrices of buffer n when sub-action $a_n = 0$ and $a_n = 1$, respectively. We then have

$$P_{b,n}(b_n, b_n^{'}, 0) = \begin{cases} \theta_n, & b_n^{'} = b_n + 1 \leq B_{\max}, \\ 1, & b_n^{'} = b_n = B_{\max}, \\ \overline{\theta}_n, & b_n^{'} = b_n < B_{\max}, \\ 0, & \text{otherwise}, \end{cases} \tag{4.1}$$

and

$$P_{b,n}(b_n, b_n^{'}, 1) = \begin{cases} \theta_n, & b_n^{'} = b_n \leq B_{\max}, \\ 1, & b_n^{'} = b_n - 1, b_n = B_{\max}, \\ \overline{\theta}_n, & b_n^{'} = b_n - 1, 0 < b_n < B_{\max}, \\ 1, & b_n^{'} = b_n = 0, \\ 0, & \text{otherwise}. \end{cases} \tag{4.2}$$

When $a_n = 0$, the buffer occupancy is increased by 1 if there is a new packet arrival and the buffer is not full; otherwise, the buffer occupancy keeps the same. When $a_n = 1$, the buffer occupancy keeps the same if there is a new arrival; otherwise it is reduced by 1. We can rewrite (4.1) and (4.2), respectively, in a matrix form as

$$\mathbf{P}_{b,n}(0) = \begin{pmatrix} \bar{\theta}_n & \theta_n & 0 & \ldots \\ 0 & \bar{\theta}_n & \theta_n & \ddots \\ \vdots & \ddots & \ddots & \ddots \\ \ldots & 0 & 0 & 1 \end{pmatrix}, \tag{4.3}$$

and

$$\mathbf{P}_{b,n}(1) = \begin{pmatrix} 1 & 0 & 0 & \dots \\ \bar{\theta}_n & \theta_n & 0 & \dots \\ 0 & \bar{\theta}_n & \theta_n & \ddots \\ \vdots & \ddots & \ddots & \ddots \\ \dots & 0 & 1 & 0 \end{pmatrix}. \tag{4.4}$$

Let $\mathbf{b} = (b_1, b_2, \dots, b_{2M})$ represent the joint state of all buffers. Define $\mathbf{b}^{'} = (b_1^{'}, b_2^{'}, \dots, b_{2M}^{'})$ as another state of the buffers. Since the arrival processes of all the buffers are independent, we can find the transition probability of the joint buffer state from $\mathbf{b}$ to $\mathbf{b}^{'}$ when action a is taken as

$$P_B(\mathbf{b}, \mathbf{b}^{'}, a) = \Pi_{n=1}^{2M} P_{b,n}(b_n, b_n^{'}, a_n). \tag{4.5}$$

As the number of non-zero elements in matrix $\mathbf{P}_{b,n}(a_n)$ is at most $2B_{\max} + 1$, we can use sparse matrix computation to reduce computational complexity when finding the state transition probability matrix. Define $\mathbf{P}_B(a) = (P_B(\mathbf{b}, \mathbf{b}^{'}, a), \forall \mathbf{b}, \mathbf{b}^{'})$. The Kronecker product of $2M$ sparse matrices can be used to find $\mathbf{P}_B(a)$, which is the joint state transition probability matrix of all the buffers when action $a = (a_1 a_2 \dots a_{2M})_2$ is taken, as follows

$$\mathbf{P}_B(a) = \mathbf{P}_{b,1}(a_1) \otimes \mathbf{P}_{b,2}(a_2) \otimes \dots \otimes \mathbf{P}_{b,2M}(a_{2M}), \tag{4.6}$$

where $\otimes$ is Kronecker product.

We now consider the channel state changes. There are $2M$ independent channels.

The state transition matrix for the channel between node n and the relay node is given by

$$\mathbf{P}_{c,n} = \begin{pmatrix} q_{0,0} & q_{0,1} & 0 & 0 & \dots & \dots & 0 \\ q_{1,0} & q_{1,1} & q_{1,2} & 0 & \dots & \dots & 0 \\ 0 & q_{2,1} & q_{2,2} & q_{2,3} & \dots & \dots & 0 \\ \vdots & \ddots & \ddots & \ddots & \dots & \ddots & \vdots \\ 0 & 0 & 0 & 0 & \dots & q_{K-2,K-1} & q_{K-1,K-1} \end{pmatrix} \tag{4.7}$$

The joint state transition probability of all the $2M$ channels can be written as

$$\mathbf{P}_C = \mathbf{P}_{c,1} \otimes \mathbf{P}_{c,2} \otimes \cdots \otimes \mathbf{P}_{c,2M}. \tag{4.8}$$

Finally, the system state transition matrix $\mathbf{P}_S(a)$ for each action a can be obtained as

$$\mathbf{P}_S(a) = \mathbf{P}_B(a) \otimes \mathbf{P}_C. \tag{4.9}$$

4.2.3 CMDP formulation

Let $p(s,a)$ be the transmission power of the relay node in state s when action $a = (a_1 a_2 \dots a_{2M})_2$ is taken. We have

$$p(s,a) = \max_{n=1}^{2M} \left\{ \frac{a_n \gamma_{th}}{g_n} \right\}. \tag{4.10}$$

That is, the transmission power is determined by the worst channel condition, if the relay multicasts to multiple end nodes.

Let $Q(s,a)$ be the total number of packets in all the buffers after action $a =$

$(a_1 a_2 \dots a_{2M})_2$ is taken. We have

$$Q(s,a) = \sum_{n=1}^{2M} \max\{b_n - a_n, 0\}. \tag{4.11}$$

According to Little's law, for a given packet arrival rate, the average packet transmission delay is proportional to the average number of packets in the queue. Therefore, $Q(s,a)$ is a direct indication of the packet transmission delay.

Let $L(s,a)$ be the probability of packet loss when the system is in state s and action a is taken. We have

$$L(s,a) = \frac{1}{2M} \sum_{n=1}^{2M} \theta_n \mathbf{I}_{b_n = B_{\max}}, \tag{4.12}$$

where $\mathbf{I}_{b_n = B_{\max}}$ is an indicator function, which is equal to 1 if the condition in the subscript holds and 0 otherwise.

Based on the above information, we can formulate the problem as a CMDP, with an objective to minimize the average packet transmission delay, subject to the average transmission power limit and the packet loss rate due to the buffer overflow. The expected long-term objective and constraints can be defined as follows:

$$\min \quad \overline{Q}(\pi) = \lim_{t\to\infty} \sup \frac{1}{t} \sum_{t'=1}^{t} E[Q(s_{t'}, a_{t'})] \tag{4.13}$$

$$\text{s.t.} \quad \overline{p}(\pi) = \lim_{t\to\infty} \sup \frac{1}{t} \sum_{t'=1}^{t} E[p(s_{t'}, a_{t'})] \le \overline{p}_{\max}, \tag{4.14}$$

$$\overline{L}(\pi) = \lim_{t\to\infty} \sup \frac{1}{t} \sum_{t'=1}^{t} E[L(s_{t'}, a_{t'})] \le \overline{L}_{\max}, \tag{4.15}$$

where $E[\cdot]$ is the expectation, and $s_{t'}$ and $a_{t'}$, respectively, are the state and action

at time t'. The objective function in (4.13), $\overline{Q}(\pi)$, is the average number of buffered packets from all end nodes, the left-hand side of (4.14) is the average transmission power of the relay node, which should be less than a pre-specified limit $\overline{p}_{\max}$, the left-hand side of (4.15) is the average packet loss of all the buffers due to overflow with $\overline{L}_{\max}$ as the pre-specified upper bound. The objective and constraints are defined as functions of policy π, which is a mapping of state $s \in \mathcal{S}$ to the action $a \in \mathcal{A}$. $p(\cdot,\cdot)$, $Q(\cdot,\cdot)$, and $L(\cdot,\cdot)$ are immediate transmission power of the relay, immediate number of packets in all the buffers, and immediate loss probability, respectively.

Based on [31], to obtain the optimal policy π^*, the CMDP formulation in (4.13)-(4.15) can be converted into a linear programming (LP). In the linear optimization problem below, $x(s,a)$ is the probability to take action a in state s, (4.19) gives the balance condition of the state transitions, (4.20) ensures that all possible states and actions are incorporated, and (4.21) ensures that only eligible actions can have a non-zero probability.

$$\min \quad \sum_{s\in\mathcal{S}}\sum_{a\in\mathcal{A}} x(s,a)Q(s,a) \tag{4.16}$$

$$\text{s.t.} \quad \sum_{s\in\mathcal{S}}\sum_{a\in\mathcal{A}} x(s,a)p(s,a) \leq \overline{p}_{\max}, \tag{4.17}$$

$$\sum_{s\in\mathcal{S}}\sum_{a\in\mathcal{A}} x(s,a)L(s,a) \leq \overline{L}_{\max}, \tag{4.18}$$

$$\sum_{a\in\mathcal{A}} x(s',a) = \sum_{s\in\mathcal{S}}\sum_{a\in\mathcal{A}} P_S(s,s',a)x(s,a), \forall s' \in \mathcal{S}, \tag{4.19}$$

$$\sum_{s\in\mathcal{S}}\sum_{a\in\mathcal{A}} x(s,a) = 1, \tag{4.20}$$

$$x(s,a)[1-\delta(s,a)] = 0, \ \forall s \in \mathcal{S}, a \in \mathcal{A}, \tag{4.21}$$

$$0 \leq x(s,a) \leq 1, \ \forall s \in \mathcal{S}, a \in \mathcal{A}. \tag{4.22}$$

Let x^* be the optimal solution to the LP problem. There exists an optimal randomized stationary policy, $\pi^*(s,a)$, for the CMDP, which can be found as [31]

$$\pi^*(s,a) = \frac{x^*(s,a)}{\sum_{a\in\mathcal{A}} x^*(s,a')}. \tag{4.23}$$

The average transmission power can be found as

$$\overline{p}(\pi^*) = \sum_{s\in\mathcal{S}}\sum_{a\in\mathcal{A}} x^*(s,a)p(s,a), \tag{4.24}$$

and the average buffer occupancy for all nodes is given by

$$\overline{Q}(\pi^*) = \frac{1}{2M}\sum_{s\in\mathcal{S}}\sum_{a\in\mathcal{A}} x^*(s,a)Q(s,a), \tag{4.25}$$

and the average packet loss rate due to buffer overflow is given by

$$\overline{L}(\pi^*) = \sum_{s\in\mathcal{S}}\sum_{a\in\mathcal{A}} x^*(s,a)L(s,a). \tag{4.26}$$

For relatively low packet arrival rate, the packet loss rate due to buffer overflow can be kept very low, and the delay performance based on the Little's Law gives very good approximation to the actual delay performance.

4.2.4 Computational complexity

In the above formulation, the total number of system states is $(B_{\max}+1)^{2M}K^{2M}$, and the total number of elements in $\mathbf{P}_S(a)$ is $\left[(B_{\max}+1)^{2M}K^{2M}\right]^2$ for each a, which can

be very large even for a moderate number of links and channel states. For example, when $B_{\max} = 2$ packets, $K = 3$, and $M = 2$, the total number of elements in the state transition matrix is approximate 4.3×10^7 for each action. On the other hand, several features of the problems can help reduce the computational complexity for calculating the state transition matrix.

The Kronecker product for sparse matrices can help to significantly reduce the number of operations. From (4.3), (4.4), and (4.7) we can see that the matrices $\mathbf{P}_{b,n}$ and $\mathbf{P}_C$ all include a lot of zeros when M, $B_{\max}$, and K are relatively large. For example, when calculating $\mathbf{P}_B(a)$ using (4.6), the result is a matrix having $(B_{\max} + 1)^{2M} \times (B_{\max} + 1)^{2M}$ elements, but at most $(2B_{\max} + 1)^{2M}$ elements are non-zero. Similarly, matrix $\mathbf{P}_C$ has at most $(3K - 2)^{2M}$ non-zero elements, and $\mathbf{P}_S(a)$ has at most $(2B_{\max}+1)^{2M}(3K-2)^{2M}$ non-zero elements. For the same parameters as in the previous paragraph, the total number of non-zero elements is approximately 1.5×10^6 for each action a, which is greatly reduced but still a huge number. Note that this number should be multiplied by the total number of eligible actions to get the total number of non-zero elements in the state transition matrix, while the number of eligible actions depends on the overhearing condition in the network in addition to the buffer and channel states.

4.2.5 CMDP for a system without overhearing

When there is no overhearing of transmissions between different end nodes, the relay node does not transmit to multiple end nodes that belong to different links. For this reason, the possible transmission options of the relay node include: not transmit, transmit to node n (one-way relaying), and transmit to both nodes n and $\hat{n}$ (i.e., the

two end nodes of a given link) using NC. In this case, the total number of possible actions is $3M+1$ and the action space is written as $\mathcal{A} = \{a, a \in [0, 3M]\}$. When $a = 0$, the action is no transmission; when $a = 3(m-1)+1 = 3m-2$, the relay transmits to the first end node of link m only using traditional relay technique; when $a = 3(m-1)+2 = 3m-1$, the relay transmits to the second end node of link m only using traditional relay technique; and when $a = 3m$, the relay transmits to both the end nodes of link m using NC. With this action space, the same method as before can be used to find the state transition matrix. However, since there are only $3M+1$ possible actions instead of 2^{2M} actions in the general case, at most $3M+1$ $\mathbf{P}_B(a)$ matrices should be found in this case. Furthermore, the elements in matrix Δ can be redefined as

$$\delta_{s,0} = 1, \tag{4.27}$$

$$\delta_{s,3(m-1)+1} = \begin{cases} 1, & \text{if } g_{2m-1} \geq g_{th} \text{ and } b_{2m} > 0, \\ 0, & \text{otherwise,} \end{cases} \tag{4.28}$$

$$\delta_{s,3(m-1)+2} = \begin{cases} 1, & \text{if } g_{2m} \geq g_{th} \text{ and } b_{2m-1} > 0, \\ 0, & \text{otherwise,} \end{cases} \tag{4.29}$$

$$\delta_{s,3m} = \delta_{s,3(m-1)+1} \times \delta_{s,3(m-1)+2}, \tag{4.30}$$

where (4.27) indicates that action $a = 0$ is feasible in all the system states; (4.28) and (4.29) indicate that the action of transmitting to one of the end nodes of a given link is feasible only if the corresponding data buffer is nonempty and the link state is above the threshold; and (4.30) indicates that the action of transmitting to both end nodes of a link is feasible only if both buffers for the link are nonempty and both the

link states are above the threshold.

With this, the transmission power of the relay node to take action a at state s is given by

$$p(s,a) = \gamma_{th} \sum_{m=1}^{M} \left(\frac{\mathbf{I}|_{a=3m-2}}{g_{2m-1}} + \frac{\mathbf{I}|_{a=3m-1}}{g_{2m}} + \frac{\mathbf{I}|_{a=3m}}{\min\{g_{2m-1}, g_{2m}\}} \right), \tag{4.31}$$

and the total number of buffered packets after action a at state s is given by

$$Q(s,a) = \sum_{n=1}^{2M} b_n - \sum_{m=1}^{M} \left(\mathbf{I}|_{a=3m-2} + \mathbf{I}|_{a=3m-1} + 2\mathbf{I}|_{a=3m} \right). \tag{4.32}$$

For the packet loss probability due to buffer overflow, the same formula as in (4.12) can be used. Submitting $Q(s,a)$, $p(s,a)$, $L(s,a)$, and $\delta(s,a)$ into the optimization problem defined by (4.16)-(4.21), we can solve $V(s,a)$ for the no-overhearing case.

4.3 Heuristic Algorithms

In certain cases of practical interest, it is not possible to use the optimal scheduling because of limited computational resources. The computational complexity for solving the CMDP is prohibitively high, although the complexity can be reduced in the "no-overhearing" case. In this section, heuristic schemes are proposed. The basic idea for the heuristic schemes is to transmit as many packets as possible subject to the transmission power limit. Below we design two schemes, the first one is for the general formulation and applies to both the overhearing and no-overhearing cases, and the second one applies to only the no-overhearing case.

4.3.1 General case

We define a weighted average of the transmission power for the relay node up to time slot t as

$$\overline{p}(t) = \beta\overline{p}(t-1) + (1-\beta)p(t), \tag{4.33}$$

where $p(t)$ is the current transmission power of the relay node. The heuristic scheme should ensure that at any time slot, $\overline{p}(t) \leq \overline{p}_{\max}$. Together with (4.33), we have

$$p(t) \leq \frac{\overline{p}_{\max} - \beta\overline{p}(t-1)}{1-\beta} \triangleq p_{\max}(t). \tag{4.34}$$

In Algorithm 1, the relay node tries to transmit to as many end nodes as possible in each time slot, provided $p(t) \leq p_{\max}(t)$. For each node n, γ_{th}/g_n gives the minimum required transmission power for the relay node, if the relay should transmit to node n. If this power is less than $p_{\max}(t)$, then the relay can transmit to node n, provided the buffer is not empty, in which case a temporary variable $\hat{p}_n$ is set to equal γ_{th}/g_n; otherwise, $\hat{p}_n$ is set to zero (i.e., no transmission to node n). All the nodes with $\hat{p}_n > 0$ form a set $\mathcal{N}_d$. This is performed in the first part (Lines 1-7) of the algorithm.

In the second part (Lines 8-16), the relay node finds the maximum number of nodes it can reach in one transmission. For each node n in $\mathcal{N}_d$, the relay node finds $\mathcal{N}_{d,n}$, which is a subset of $\mathcal{N}_d$ and includes all possible receiver nodes that the relay node can transmit to together with node n in one transmission. Specifically, node v can be included in $\mathcal{N}_{d,n}$ if it satisfies the overhearing condition with all the existing nodes in $\mathcal{N}_{d,n}$. After $\mathcal{N}_{d,n}$ is formed for all nodes $n \in \mathcal{N}_d$, the relay node decides to transmit to the nodes in set $\mathcal{N}_{d,n*}$, which has the largest size among all $\mathcal{N}_{d,n}$'s, and

the transmission power is set accordingly.

Algorithm 1 Heuristic algorithm for the general case

1: **for** $n = 1 : 2M$ **do**
2: **if** $b_{\hat{n}} > 0$ and $\gamma_{th}/g_n < p_{\max}(t)$ **then**
3: $\hat{p}_n = \gamma_{th}/g_n$ and $\mathcal{N}_d = \{n\}$
4: **else**
5: $\hat{p}_n = 0$
6: **end if**
7: **end for**
8: **for** $n \in \mathcal{N}_d$ **do**
9: $\mathcal{N}_{d,n} = \{n\}$
10: **for** $v \in \mathcal{N}_d \setminus \mathcal{N}_{d,n}$ **do**
11: **if** $O_{u\hat{v}} = O_{v\hat{u}} = 1$ for all $u \in \mathcal{N}_{d,n}$ **then**
12: $\mathcal{N}_{d,n} = \mathcal{N}_{d,n} \cup \{v\}$
13: $\hat{p}_n = \max\{\hat{p}_n, \gamma_{th}/g_v\}$
14: **end if**
15: **end for**
16: **end for**
17: $n^* = \arg\max_n |\mathcal{N}_{d,n}|$ and $p(t) = \hat{p}_{n^*}$

4.3.2 No-overhearing case

When overhearing is not allowed, Algorithm 1 can still be used to schedule the transmissions, but the special feature of no-overhearing between end nodes allows designing a better scheme that can further improve the packet transmission performance. Algorithm 2 is designed to minimize both the average and maximum packet transmission delay. The first part (Lines 1-9) of the algorithm is to find the nodes that the relay node can transmit to based on both buffer and transmission power. If both conditions are satisfied, U_n is set to 1, and $\hat{p}_n$ records the required transmission power to reach the node. When this process is done for all the end nodes, the relay node can transmit to one and only one end node of each link in set $\mathcal{M}_1$, and can transmit to both end

nodes of each link in set $\mathcal{M}_2$. In the second part (Lines 10-20) of the algorithm, the relay node first checks $\mathcal{M}_2$. If $\mathcal{M}_2$ is not empty, it uses NC and transmits to the link that results in the longest instantaneous delay. In Line 11, Q_{2m-1}/θ_{2m-1} and Q_{2m}/θ_{2m}, respectively, are the instantaneous delay of the first and second queues of link m. If set $\mathcal{M}_2$ is empty, it then checks $\mathcal{M}_1$. If $\mathcal{M}_1$ is not empty, it transmits to the node that results in the longest instantaneous delay. In this algorithm, the emphasis is not only regarding how many packets can be combined by the relay node in one transmission, but also which link to serve.

Algorithm 2 Heuristic algorithm for no-overhearing case

1: **for** $n = 1 : 2M$ **do**
2: **if** $b_{\hat{n}} > 0$ and $\gamma_{th}/g_n < p_{\max}(t)$ **then**
3: $\hat{p}_n = \gamma_{th}/g_n$ and $U_n = 1$
4: **else**
5: $\hat{p}_n = 0$ and $U_n = 0$
6: **end if**
7: **end for**
8: $\mathcal{M}_1 = \{m | m = 1 : M, U_{2m-1} + U_{2m} = 1\}$
9: $\mathcal{M}_2 = \{m | m = 1 : M, U_{2m-1} = U_{2m} = 1\}$
10: **if** $\mathcal{M}_2 \neq \emptyset$ **then**
11: $m^* = \arg\max_{m \in \mathcal{M}_2} (Q_{2m-1}/\theta_{2m-1} + Q_{2m}/\theta_{2m})$
12: Transmit to nodes $2m^* - 1$ and $2m^*$ using NC, $p(t) = \max\{\hat{p}_{2m^*-1}, \hat{p}_{2m^*}\}$
13: **else**
14: $m^* = \arg\max_{m \in \mathcal{M}_1} (Q_{2m-1}/\theta_{2m-1} + Q_{2m}/\theta_{2m})$
15: **if** $U_{2m^*-1} = 1$ **then**
16: Transmit to node $2m^* - 1$, $p(t) = \hat{p}_{2m^*-1}$
17: **else**
18: Transmit to node $2m^*$, $p(t) = \hat{p}_{2m^*}$
19: **end if**
20: **end if**

4.4 Numerical Results

In this section, we generate numerical results using both the optimum solution from the CMDP model and the proposed heuristic schemes. The channel model is the same as in Chapter 3.

Default parameters are as follows: $\beta = 0.999$, $\gamma_{th} = 10$ dB, and the packet arrival rate from each end node to the relay node is $\theta = 0.1$ packets per time slot. For most simulation results, we choose a fixed distances between the relay node and each end node is ($d = 200$ m). However, to examine a more realistic scenario, for the heuristic algorithms in Figs. 4.7– 4.9 the distance (d) is uniformly distributed on the interval $[100, 300]$. The reason we consider fixed distance for the optimal results is that FSMC formulation needs fixed values of average channel gain and distance. Therefore, to get a uniform distribution over distance, we have to solve the MDP problem for a number of iterations which is very time-consuming due to the complexity of the MDP problem.

We first compare the performance of the first proposed scheme to the optimum solution. Due to the high computational complexity, only small values of M, K, and $B_{\max}$ can be used in order to generate the optimum solutions within a reasonable amount of time. Larger values of M, K, and $B_{\max}$ will be used to simulate the performance of the heuristic schemes later on. Throughout the simulation, we adjust the packet arrival rates so that the packet loss rate due to buffer overflow is very small (below 1%).

Figs. 4.2–4.5 show the comparison between the first heuristic scheme and optimum solutions. Figs. 4.2 and 4.3, respectively, show the average transmission power and delay performance for $M = 2$, and Figs. 4.4 and 4.5 show the results for $M = 3$.

When generating these results, the heuristic schemes are simulated first, and the resulted average packet loss rates are fed into the optimization problem as $\overline{L}_{\max}$, based on which performance of the optimum solutions is obtained. Figs. 4.2 and 4.4 show that the average transmission power using the heuristic scheme is almost the same as the optimum. This shows that the heuristic scheme can follow the average transmission power limit as good as the optimum. When $\overline{p}_{\max}$ is relatively small, the actual average transmission power of the relay node is the same as $\overline{p}_{\max}$. This is because the transmission opportunity of the relay node is mainly determined by the average transmission power limit. The relay node should transmit whenever the transmission power constraints are satisfied. As $\overline{p}_{\max}$ increases, the transmission power causes less constraint on the transmission opportunity of the relay node. As a result, packets do not have to be buffered for a long time before the channel condition is good enough. As the relay node seldom needs to use up all its power budget, the actual average transmission power becomes lower than $\overline{p}_{\max}$. When $\overline{p}_{\max}$ exceeds a certain value, the constraint on average transmission power becomes further looser, and most packets can be transmitted with a very short delay. Further increasing the average transmission power limit does not help speed up the packet transmissions very much. This is also shown in Figs. 4.3 and 4.5 where the average delay curves are almost flat when $\overline{p}_{\max}$ is large. In this case, the transmission power of the relay node is completely determined by the packet arrival process, not the power limit. Therefore, the average transmission power of the relay node is also flat as $\overline{p}_{\max}$ further increases as shown in Figs. 4.2 and 4.4.

By comparing the results of overhearing and no-overhearing cases, it is seen that in general the no-overhearing case may require higher transmission power and result

in longer average packet transmission delay. This indicates that overhearing provides more chances for using NC, which makes it possible for the relay node to transmit packets with shorter delay and at lower transmission power. On the other hand, Figs. 4.2 and 4.4 show that when $\overline{p}_{\max}$ is relatively small, the average transmission power for both cases is about the same. Figs. 4.3 and 4.5 show that when $\overline{p}_{\max}$ is relatively small, the no-overhearing case can result in much higher average delay than the overhearing case; while this difference becomes less obvious as $\overline{p}_{\max}$ increases. The reason for this is that when $\overline{p}_{\max}$ is small, the relay node can transmit only when the channel state is very good, and the difference between the actual transmission power and $\overline{p}_{\max}$ is very small, whether or not the transmission is to a single, two, or more end nodes. When $\overline{p}_{\max}$ is relatively larger, there is more flexibility for the actual transmission power, and more NC chances are available for both the overhearing and no-overhearing cases, and eventually the power limit is loose enough to allow most packets to be transmitted as soon as they arrive without much queueing delay. In this case, the average transmission power in the no-overhearing case is higher than the overhearing case.

By further comparing Figs. 4.2 and 4.4 we can see that the basic trend of the average power versus $\overline{p}_{\max}$ is the same, although the average power for $M = 3$ is higher than that for $M = 2$. By comparing Figs. 4.3 and 4.5 we can see that the average transmission delay for $M = 3$ is lower than that for $M = 2$, because a smaller buffer size is used for the $M = 3$ case.

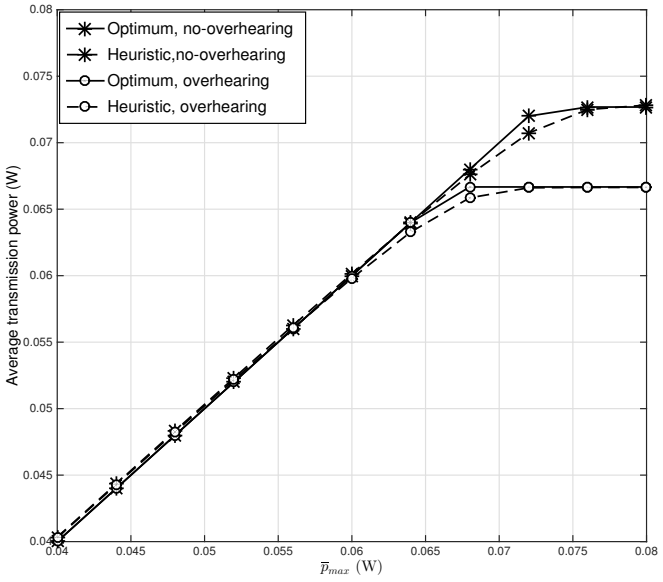

Figure 4.2: Average power versus $\overline{p}_{\max}$, $M = 2$, $K = 3$, $B_{\max} = 2$

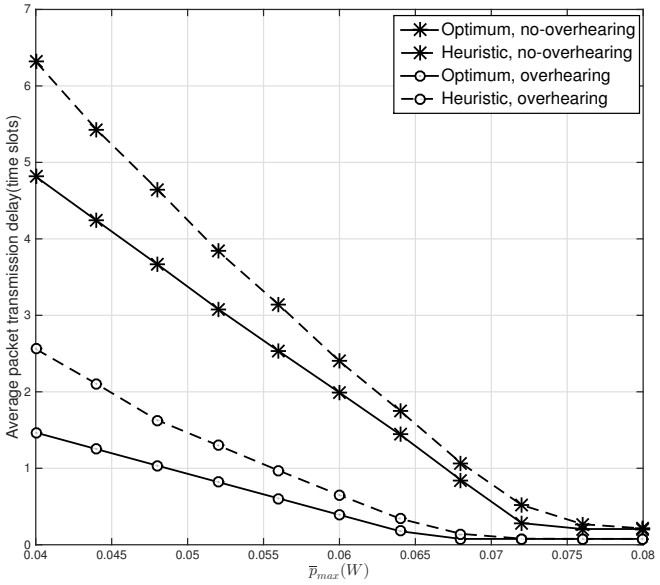

Figure 4.3: Average delay versus $\overline{p}_{\max}$, $M = 2$, $K = 3$, $B_{\max} = 2$

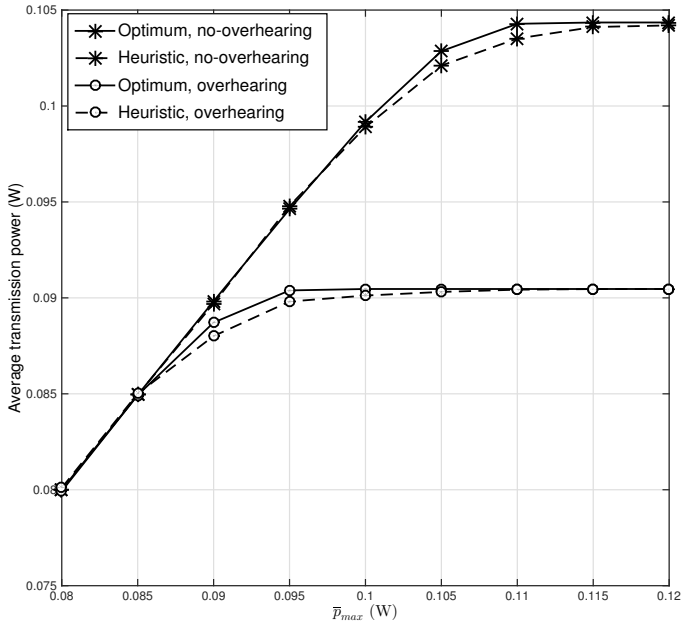

Figure 4.4: Average power versus $\overline{p}_{\max}$, $M = 3$, $K = 2$, $B_{\max} = 1$

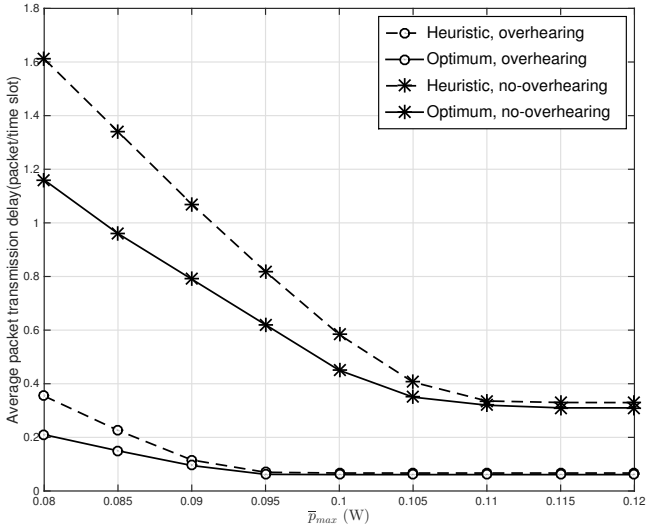

Figure 4.5: Average delay versus $\overline{p}_{\max}$, $M = 3$, $K = 2$, $B_{\max} = 1$

Figs. 4.6 and 4.7, respectively, show the average packet transmission delay and average relay node transmission power versus the packet arrival rate at different fading rates in the overhearing case; and Figs. 4.8 and 4.9 show the delay and power results in the no-overhearing case. From Figs. 4.6 and 4.8 it can be seen that the average packet transmission delay increases with the packet arrival rate; for the same arrival rate and fading rate, larger $\overline{p}_{\max}$ results in lower average delay due to increased transmission opportunities; and larger fading rate also reduces the average packet transmission delay because the buffered packets do not have to wait for a long time before the channel enters good conditions. By comparing Figs. 4.6 and 4.8 we can see that overhearing can reduce the average packet transmission delay. From Figs. 4.7 and 4.9 it can be seen that as θ increases, the average transmission power of the relay node increases and then keeps constant. When θ is small, increasing θ requires more transmissions from the relay node, and the relay node may have to transmit when the channel condition is not very good, and this increases the average transmission power. On the other hand, the average transmission power stops increasing with the arrival rate once the latter is above a certain value that is sufficient to keep the buffer nonempty all the time. In this case, the relay node transmits all the time, provided the channel conditions allow it to do so, and the average transmission power is fully determined by the channel condition. For the same $\overline{p}_{\max}$ limit, different fading rates result in almost the same average transmission power, because the fading rate only affects how quickly the next good channel condition comes, but not the average link gains. By comparing Figs. 4.7 and 4.9 it can be seen that the overhearing condition does not significantly affect the average transmission power of the relay node. This observation is consistent with that from Figs. 4.2 and 4.4 when $\overline{p}_{\max}$ is set to be

relatively small.

When overhearing is not allowed, Figs. 4.10, 4.11, and 4.12 show the maximum packet transmission delay, average packet transmission delay, and average transmission power of the relay node when using the two proposed schemes. It is seen that using the second scheme achieves almost the same average data transmission delay and consumes almost the same average transmission power as using the first scheme, but always achieves lower maximum transmission delay. This is because of the fact that in the second scheme the relay node always selects to transmit for the link that results in the longest instantaneous delay, whereas in the first scheme the decision is only based on total number of packets that can be combined in one transmission.

Fig. 4.12 shows that the average transmission power of the relay node increases with γ_{th} and then keeps constant. When γ_{th} is small, the relay node does not need to use all of its power budget to reach γ_{th}. In this case, increasing γ_{th} increases the average transmission power until it reaches the maximum transmission power. After this point, the transmission power cannot be increased, and increasing γ_{th} will result in higher transmission delay. That is, the relay can only transmit when the channel is in very good condition.

In Figs. 4.13 and 4.14, we compare the performance of the proposed heuristic schemes with several other scheduling schemes. The "one-way relaying" scheme works in the same way for both overhearing and no-overhearing cases, and the relay node always transmits to the node with the best channel condition, provided the buffer is not empty. In the "two-way relaying" scheme, the relay node always uses NC. In the no-overhearing case, the relay node transmits to the two end nodes of the link that results in the longest instantaneous delay; and in the overhearing case, the

relay node transmits to as many pairs of the end nodes as possible, provided that the overhearing conditions are satisfied, and there are buffered packets. In both the one-way and two-way scheduling schemes, the transmission power of the relay node is set in the same way as in the proposed schemes. In addition, the "no power allocation" scheduling works similarly to Algorithm 1 for the overhearing case and Algorithm 2 for the no-overhearing case, except that $p(t)$ can take only $p_{\max}$ or 0.

As it can be observed from Fig. 4.14, having higher $\overline{p}_{\max}$ helps reduce the packet transmission delay for all the scheduling schemes, and the proposed two scheduling schemes achieve the lowest delay. By comparing the seven curves in Fig. 4.14, it is seen that the two "no power allocation" schemes result in the highest delay. This is because that the relay node always uses the maximum power when it transmits, which limits its transmission opportunities due to the average transmission power limit (which is normally lower than the maximum instantaneous power limit). On the other hand, all other scheduling schemes dynamically adjust the transmission power of the relay node, so that when the link condition is good, the relay node transmits at lower power, and overall the relay node can have more transmission opportunities, which reduce the average packet transmission delay. Among all the five scheduling schemes that apply power allocations, using two-way relaying in the no-overhearing case results in the worst delay. This is because of the fact that the restriction on using only NC limits the transmission opportunities, while no-overhearing further reduces the chance of combining multiple packets into one transmission.

Fig. 4.13 also shows that the "no power allocation" schemes indeed always reach the full average power limit. On the other hand, the two-way relaying scheduling

schemes for both overhearing and no-overhearing have much lower average transmission power than the other scheduling schemes, because they result in the minimum number of transmissions of the relay node. In contrast, both the proposed scheduling schemes can take better advantage of the given transmission power limit for improving the average packet transmission delay. The one-way relay scheme also results in much higher delay than the proposed schemes, and this is shown more clearly in part (b) of Fig. 4.14, which is a zoomed version of part (a).

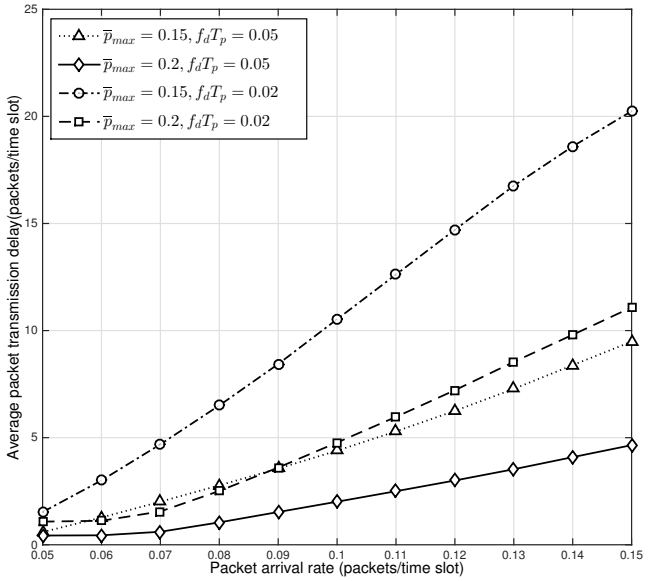

Figure 4.6: Overhearing: average delay versus θ, $M = 4$, $K = 8$, $B_{\max} = 20$

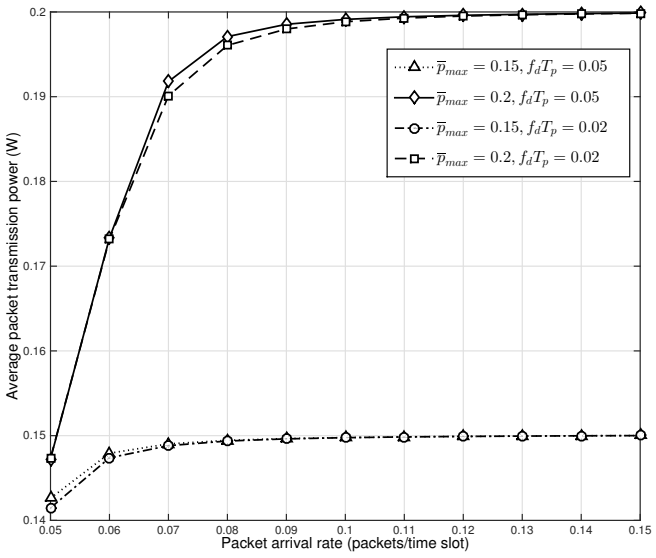

Figure 4.7: Overhearing: average power versus θ, $M = 4$, $K = 8$, $B_{\max} = 20$

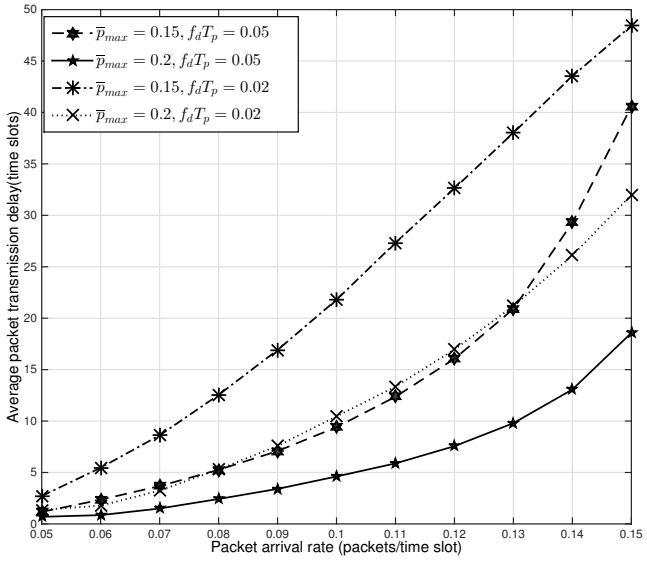

Figure 4.8: No-overhearing: average delay versus θ, $M = 4$, $K = 8$, $B_{\max} = 20$

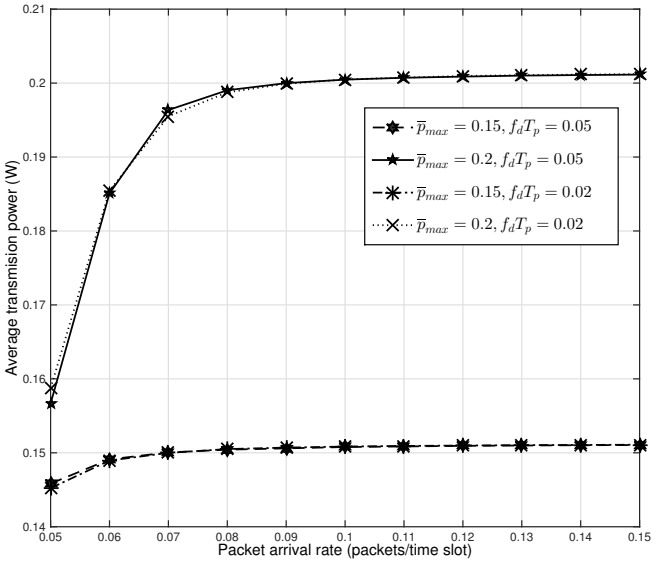

Figure 4.9: No-overhearing: average power versus θ, $M = 4$, $K = 8$, $B_{\max} = 20$

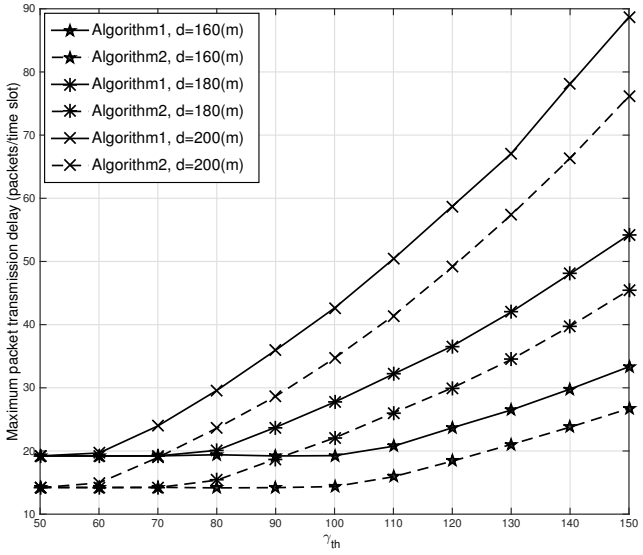

Figure 4.10: No-overhearing, maximum delay versus γ_{th}, $\overline{p}_{\max} = 0.25$, $M = 6$, $K = 8$, $B_{\max} = 20$

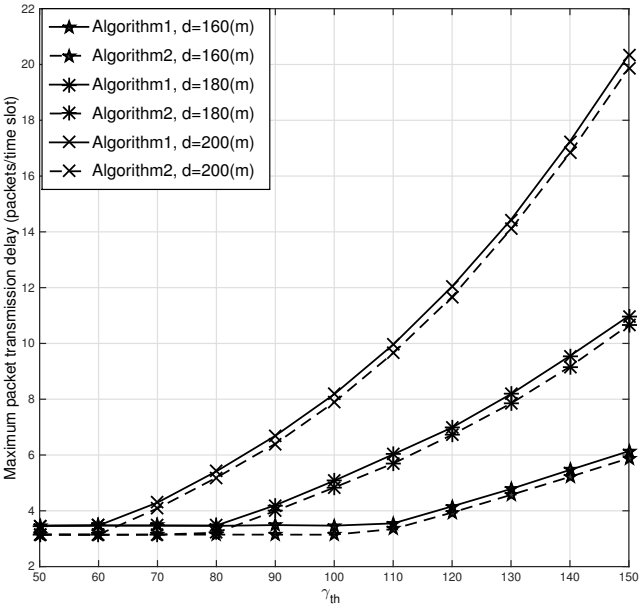

Figure 4.11: No-overhearing, average delay versus γ_{th}, $\overline{p}_{\max} = 0.25$, $M = 6$, $K = 8$, $B_{\max} = 20$

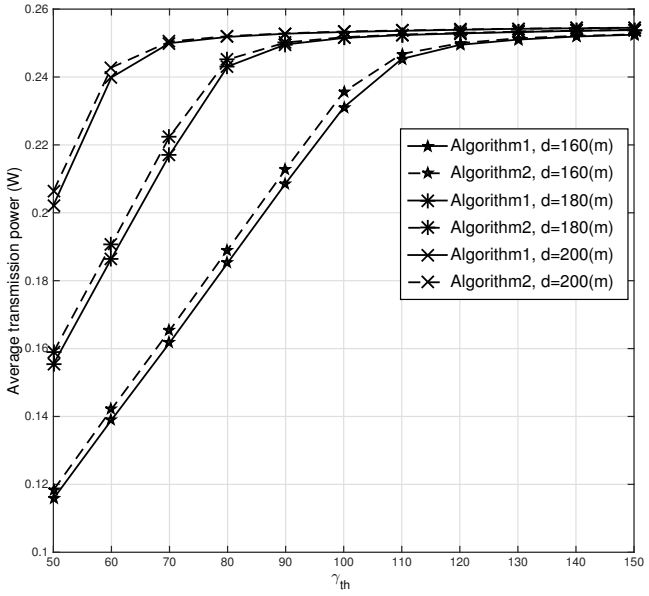

Figure 4.12: No-overhearing, average power versus γ_{th}, $\overline{p}_{\max} = 0.25$, $M = 6$, $K = 8$, $B_{\max} = 20$

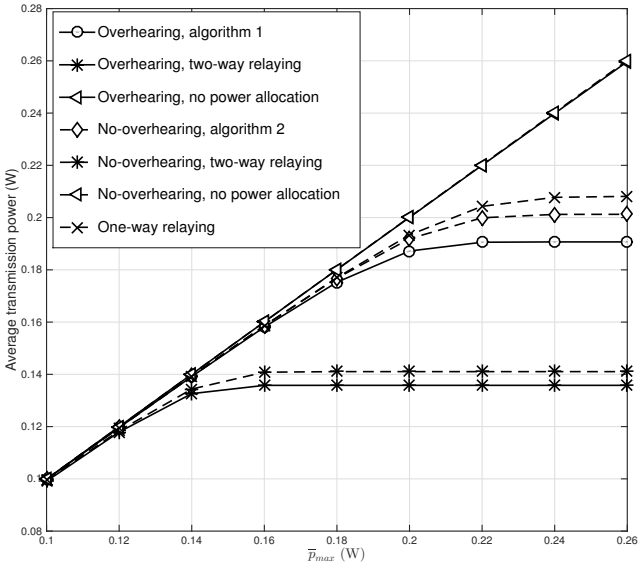

Figure 4.13: Average power versus $\overline{p}_{\max}$ for different schemes, $M = 2$, $K = 8$, $B_{\max} = 20$

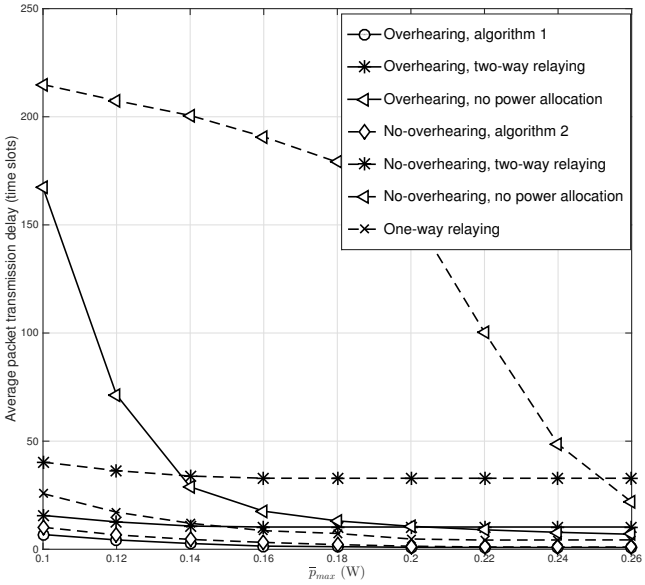

(a)

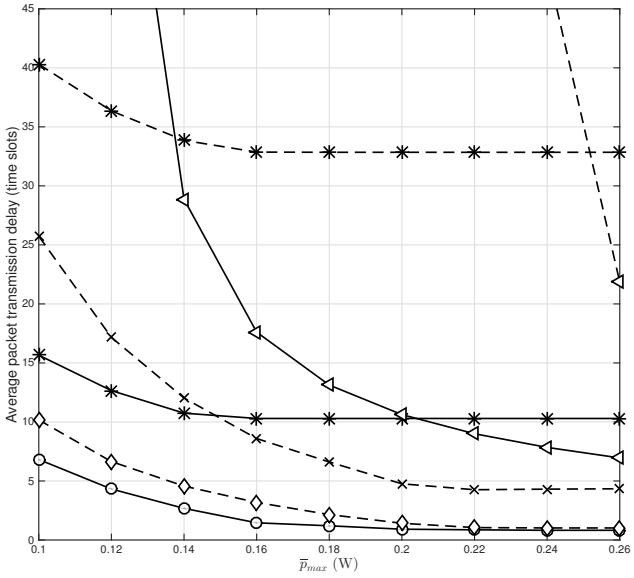

(b) Larger view of part (a) for average packet delay below 45 time slots

Figure 4.14: Average delay versus $\overline{p}_{\max}$ for different schemes, $M = 2$, $K = 8$, $B_{\max} = 20$

4.5 Summary

We have studied packet transmission scheduling and power allocation in a network of bidirectional relaying links. A CMDP model has been developed, which finds the optimum strategy for combining packets into one transmission as well as the transmission power of the relay node, given the maximum and average transmission power limits. Heuristic schemes are designed, one for the general case of overhearing, and another for the no-overhearing case. Our results indicate that the proposed schemes can closely follow the transmission power constraints, while providing close-to-optimum average transmission delay under some conditions. Furthermore, the overhearing condition does not very much affect the average transmission power of the relay node, but does affect the packet transmission delay performance.

Our work in Chapters 2-4 has demonstrated that by using network coding, which is one of the typical applications of taking advantage of the broadcast nature of wireless communications, network performance can be improved in different aspects. On the other hand, broadcast does bring some negative features to network resource utilization and QoS provisioning, one of which is that if a transmission is to reach multiple receivers, the weakest link always limits the performance, and such constraint becomes even more complicated when co-channel interference exists. We will study resource allocations in one of this type applications in the next chapter.

Chapter 5

Resource Allocation in Multicast Device-to-Device Communications Underlaying LTE Networks

In the previous three chapters, we have seen that taking advantage of the broadcast feature of wireless communications by using network coding and opportunistic scheduling can improve the network performance. On the other hand, co-channel interference caused by the broadcast nature of the wireless channel is a fundamental issue since it degrades the QoS of a wireless network. In this chapter, we present a framework for resource allocations in multicast device-to-device (D2D) communications underlaying a cellular network, where a number of D2D multicast groups share the channels with the cellular users (CUs). Our focus is on transmission power of the D2D transmitters and CUs, so that co-channel interference is controlled and total transmission throughput of the D2D groups and the CUs is maximized. We will start with a brief survey on D2D communications underlaying cellular networks and related

work on resource allocations, and then introduce our proposed work.

5.1 Background and Related Works

D2D communication is a technology component for Long Term Evolution-Advanced (LTE-A) of the Third Generation Partnership Project (3GPP) [82]. In D2D communication, CUs in proximity can exchange information over a direct link rather than transmitting and receiving signals through a cellular base station (BS). D2D users communicate directly while remaining controlled under the BS. Compared to routing through a BS, CUs in proximity can save energy and resources when communicating directly with each other. Moreover, D2D users may experience high data rate and low transmission delay due to the short-range direct communication [83]. Reducing the network load by offloading cellular traffic from the BS and other network components to a direct path between users is another benefit of D2D communication that can reduce the network load and increase its effective capacity. Other benefits and usage cases are discussed in [84].

The majority of the literature in D2D communications uses the cellular spectrum for both D2D and cellular communications, also known as in-band D2D [85]. Generally, in-band D2D falls into two categories, underlay and overlay [86]. Underlay in-band D2D can improve the spectrum efficiency of cellular networks by reusing cellular resources. Its main drawback lies in the interference caused by D2D users to cellular communications. Thus, efficient interference management and resource allocation are required to guarantee a target performance level of the cellular communication [87, 88]. In order to avoid this interference issue, it has also been proposed to dedicate part of the cellular resources to D2D communications in overlay in-band

D2D. In this case, designing a resource allocation scheme is crucial to maximize the utilization of dedicated cellular resources [89]. Other works consider out-of-band instead of in-band D2D communications so that the cellular spectrum would not be affected by D2D communications [90]. Out-of-band D2D communication faces challenges in coordinating the communication over two different bands because usually D2D communication happens on a second radio interface (e.g., WiFi Direct and Bluetooth) [91].

Most of the work in D2D resource allocation targets the unicast scenario where a single or multiple D2D pairs reuse the resources of CUs. In [85], the authors consider throughput maximization where by allowing D2D communication to underlay the cellular network, the overall throughput in the network can be increased compared to the case where all D2D traffic is relayed by the cellular network. Some other works such as [91], [92] consider D2D communication reliability while guaranteeing a certain level of SINR or outage probability. The works in [93–95] consider both throughput and reliability simultaneously. In [93], throughput is maximized for a network with a single D2D pair and a single CU subject to spectral efficiency restrictions and energy constraints. There are only a few works dealing with scenarios with multiple D2D users and CUs. For example, the quality-of-service (QoS) requirements for both CUs and D2D users have been investigated in [94] and [95]. In [94], a heuristic algorithm has been proposed to solve the MINLP resource allocation problem that aims to decrease interference to the cellular network and maximize the total throughput. The authors in [95] present a framework of resource allocation for D2D communications underlaying cellular networks to maximize the overall network throughput of existing CUs and admissible D2D pairs while guaranteeing the QoS requirements for both CUs

and D2D pairs. A scheme based on maximum weight bipartite matching is proposed to determine a specific CU partner for each admissible D2D pair.

Multicast D2D transmissions, where the same packets for a UE are sent to multiple receivers, are important for scenarios such as multimedia streaming, device discovery, and public safety. Especially, D2D multicast communications are required features in public safety services like police, fire, and ambulance [82]. Compared to communicating with each receiver separately in unicast D2D, multicast D2D transmission reduces overhead and saves resources. However, unlike the more commonly studied unicast D2D (see e.g. [93] [95]), multicast D2D has its own challenges. Within a multicast group, the data rates attainable at different receivers are different because of the diverse link conditions between each receiver and the transmitter. A common approach is to transmit at the lowest rate of all users within a group determined by the user with the worst channel condition. This assures that multicast services can be provided to all users. On the one hand, as all multicast users within a group receive the same data rate, the total sum rate grows with the number of active users of the group. On the other hand, the lowest transmission rate typically decreases as the number of users increases since it is based on the user with the Least Channel Gain (LCG) [96].

As discussed in [96] there are lots of works in multicast scheduling and resource allocation for OFDMA-based systems. They can be broadly classified into two types: single-rate and multi-rate transmissions. In single-rate broadcast, the BS transmits to all users in each multicast group at the same rate irrespective of their non-uniform achievable capacities, whereas in multirate broadcast, the BS transmits to each user in each multicast group at different rates based on what each user can handle. All of the

works mentioned in [96] targeted cellular networks where the multicast transmitter is the BS. However, in multicast D2D, UEs are multicast transmitters and the QoS requirements for both the D2D links and the cellular links should be satisfied.

In this chapter, we consider multicast D2D communications underlaying cellular networks and present a joint power and channel allocation scheme to maximize the total throughput of all CUs and D2D groups within a cell. We formulate the general problem of power and channel allocation as an MINLP where one D2D group can reuse the channels of multiple CUs and the channel of each CU can be reused by multiple D2D groups. To guarantee the QoS requirements for both CUs and D2D groups, a minimum SINR constraint is imposed. A variant of the generalized bender decomposition (GBD) is applied to optimally solve the MINLP problem. We further propose an exact solution to a special case of the general problem. Specifically, inspired by the work in [95], we use the maximum weight bipartite matching algorithm for the case where each D2D group can reuse the channel of at most one CU and each CU can share their resources with at most one D2D group. Next, we propose a greedy algorithm with a somewhat high complexity but close-to-optimal performance. A low-complexity heuristic solution is then devised that trades computation complexity with performance.

The remainder of the chapter is organized as follows. In Section 5.2, the system model is described and the problem of power and channel allocation for underlay multicast D2D communication is formulated. Section 5.3 describes the generalized bender decomposition method to solve the general problem, and the solution is given in Section 5.4. The matching-based optimal resource allocation for one special case is presented in Section 5.4, and the greedy and the heuristic algorithms are presented

in Section 5.5. Numerical results are demonstrated in Section 5.6, and Section 5.7 concludes the chapter.

5.2 System Model and Problem Formulation

We study resource allocation for D2D group communications underlaying uplink (UL) transmissions in LTE networks. UL resource sharing is considered since reusing downlink resources is more difficult and less effective than reusing uplink resources in the worst case of a fully loaded cellular network, as demonstrated in [97]. Consider K groups of D2D group users coexisting with M CUs. We assume a fully loaded cellular network. That is, there are M channels, each occupied by one CU. We use $m \in \mathcal{M} = \{1, 2, \ldots, M\}$ to index both the mth CU and the channel it occupies, and $k \in \mathcal{K} = \{1, 2, \ldots, K\}$ to index the kth D2D group. We consider a single cell scenario and assume that advanced intercell interference mitigation is applied on top of our scheme. Also, we assume that each CU sends the channel information between itself and D2D receivers through control channels to the BS. Within a D2D group, there is only one user that multicasts messages to the remaining users. Each D2D user only belongs to one D2D group. We use $\mathcal{D}_k$ to represent the set of D2D receivers in the kth multicast group, and $|\mathcal{D}_k|$ is the total number of receivers in the group. As a special case, when $|\mathcal{D}_k| = 1$, the scenario becomes unicast.

Define a set of binary variables y_{km} with $y_{km} = 1$ if the kth D2D group reuses channel m, and $y_{km} = 0$ otherwise. In the general case, each D2D group splits its multicast traffic among maximally C_1 channels, and each channel can be reused by

at most C_2 D2D groups, where $C_1 \leq M$ and $C_2 \leq K$. That is,

$$\sum_{m=1}^{M} y_{k,m} \leq C_1, \ \forall k \in \mathcal{K}, \tag{5.1}$$

$$\sum_{k=1}^{K} y_{k,m} \leq C_2, \ \forall m \in \mathcal{M}. \tag{5.2}$$

The channel quality of receiver d in the kth D2D group at channel m is given by

$$\beta_{k,m,d}^{D2D} = \frac{G_{k,m,d}^{D2D}}{P_{noise} + P_m^{Cell} G_{k,m,d}^{C2D} + \sum_{k' \neq k} P_{k',m}^{D2D} G_{k,k',d}^{D2D}}, \forall k \in \mathcal{K}, \ m \in \mathcal{M}, d \in \mathcal{D}_k, \tag{5.3}$$

where P_{noise} is the aggregate power of background noise, $G_{k,m,d}^{D2D}$ is the link gain to D2D receiver d from the D2D transmitter in group k over channel m, $G_{k,m,d}^{C2D}$ is the link gain from CU m to D2D receiver d in group k, P_m^{Cell} is the transmission power of CU m, $P_{k,m}^{D2D}$ is the transmission power of the kth D2D group transmitter at channel m, and $G_{k,k',d}^{D2D}$ the link gain from the transmitter at D2D group k' to receiver d at D2D group k.

For the kth D2D group, its transmission condition in channel m is determined by the receiver with the worst condition. Define

$$\beta_{k,m}^{D2D} = \min_{d \in \mathcal{D}_k} \beta_{k,m,d}^{D2D}. \tag{5.4}$$

Then, the normalized transmission rate (bit/s/Hz) of the kth D2D group is given by

$$r_k^{D2D} = \sum_{m=1}^{M} y_{k,m} \log_2(1 + P_{k,m}^{D2D} \beta_{k,m}^{D2D}). \tag{5.5}$$

The aggregate transmission rate of the kth D2D group is given by

$$R_k^{D2D} \leq |\mathcal{D}_k| r_k^{D2D} \tag{5.6}$$

$$= \sum_{m=1}^{M} y_{k,m} |\mathcal{D}_k| \log_2(P_{k,m}^{D2D} \beta_{k,m}^{D2D}). \tag{5.7}$$

For CU m, its channel quality is given by

$$\beta_m^{Cell} = \frac{G_m^{Cell}}{P_{noise} + \sum_{k=1}^{K} y_{k,m} P_{k,m}^{D2D} G_{k,m}^{D2C}}, \tag{5.8}$$

where G_m^{Cell} is the link gain of CU m to the cellular base station, and $G_{k,m}^{D2C}$ is the link gain from the kth D2D transmitter to the cellular base station at channel m. Therefore, the normalized transmission rate for CU m is

$$R_m^{Cell} \leq \log_2(1 + P_m^{Cell} \beta_m^{Cell}). \tag{5.9}$$

A threshold is set for the SINR of each D2D group and CU transmission. For the kth D2D group,

$$P_{k,m}^{D2D} \beta_{k,m}^{D2D} \geq y_{k,m} \gamma_{th}^{D2D}, \tag{5.10}$$

and for CU m,

$$P_m^{Cell} \beta_m^{Cell} \geq \gamma_{th}^{Cell}. \tag{5.11}$$

Given these SINR threshold constraints, we can approximate the capacity in higher SINR regimes by removing the term "1" from the logarithm functions in both (5.5)

and (5.9). The maximum power constraints for CUs and D2D groups, respectively, are given by

$$P_m^{Cell} \leq P_{\max}^{Cell},\ \forall m \in \mathcal{M}, \tag{5.12}$$

and

$$\sum_{m=1}^{M} P_{k,m}^{D2D} \leq P_{\max}^{D2D},\ \forall k \in \mathcal{K}. \tag{5.13}$$

The objective is to maximize the aggregate data transmission rate of all the D2D groups and CUs. Combining (5.1) – (5.13), we formulate the joint power control and channel allocation problem to maximize the sum throughput of D2D group groups and cellular users as follows,

$$\text{P1.} \quad \max \left(\sum_{k=1}^{K} R_k^{D2D} + \sum_{m=1}^{M} R_m^{Cell} \right) \tag{5.14}$$

$$\text{s.t.} \quad \beta_{k,m}^{D2D} \leq \beta_{k,m,d}^{D2D},\ \forall k \in \mathcal{K}, m \in \mathcal{M},\ d \in \mathcal{D}_k, \tag{5.15}$$

$$y_{k,m} \in \{0,1\},\ \forall k \in \mathcal{K}, m \in \mathcal{M}, \tag{5.16}$$

$$\text{Constraints(5.1)-(5.3), (5.7)-(5.13).}$$

Table 5.1 lists all the parameters and variables used in the problem formulation.

Clearly, P1 is a Mixed Integer Nonlinear Programming (MINLP) problem. In general, MINLP problems are NP-hard and thus no efficient polynomial-time solutions exist. In the general case, when C_1 and C_2 are arbitrary values, we will use GBD [98] to solve the problem optimally in the next section.

Based on the values of C_1 and C_2, several special cases exist. For example, when $C_1 = 1$ and $C_2 = 1$, each D2D group can reuse the channels of at most one CU and each CU can share their channels with at most one D2D group. Another special case

of interest is when $C_2 = 1$. In this case, to increase the spectrum utilization, we allow each D2D group to reuse the resources of multiple CUs, but each CU cannot share its resource with more than one D2D group. Here, there is no interference among D2D groups and this setting is useful when the number of D2D groups is much less than the number of CUs. All the special cases can be resolved via GBD. However, it turns out that a polynomial algorithm can be devised when $C_1 = 1$ and $C_2 = 1$ as will be discussed in Section 5.4.

It is worth mentioning that channel measurement is an indispensable component of resource allocations in D2D communications. Depending on the control mode, the measurement results may be reported to the BS or the mobile users. First, the BS should collect all required channel information in order to allocate channels to each D2D group and find the transmission power for all transmitters. After that, the calculated power values need to be passed to individual transmitters, and the channel allocation information should be passed to the D2D transmitters. Collecting the channel information between a mobile user and the BS and between two mobile users can be performed during the device discovery process using the discovery signal. The overhead can be reduced for short and low mobility user to user or BS to user links as the channel should have fewer taps and vary slowly.

Table 5.1: Table of notations

Notation	**Description**
$\mathcal{M}$	Set of cellular users (CU)
$\mathcal{K}$	Set of D2D groups
$\mathcal{D}_k$	Set of receivers in kth D2D group
$\mathcal{A}$	Set of admissible or successful D2D groups
$y_{k,m}$	Binary variable, =1 if kth D2D group reuses CU m's channel, and =0 otherwise
C_1	Maximum number of channels to be reused by each D2D group
C_2	Maximum number of D2D groups sharing each CU channel
P_{noise}	Aggregate power of background noise
$G^{D2D}_{k,m,d}$	Link gain to D2D receiver d from D2D transmitter in group k at channel m
$G^{C2D}_{k,m,d}$	Link gain from CU m to D2D receiver d in group k
$G^{D2D}_{k,k',d}$	Link gain from the transmitter at D2D group k' to receiver d at D2D group k
G^{Cell}_{m}	Link gain of CU m to the cellular BS
$G^{D2C}_{k,m}$	Link gain from the kth D2D transmitter to the cellularBS at channel m
$P^{D2D}_{k,m}$	Transmission power of the kth D2D group transmitter at channel m
P^{Cell}_{m}	Transmission power of CU m
$\beta^{D2D}_{k,m,d}$	Channel quality of receiver d in the kth D2D group at channel m
β^{Cell}_{m}	Channel quality of CU m
R^{D2D}_{k}	Normalized transmission rate of the kth D2D group
R^{Cell}_{m}	Normalized transmission rate for CU m
R^{sum}	The summation of D2D and cellular throughput
γ^{D2D}_{th}	SINR threshold for all D2D groups
γ^{Cell}_{th}	SINR threshold for all CUs
$f_i(\lvert\mathcal{D}_\mathcal{K}\rvert)$	The complexity of solving problem Pi

5.3 Generalized Bender Decomposition

The MINLP problem in P1 has the special property that when the binary variables ($y_{k,m}$'s) are fixed, the problem becomes a geometric programming problem with continuous variables ($P_{k,m}^{D2D}$'s and P_m^{Cell}'s), which can be transformed to a convex problem. A well-known solution to this type of problems is GBD [98]. However, non-trivial transformations are needed to ensure the separability of the problem with respect to the binary variables. This allows efficient solutions using GBD with guaranteed convergence. We next discuss the details of the proposed solution to P1.

5.3.1 Problem transformation

Let $\mathcal{X} = [P_{k,m}^{D2D}, P_m^{Cell}, R_k^{D2D}, R_m^{Cell}, \beta_{k,m}^{D2D}, \beta_m^{Cell}, k \in \mathcal{K}, m \in \mathcal{M}]$ represent the set of all continuous variables and $\mathcal{Y} = [y_{k,m}, k \in \mathcal{K}, m \in \mathcal{M}]$ represent the binary variables. We modify the constraints in problem P1 to separate binary variables $\forall y \in \mathcal{Y}$ from the continuous variables $\forall x \in \mathcal{X}$ and make the problem linear in terms of y's when the continuous variables are fixed. Problem P1 can be transformed to

$$\text{P2.} \quad \max_{x\in\mathcal{X}, y\in\mathcal{Y}} f(x,y) = \max\left(\sum_{k=1}^{K} R_k^{D2D} + \sum_{m=1}^{M} R_m^{Cell}\right) \tag{5.17}$$

$$\text{s.t.} \quad \beta_{k,m}^{D2D} \leq \frac{G_{k,m,d}^{D2D}}{P_{noise}+P_m^{Cell}G_{k,m,d}^{C2D}+\sum_{k'\neq k} P_{k',m}^{D2D}G_{k,k',d}^{D2D}}, \forall k \in \mathcal{K}, m \in \mathcal{M},\ d \in \mathcal{D}_k, \tag{5.18}$$

$$R_k^{D2D} \leq \sum_{m=1}^{M} \left[|\mathcal{D}_k| \log_2(P_{k,m}^{D2D}\beta_{k,m}^{D2D}) + C(1-y_{k,m})\right], \forall k \in \mathcal{K} \tag{5.19}$$

$$|\mathcal{D}_k| \log_2(P_{k,m}^{D2D}\beta_{k,m}^{D2D}) + C(1-y_{k,m}) \leq Cy_{k,m}, \forall k \in \mathcal{K}, m \in \mathcal{M}, \tag{5.20}$$

$$\beta_m^{Cell} \leq \frac{G_m^{Cell}}{P_{noise} + \sum_{k=1}^{K} P_{k,m}^{D2D}G_{k,m}^{D2C}},\ \forall m \in \mathcal{M}, \tag{5.21}$$

$$\frac{P_{k,m}^{D2D}}{P_{\max}^{D2D}} \leq y_{k,m} + \epsilon \leq CP_{k,m}^{D2D},\ \forall k \in \mathcal{K}, m \in \mathcal{M}, \tag{5.22}$$

$$y_{k,m} \in \{0,1\},\ \forall k \in \mathcal{K}, m \in \mathcal{M}, \tag{5.23}$$
$$\text{Constraints } (5.1)-(5.2) \text{ and } (5.9)-(5.13),$$

where C is a very large number and $\epsilon > 0$ is a very small number. Constraint (5.18) combines constraints (5.3) and (5.15) in problem P1. Constraints (5.19) and (5.20) together are equivalent to constraint (5.7) in problem P1. In (5.19), when $y_{k,m} = 1$, the second term in the summand, namely, $1 - y_{k,m}$ is zero, and the sum of the two terms inside the summation is the same as the term inside the summation on the right-hand side in (5.7) for the same k and m. When $y_{k,m} = 0$, second term in the summand (5.19) is a large number, and the constraint is automatically satisfied; while constraint (5.20) guarantees that the corresponding rate for the kth D2D group at channel m is zero when the channel is not allocated to the D2D group.

The introduction of constraint (5.22) makes $P_{k,m}^{D2D}$ very small whenever $y_{k,m}$ is zero. This eliminates the binary variables $y_{k,m}$ in (5.8) and results in constraint (5.21). To this end, we have obtained in P2 a geometric MINLP problem with separable continuous and binary variables.

5.3.2 Solution Using GBD

The basic idea of GBD is to decompose the original MINLP problem into a primal problem and a master problem, and solve them iteratively. The primal problem corresponds to the original problem with fixed binary variables. Solving this problem provides the information about the lower bound and the Lagrange multipliers corresponding to the constraints. The master problem is derived through nonlinear duality

theory using the Lagrange multipliers obtained from the primal problem. The solution to the master problem gives the information about the upper bound as well as the binary variables that can be used in the primal problem in next iteration. When the upper bound meets the lower bound, the iterative process converges.

Primal problem The primal problem results from fixing the $y_{k,m}$ variables to a particular 0-1 combination denoted by $y_{k,m}^{(i)}$, where i stands for the iteration counter. After replacing the variable $y_{k,m}$ with its current value in problem P2, the formulation for the primal problem at iteration i is given by

$$\text{P3.} \quad \max_{x\in\mathcal{X},y\in\mathcal{Y}} f(x,y^{(i)}) = \max\left(\sum_{k=1}^{K} R_k^{D2D} + \sum_{m=1}^{M} R_m^{Cell}\right) \tag{5.24}$$

$$\text{s.t.} \quad \beta_{k,m}^{D2D} \leq \frac{G_{k,m,d}^{D2D}}{P_{noise}+P_m^{Cell}G_{k,m,d}^{C2D}+\sum_{k'\neq k} P_{k',m}^{D2D}G_{k,k',d}^{D2D}}, \forall k\in\mathcal{K}, m\in\mathcal{M},\ d\in\mathcal{D}_k, \tag{5.25}$$

$$R_k^{D2D} \leq \sum_{m=1}^{M}\left[|\mathcal{D}_k|\log_2(P_{k,m}^{D2D}\beta_{k,m}^{D2D}) + C(1-y_{k,m}^{(i)})\right], \forall k\in\mathcal{K}, \tag{5.26}$$

$$|\mathcal{D}_k|\log_2(P_{k,m}^{D2D}\beta_{k,m}^{D2D}) + C(1-y_{k,m}^{(i)}) \leq Cy_{k,m}^{(i)}, \forall k\in\mathcal{K}, m\in\mathcal{M}, \tag{5.27}$$

$$\beta_m^{Cell} \leq \frac{G_m^{Cell}}{P_{noise}+\sum_{k=1}^{K} P_{k,m}^{D2D}G_{k,m}^{D2C}},\ \forall m\in\mathcal{M}, \tag{5.28}$$

$$\frac{P_{k,m}^{D2D}}{P_{\max}^{D2D}} \leq y_{k,m}^{(i)} + \epsilon \leq CP_{k,m}^{D2D},\ \forall k\in\mathcal{K}, m\in\mathcal{M}, \tag{5.29}$$

$$P_{k,m}^{D2D}\beta_{k,m}^{D2D} \geq y_{k,m}^{(i)}\gamma_{th}^{D2D},\ \forall k\in\mathcal{K}, m\in\mathcal{M}, \tag{5.30}$$

Constraints (5.9), (5.11), (5.12), (5.13).

Since the optimal solution to this problem (if exists) is also a feasible solution to problem P1, the optimal value $f(x^*, y^{(i)})$ provides a lower bound to the original problem. In general, not all choices of binary variables lead to a feasible primal problem. Therefore, for a given choice of $y_{k,m}$'s, there are two cases for primal problem

P3: feasible problem and infeasible problem. In the following, we consider each of these cases.

- Feasible Primal: If the primal problem at iteration i is feasible, its solution provides information on the transmission power of D2D and cellular transmitters, $f(x^*, y^{(i)})$, and the optimal multiplier vectors, $\lambda_q^{(i)}$, $q = 1, 2, \ldots, Q$ for the Q inequality constraints in Problem P3. Subsequently, using this information we can formulate the Lagrange function for all inequality constraints $G_q(x, y^{(i)}) \leq 0$ for $q = 1, 2, \ldots, Q$ as

$$L(x, y^{(i)}, \lambda^{(i)}) = f(x, y^{(i)}) + \sum_{q=1}^{Q} \lambda_q^{(i)} G_q(x, y^{(i)}), \tag{5.31}$$

  where $\lambda^{(i)} = [\lambda_q^{(i)}, q = 1, 2, \ldots, Q]$.

- Infeasible Primal: If the primal problem is infeasible, to identify a feasible point we can formulate an l_1-minimization problem as

$$\text{P3.1.} \quad \min \sum_{q=1}^{Q} \alpha_q \tag{5.32}$$

$$\text{s.t.} \quad G_q(x, y^{(i)}) \leq \alpha_q, q = 1, 2, ..., Q, \tag{5.33}$$

$$\alpha_q \geq 0, q = 1, 2, ..., Q. \tag{5.34}$$

  Note that if $\sum_{q=1}^{Q} \alpha_q = 0$, then P3 is feasible. Otherwise, the solution to this feasibility problem (FP) provides information on the Lagrange multipliers, denoted as $\bar{\lambda}_q^{(i)}$; the Lagrange function resulting from the feasibility problem at

iteration i can be defined as

$$\bar{L}(x, y^{(i)}, \bar{\lambda}^{(i)}) = \sum_{q=1}^{Q} \bar{\lambda}_q^{(i)} (G_q(x, y^{(i)}) - \alpha_q). \tag{5.35}$$

It is worth mentioning that two different types of Lagrange functions are calculated depending on whether the primal problem is feasible or infeasible. Also, the lower bound is obtained only from the feasible primal problem.

Master Problem The master problem is derived from the non-linear duality theory [98]. The original problem P2 can be written as:

$$\begin{aligned} &\max_{y \in \mathcal{Y}} \sup_{x \in \mathcal{X}} f(x, y) \\ \text{s.t.} \quad &G_q(x, y) \leq 0, q = 1, 2, ..., Q. \end{aligned} \tag{5.36}$$

Let also define set $\mathcal{V}$ as

$$\mathcal{V} = \{y : G_q(x, y)) \leq 0 \text{ for some } x \in \mathcal{X}\}. \tag{5.37}$$

Using the Lagrange function in (5.31) and duality theory, we obtain

$$\begin{aligned} \max f(x, y^{(i)}) &= \max_{y^{(i)}} (\min_{\lambda^{(i)}} \sup_{x} L(x, y^{(i)}, \lambda^{(i)}), \\ &= \max \eta \\ \text{s.t. } \eta &\leq \sup_{x} L(x, y^{(i)}, \lambda^{(i)}), \ \forall \lambda \geq 0, \\ y^{(i)} &\in \mathcal{Y} \cap \mathcal{V} \end{aligned} \tag{5.38}$$

It is shown in [98] that a point $y \in \mathcal{Y}$ belongs also to the set $\mathcal{V}$ if and only if they satisfy the following system:

$$\inf_{x} \bar{L}(x, y^{(i)}, \bar{\lambda}^{(i)}) \leq 0, \ \forall \bar{\lambda}^{(i)} \in \Lambda, \tag{5.39}$$

where

$$\Lambda = \left\{ \bar{\lambda}_q \geq 0, \sum_{q=1}^{Q} \bar{\lambda}_q = 1 \right\}.$$

Substituting (5.39) for $y \in \mathcal{Y} \cap \mathcal{V}$ into (5.38) we can make the constraints over set $\mathcal{V}$ explicit and obtain the following master problem:

$$\text{P4.} \quad \max_{y^{(i)} \in \mathcal{Y}} \eta \tag{5.40}$$

$$\text{s.t.} \quad \eta \leq \sup_{x} L(x, y^{(i)}, \lambda^{(i)}), \ \forall \lambda^{(i)} \geq 0, \tag{5.41}$$

$$\inf_{x} \bar{L}(x, y^{(i)}, \bar{\lambda}^{(i)}) \leq 0, \ \forall \bar{\lambda}^{(i)} \in \Lambda, \tag{5.42}$$

$$\text{Constraints (5.1), (5.2).}$$

The master problem P4 is similar to the original problem P2, but has two inner optimization problems that need to be considered for all λ and $\overline{\lambda}$ obtained from the primal problem in every iteration. Therefore, it has a very large number of constraints. Because of the separability of binary variables $\forall y \in \mathcal{Y}$ and continuous variables $\forall x \in \mathcal{X}$, and the linearity with regard to binary variables, we can adopt Variant 2 of GBD (V2-GBD) in [98]. It is proven in [98] that under the conditions for V2-GBD, the Lagrange function evaluated at the solution of the corresponding primal is a valid under-estimator of the inner optimization problem in P4. Therefore,

the relaxed master problem can be formulated as,

$$\text{P5.} \quad \max_{y^{(i)} \in \mathcal{Y}} \eta \tag{5.43}$$

$$\text{s.t.} \quad \eta \leq L(x, y^{(i)}, \lambda^{(i)}),\ \forall \lambda^{(i)} \geq 0, \tag{5.44}$$

$$\bar{L}(x, y^{(i)}, \bar{\lambda}^{(i)}) \leq 0,\ \forall \bar{\lambda}^{(i)} \in \Lambda, \tag{5.45}$$

$$\text{Constraints (5.1), (5.2).}$$

The relaxed problem provides an upper bound to the master problem and can be used to generate the primal problem in the next iteration.The same procedure is then repeated until convergence. Over the iterations, the sequence of upper bounds are non-increasing and the set of lower bounds are non-decreasing. The two sequences are proven to converge, and the algorithm will stop at the optimal solution within a finite number of iterations [99]. Algorithm 1 summarizes the GBD procedure.

Algorithm 1 GBD Algorithm

First iteration, $i = 1$
Select an initial value for $y^{(i)}$, which makes the primal problem feasible.
Solve the primal problem in P3 and obtain the Lagrange function
$UBD^{(i)} = \infty$, $LBD^{(i)} = 0$
while $UBD^{(i)} - LBD^{(i)} > 0$ **do**
    $i = i + 1$
    Solve the relaxed master problem P5 to obtain η^* and y^*
    Set $UBD^{(i)} = \eta^*$
    Solve the primal problem P3 with fixed $y^{(i)} = y^*$
    if the primal problem is feasible **then**
        Obtain optimal solution x^* and the Lagrange function $L(y, y^{(i)}, \lambda^{(i)})$
        Set $LBD^{(i)} = \max(LBD^{(i-1)}, f^{(i)}(x^*, y^{(i)}))$
    else
        Solve the feasibility-check problem P3.1 to obtain the optimal solution x^* and the Lagrange function $\bar{L}(x, y^{(i)}, \bar{\lambda}^{(i)})$
    end if
end while

5.4 Matching-based Optimal Resource Allocation

In this section, we consider the MINLP problem in P1 for the special case $C_1 = 1$ and $C_2 = 1$. This case can be cast as a bipartite matching problem and thus can be solved polynomially. To formulate the bipartite problem, we divide P1 into two subproblems. In the first step, for each D2D group k and each CU m, we find their transmission power so that the sum throughput of the D2D group and the CU is maximized. If this problem is feasible, D2D group k is allowed to reuse the channel of CU m and is marked as a candidate partner in the second step; otherwise group k is excluded from the list of feasible partners. The second step is then to find the best CU partner for each D2D group among all feasible candidates so that the total throughput of all D2D groups and CUs is maximized.

Feasibility check and power allocation

In order to determine whether D2D group k can reuse channel m and to find the transmission power of the feasible D2D group and CU, we have problem P6 as follows:

$$\text{P6.} \quad \max \left(R_{k,m}^{D2D} + R_{k,m}^{Cell}\right) \tag{5.46}$$

$$\text{s.t.} \quad R_{k,m}^{D2D} = |\mathcal{D}_k| \log_2(P_{k,m}^{D2D} \beta_{k,m}^{D2D}), \tag{5.47}$$

$$R_{k,m}^{Cell} = \log_2 \left(P_m^{Cell} \beta_m^{Cell}\right), \tag{5.48}$$

$$P_{k,m}^{D2D} \beta_{k,m}^{D2D} \geq \gamma_{th}^{D2D}, \tag{5.49}$$

$$P_m^{Cell} \beta_m^{Cell} \geq \gamma_{th}^{Cell}, \tag{5.50}$$

$$\beta_m^{Cell} = \frac{G_m^{Cell}}{P_{noise} + P_{k,m}^{D2D} G_{k,m}^{D2C}}, \tag{5.51}$$

$$\beta_{k,m}^{D2D} \leq \frac{G_{k,m,d}^{D2D}}{P_{noise} + P_m^{Cell} G_{k,m,d}^{C2D}}, \ \forall d \in \mathcal{D}_k, \tag{5.52}$$

$$P_m^{Cell} \leq P_{\max}^{Cell}, \tag{5.53}$$

$$\sum_{m=1}^{M} P_{k,m}^{D2D} \leq P_{\max}^{D2D}. \tag{5.54}$$

P6 is a reduced version of P1 by limiting it to only one D2D group and one CU with the objective of maximizing their sum throughput. Clearly, P6 is a geometric programming problem and can be transformed to a convex optimization problem using geometric programming techniques [100]. We solve problem P6 for all k and m pairs. Define a candidate channel set $\mathcal{C}_k$ for D2D group k. If the problem is feasible, D2D group k is admissible to channel m (i.e., eligible to use channel m), then m is added to $\mathcal{C}_k$. For $m \in \mathcal{C}_k$, denote the optimal throughput for the kth D2D transmitter and the mth CU as $R_{k,m}^{*D2D}$ and $R_{k,m}^{*Cell}$, respectively, and the optimal sum throughput as $R_{k,m}^{sum} = R_{k,m}^{*D2D} + R_{k,m}^{*Cell}$. For $m \notin \mathcal{C}_k$, we set $R_{k,m}^{*D2D} = 0$, $R_{k,m}^{*Cell} = \log_2\left(\frac{P_{\max}^{Cell} G_m^{Cell}}{P_{noise}}\right)$, and thus $R_{k,m}^{sum} = R_{k,m}^{*Cell}$.

Maximizing total throughput

Given the maximum achievable throughput for each D2D group when reusing each cellular channel, to find the optimal channel allocation that maximizes the total throughput we have,

$$\text{P7.} \quad \max_{y_{k,m}} \sum_{k=1}^{K} \sum_{m=1}^{M} y_{k,m} R_{k,m}^{sum} \tag{5.55}$$

$$\text{s.t.} \quad \sum_{k=1}^{K} y_{k,m} \leq 1, \ \forall m \in \mathcal{M}, \tag{5.56}$$

$$\sum_{m=1}^{M} y_{k,m} \leq 1, \ \forall k \in \mathcal{K}, \tag{5.57}$$

$$y_{k,m} \in \{0,1\}, \ \forall k \in \mathcal{K}, \ m \in \mathcal{M}. \tag{5.58}$$

P7 is in effect the maximum weight bipartite matching problem, where the D2D groups and the cellular channels are two groups of vertices in the bipartite graph, and the edge connecting D2D group k and channel m has a weight $R_{k,m}^{sum}$. The Hungarian algorithm [101] can be used to solve the bipartite matching problem in polynomial time.

To determine the computational complexity, consider $M \geq K$ and the complexity of solving P6 is a function of the size of each D2D group, denoted as $f_6(|\mathcal{D}_\mathcal{K}|)$. Therefore, the time complexity of the matching-based optimal resource allocation is $\mathbf{O}(M \times K \times f_6(|\mathcal{D}_\mathcal{K}|)) + \mathbf{O}(M^3)$, where the first and second terms correspond to the computation time in the first and second steps, respectively.

5.5 Greedy and Heuristic Channel Allocation Algorithms

The MINLP problem in P1 is an NP-hard problem, and the computation complexity grows exponentially with the problem size in the worst case. In other words, GBD may converge in an exponential number of iterations. In this section, we first propose a greedy algorithm and then a heuristic solution to the general MINLP problem in P1.

Algorithm 2 Greedy algorithm

$\mathcal{M}$: Set of cellular users
$\mathcal{K}$: Set of all D2D groups
$e_{k,m} = 1,\ \forall k \in \mathcal{K}, m \in \mathcal{M}$
$Y = [y_{k,m} |\ y_{k,m} = 0,\ \forall k \in \mathcal{K}, m \in \mathcal{M}]$
$\mathcal{S} = \emptyset$
while $\sum_{k=1}^{K} \sum_{m=1}^{M} e_{k,m} \geq 1$ **do**
  $E = [e_{k,m} |\ e_{k,m} = 1,\ \forall k \in \mathcal{K}, m \in \mathcal{M}]$
  $T_{k,m}^{sum} = \sum_{m'=1}^{M} \log_2 \left(\frac{P_{\max}^{Cell} G_{m'}^{Cell}}{P_{noise}} \right),\ \forall k \in \mathcal{K}, m \in \mathcal{M}$
  for each $e_{k,m} \in E$ **do**
    $y_{k,m} = 1$
    if (k, m) is *Admissible* **then**
      Solve P3 to find $P_{k',m'}^{D2D}$ and $P_{m'}^{Cell},\ \forall (k', m') \in [\mathcal{S} \cup (k, m)]$
      if P3 is feasible **then**
        $T_{k,m}^{sum} = \sum_{(k',m') \in [\mathcal{S} \cup (k,m)]} y_{k',m'} |\mathcal{D}_{k'}| \log_2 (P_{k',m'}^{D2D} \beta_{k',m'}^{D2D}) + \sum_{m'=1}^{M} \log_2 \left(P_{m'}^{Cell} \beta_{m'}^{Cell} \right)$
      else
        $e_{k,m} = 0$
      end if
    else
      $e_{k,m} = 0$
    end if
    $y_{k,m} = 0$
  end for
  $(k^*, m^*) = \arg\max_{\forall (k,m)} T_{k,m}^{sum}$
  $y_{k^*,m^*} = 1$
  $e_{k^*,m^*} = 0$
  $\mathcal{S} = \mathcal{S} \cup (k^*, m^*)$
end while

5.5.1 A greedy algorithm

Algorithm 2 shows the greedy resource allocation algorithm. The key idea of the greedy algorithm is that, in each iteration, it selects a CU and D2D group pair that maximizes the resulting sum throughput of all selected pairs. The algorithm terminates when no more pair can be included.

In this algorithm, we first initialize all edges of a $K \times M$ bipartite graph, $e_{k,m}$, to one in line 3. The $K \times M$ assignment matrix $\mathbf{Y}$ is initialized to zero. $\mathcal{S}$ is the set of selected CU and D2D pairs that maximize the sum throughput and are initialized to zero at first. Matrix E includes all edges ($e_{k,m}$) with the value of one. The inner loop (lines 8-23) finds the sum throughput, $T^{sum}_{k,m}$, of all pairs in set $\mathcal{S}$ after an admissible pair (k, m) is added to $\mathcal{S}$. In line 10, to find if (k, m) is *admissible*, the algorithm checks constraints (5.1) and (5.2) for a given (k, m) pair. If either of these constraints is violated for the current (k, m), the procedure sets $e_{k,m}$ and $y_{k,m}$ to zero and moves to the next pair. Otherwise, the algorithm solves problem P3 and finds $T^{sum}_{k,m}$. In the outer loop, the pair (k^*, m^*) that maximizes $T^{sum}_{k,m},\ \forall (k, m) \in \mathcal{S}$ (line 24) is found and removed from E. The outer loop is iterated until $e_{k,m} = 0,\ \forall k \in \mathcal{K}$ and $m \in \mathcal{M}$.

Since a total of $\min\{M \times C_2, K \times C_1\}$ pairs can be found in the procedure, and in each iteration of the outer loop, only one such pair can be added, the computational complexity of the greedy algorithm is $\mathbf{O}(\min\{M \times C_2, K \times C_1\} \times K \times M \times f_3(|\mathcal{D}_\mathcal{K}|))$, where $f_3(|\mathcal{D}_\mathcal{K}|)$ is the complexity of solving P3 as a function of the size of each D2D group. The high complexity of the greedy algorithm mainly arises from the need to solve the optimization problem P3 up to $K \times M$ times to find the best pair in each iteration.

Algorithm 3 Heuristic algorithm

$\mathcal{M}$: List of cellular users in decreasing order of G_m^{Cell}
$\mathcal{K}$: List of all D2D groups
$G_{m,k}^{C2D} = \min_{d \in \mathcal{D}_k} G_{k,m,d}^{C2D},\ \forall k \in \mathcal{K}, m \in \mathcal{M}$
$G_{k,k'}^{D2D} = \min_{d \in \mathcal{D}'_k} G_{k,k',d}^{D2D},\ \forall k \in \mathcal{K}, m \in \mathcal{M}$
$y_{k,m} = 0,\ \forall k \in \mathcal{K}, m \in \mathcal{M}$
$P_m^{Cell} = P_{\max}^{Cell},\ \forall m \in \mathcal{M}$
$P_{k,m}^{D2D} = 0,\ \forall k \in \mathcal{K}, m \in \mathcal{M}$
$m = 1$
while $m \leq M$ **do**
  $\mathcal{K}' = \{\forall k \in \mathcal{K} | \sum_{m=1}^{M} y_{k,m} < C_2\}$
  while $\sum_{k=1}^{K} y_{k,m} < C_1$ or $\mathcal{K}' \neq \emptyset$ **do**
    $k^* = \arg\min_{k \in \mathcal{K}'} \left(\sum_{k'=1}^{K} P_{k',m}^{D2D} G_{k,k'}^{D2D} + P_m^{Cell} G_{m,k}^{C2D} \right)$
    $y_{k^*,m} = 1$
    Solve P3 to find $P_{k^*,m}^{D2D}$ and P_m^{Cell}
    if P3 is feasible **then**
      D2D k^* transmits on channel m
      $y_{k^*,m} = 1$
    else
      $y_{k^*,m} = 0$
    end if
    $\mathcal{K}' = \mathcal{K}' \setminus \{k^*\}$
  end while
  $m = m + 1$
end while

5.5.2 A heuristic algorithm

Since the complexity of the greedy algorithm is high, we propose a heuristic algorithm with less complexity in Algorithm 3. In the following, we explain some intuition behind the algorithm.

To increase cellular and D2D throughputs, it is desirable to have higher SINR. From (3) and (7), it can be deduced that having smaller values of $G^{C2D}_{k,m,d}$ and $G^{D2D}_{k,k',d}$ reduces interference from CU m to D2D group k and from D2D group k to D2D group k', respectively, resulting in higher $\beta^{D2D}_{k,m}$ and D2D throughput. Furthermore, higher values of G^{Cell}_{m} lead to higher cellular throughput. Therefore, Algorithm 3 tries to pair up a CU that has a high link gain to the BS and a D2D group that has low interference to the CU.

Starting from $m = 1$, the outer loop in Algorithm 3 iterates through all CUs. For each m, the algorithm finds at most C_1 best D2D groups to share the channel m in the inner loop. Line 12 shows the criteria for choosing the D2D group that receives the minimum interferences from CU m and all other D2D groups using the same channel. In line 14, based on the current value of $y_{k,m}$, problem P3 is solved to find the optimal transmission power for each CU and D2D group. If P3 is feasible, D2D group k^* will reuse the channel m and we have $y_{k^*,m} = 1$, otherwise $y_{k^*,m} = 0$ in line 20. In both cases, k^* is removed from the D2D group list for the next iteration. The inner loop stops iterating after finding C_1 D2D groups for CU m or after at most K iterations. It is worth mentioning that each D2D group cannot reuse more than C_2 CUs. That is accomplished by introducing $\mathcal{K}'$ that keeps track of all D2D groups with less than C_2 assigned channels in line 10.

In this algorithm, problem P3 is solved $M \times C_1$ times in the worst case, and

thus the complexity of the heuristic algorithm is $\mathbf{O}(M^2) + \mathbf{O}(M \times K \times f_3(|\mathcal{D}_\mathcal{K}|))$. This is much less than the complexity of the greedy algorithm. However, as will be demonstrated in the simulation, the improvement in computation complexity comes at the cost of lower performance.

We summarize the computational complexity of GBD, greedy and heuristic algorithms in Table 5.2 in the worst case.

Table 5.2: Worst case complexity comparison

Algorithm	**Worst Case Complexity**
GBD	Exponential
Greedy	$\mathbf{O}(\min\{M \times C_2, K \times C_1\} \times K \times M \times f_3(\|\mathcal{D}_\mathcal{K}\|))$
Heursitic	$\mathbf{O}(M^2) + \mathbf{O}(M \times K \times f_3(\|\mathcal{D}_\mathcal{K}\|))$

5.6 Performance Evaluation

We consider a single cell network as illustrated in Fig. 5.1, where cellular users are uniformly distributed in the cell. In our evaluation, we only consider the CUs whose SINRs are above the specified threshold before including D2D groups to the cell. The distance-based path loss and slow Rayleigh fading are adopted as the channel model. The probability density function of the instantaneous link gain at any time is given by

$$f_G(x) = \frac{1}{\bar{G}} e^{-x/\bar{G}}, \tag{5.59}$$

where $\bar{G}$ is the average link gain between the transmitter and the receiver and can be calculated based on the distance-based path loss model. The proposed algorithms

have been implemented in Matlab together with the CVX convex optimization package [102]. Default parameters used in the simulations are given in Table 5.3. We run two sets of experiments to evaluate the performance of the proposed algorithms, namely, regularly placed D2D clusters and randomly placed D2D clusters. A larger M is used for the regular placement of users, since the results are collected based on one placement of the users. For the randomly placed users, each result is collected by averaging over a large number of different placements of users. Therefore, each result for the randomly placed users takes much longer time to compute than that for the regular placement. In order to keep the total simulation time to be reasonable, we have to use smaller M in the random placement.

Table 5.3: Default Simulation Parameters

Parameter	**Value**
Cell radius (R)	1 km
Number of D2D receivers in each group	3
P_{noise}	-114 dBm
Pathloss exponent (α)	3
$P_{\max}^{D2D}$	20 dBm
$P_{\max}^{Cell}$	20 dBm
$\gamma_{th} = \gamma_{th}^{Cell} = \gamma_{th}^{D2D}$	10 dB
D2D cluster size(r)	50 m

Regularly placed D2D clusters In Fig. 5.1, D2D groups are manually placed in six different locations and D2D transmitters and receivers are placed in the fixed locations within each group with radius r. This scenario allows us to have a better

understanding of the channel selection for D2D users and how it is impacted by geographical spacing. In the figure, D2D transmitters are labeled with their coordinates. The GBD algorithm finds the CU partner (or equivalent, the CU channel) for each D2D group among 40 CUs when $C_1 = 2$ and $C_2 = 2$. The straight lines in Fig. 5.1 connect D2D groups with their respective CU partners. As shown in the figure, the chosen CU partners, tend to be close to the base station to ensure the rate of the CUs. Meanwhile, the CU partners are away from the respective D2D users to reduce mutual interference between the CUs and the D2D users. Note that even for CUs at the cell edges, their SINR constraints are satisfied as guaranteed by P1.

Fig. 5.2 compares the maximum cellular throughput (without D2D users), $R_{\max}^{Cell}$, the throughput of cellular users (with D2D users), R^{Cell}, and D2D throughput, R^{D2D}, defined as follows,

$$R_{\max}^{Cell} = \sum_{m=1}^{M} \log_2 \left(\frac{P_{\max}^{Cell} G_m^{Cell}}{P_{noise}} \right), \tag{5.60}$$

$$R^{Cell} = \sum_{m=1}^{M} R_m^{Cell}, \tag{5.61}$$

$$R^{D2D} = \sum_{k \in \mathcal{A}} R_k^{D2D}, \tag{5.62}$$

where $\mathcal{A}$ is the set of D2D groups that are allowed to reuse at least one cellular channel. As can be observed in Fig. 5.2, the overall network throughput, $R^{sum} = R^{Cell} + R^{D2D}$, is greater than the maximum throughput before including D2D users, $R_{\max}^{Cell}$. With the introduction of D2D users, the overall throughput increases by 25% to 125%. This comes at the cost of reduced cellular throughput as $R_{\max}^{Cell} > R^{Cell}$ since adding

D2D users causes interference to cellular users and decreases their throughput. However, the reduction is relatively small, compared to the D2D throughput. Moreover, although a larger D2D cluster size leads to lower D2D channel gain and lower D2D throughput, it does not affect the cellular throughput very much.

Fig. 5.3 shows D2D and sum rates versus C_1 for different values of C_2. Both rates increase with C_1 since the number of available channels for each D2D group increases and hence D2D rate increases. However, when $C_2 = 1$, both the D2D and sum rates flatten out after a certain value of C_1. In this case, each CU can serve at most one D2D group, and increasing C_1 does not increase the rate since there are not enough channels to allow all the D2D groups to reuse C_1 channels. Also, from this figure we see that cellular throughput, which is the difference between the sum rate and the D2D rate, decreases as C_1 increases. This is because of the fact that the interference from D2D groups on CUs increases with C_1. On the other hand, increasing C_2 increases the D2D and sum rate for higher values of C_1 since each CU can serve more D2D groups and hence there are more available channels for D2D groups. However, for lower values of C_1, since there are enough CUs in the cell to be reused by D2D groups, increasing C_2 does not change the D2D and sum rates significantly.

Fig. 5.4 shows the convergence of the GBD in Algorithm 1. As it is mentioned in this algorithm, in the first iteration $UBD^{(1)} = \infty$, $LBD^{(1)} = 0$. The second iteration starts with a initial value of $\mathbf{Y}$. It is shown in this figure the LBD results from solving primal problem and the UBD from solving master problem converge in iteration 5.

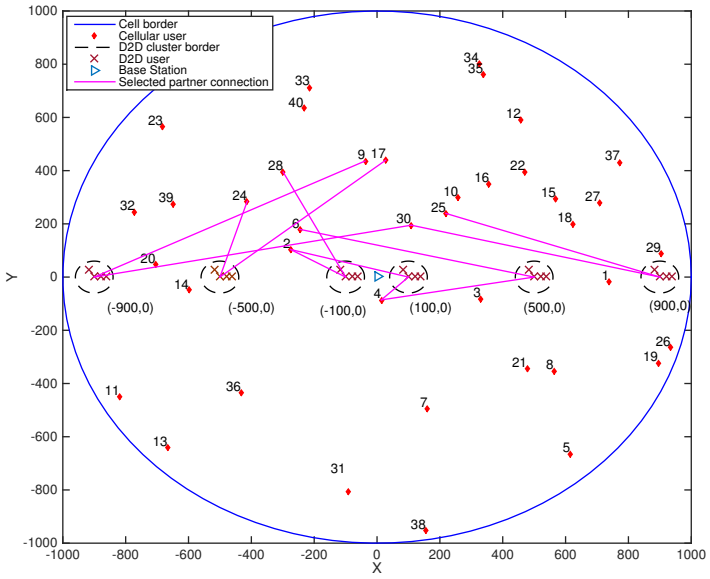

Figure 5.1: Regularly placed D2D clusters in a cell, $C_1 = 2, C_2 = 2$, $M = 40$.

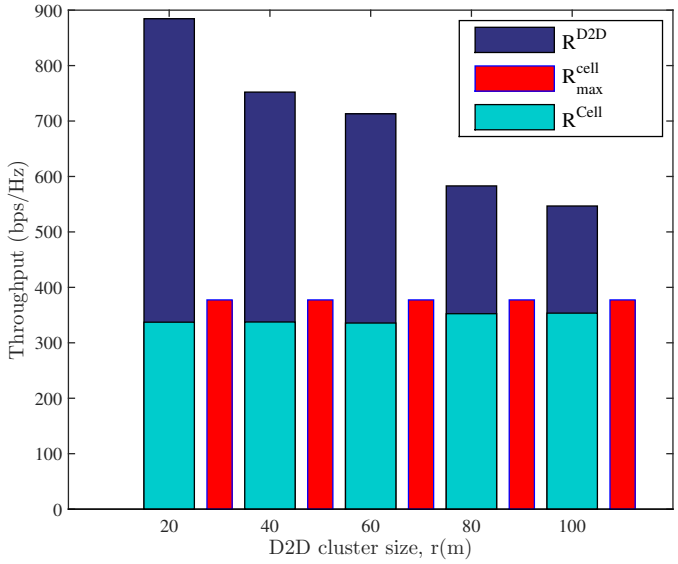

Figure 5.2: Throughput comparison for different cluster sizes, $C_1 = 2, C_2 = 2$, $M = 40$, and $K = 6$.

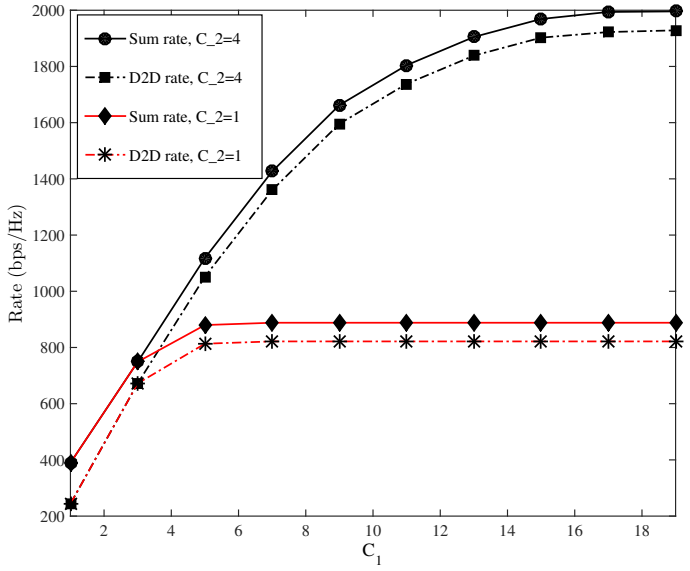

Figure 5.3: Throughput comparison for different values of C_1 and C_2, $M = 20$, and $K = 6$.

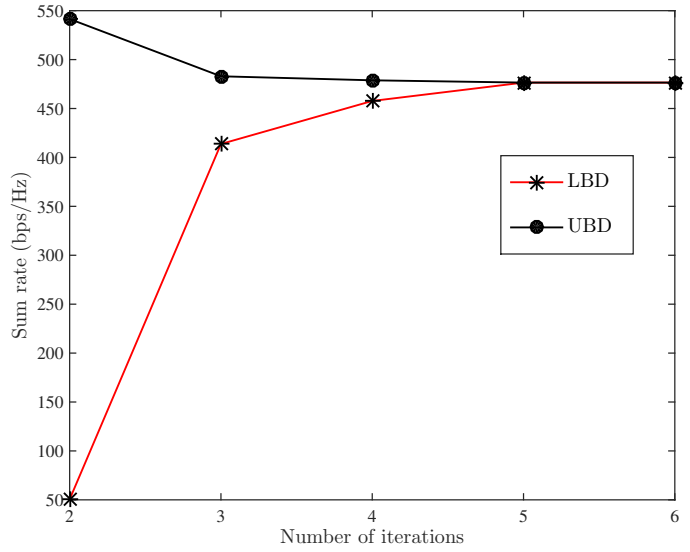

Figure 5.4: Convergence of the GBD algorithm, $C_1 = 2$, $C_2 = 2$, $M = 20$, and $K = 6$.

Randomly placed D2D users In the second set of experiments, we follow the clustered distribution model in [103], where clusters of radius r are randomly located in a cell and the D2D users in each group are randomly distributed in the corresponding cluster. Four metrics are used to evaluate the performance: the sum throughput, R^{sum}, the D2D throughput, R^{D2D}, the success rate, and the fairness index. The success rate is defined as the ratio of the number of D2D groups that found their CU partners ($|\mathcal{A}|$) and the total number of D2D groups. Fairness index is defined as follows,

$$f(R_1^{D2D}, R_2^{D2D}, \ldots, R_k^{D2D}) = \frac{(\sum_{k\in\mathcal{A}} R_k^{D2D})^2}{|\mathcal{A}| \sum_{k\in\mathcal{A}} (R_k^{D2D})^2}. \tag{5.63}$$

The fairness index is a positive number with the maximum value of 1 suggesting an equal D2D throughput among all feasible D2D groups.

The results in this section have been generated for two sets of C_1 and C_2 values: in part (a) of all the figures, $C_1 = 4$ and $C_2 = 3$; and in part (b), $C_1 = 1$ and $C_2 = 1$. In the case of $C_1 = 1$ and $C_2 = 1$, both GBD and the matching-based algorithm return the same results since both are optimal.

Figs. 5.5 – 5.8 compare the performance of GBD, the greedy and the heuristic algorithms for different D2D cluster sizes (r) and different cell radii (R). From these figures, we observe that both the sum and the D2D throughput as well as the success rate decrease with the D2D cluster size. Since the channel gain of D2D link decreases when the cluster radius increases, more transmission power is required for the D2D groups to satisfy the SINR threshold constraint. This in turn causes more interference to the reused CU partner. Furthermore, it is seen from these figures that the sum throughput, the D2D throughput and the success rate of all three algorithms increase

with the cell radius. This is because increasing the cell radius increases the distance between the CUs and D2D receivers and also the average distance of individual nodes to the BS. Hence, the interference from CUs to D2D receivers and the interference from D2D transmitters at the BS is decreased. Recall that the D2D rate is the maximum throughput achieved by the admitted D2D groups. It is worth mentioning that increasing the cell size leads to reduction in the cellular throughput due to the decreased link gain between the CUs and the base station. However, with the current simulation parameters, R^{D2D} is the dominating part of the sum rate and, therefore, R^{sum} increases with the cell size in both parts (a) and (b).

It can be also seen from Fig. 5.5 that the optimal solutions, GBD algorithm for part (a) and matching-based algorithm for part (b), has the highest sum rates. In comparison, the greedy algorithm achieves close-to-optimal sum rate, while the heuristic algorithm has a lower sum rate compared to the other two algorithms, but it has the lowest complexity among them. Note that in Fig. 5.6, the D2D rate of the greedy algorithm exceeds that of the optimal solution for some D2D cluster sizes. This does not contradict the optimality of GBD since the objective of P1 is to maximize the sum rate not the D2D rate.

Fig. 5.8 shows that the D2D fairness indices achieved by all algorithms are greater than 90%. Note that the fairness index calculates the fairness among all *admitted* D2D groups. Therefore, we can conclude that there is not much difference among D2D rates of all admitted D2D groups.

In Figs. 5.9 – 5.12 the performance of all proposed algorithms for different SINR thresholds ($\gamma_{th}^{D2D} = \gamma_{th}^{Cell} = \gamma_{th}$) with different numbers of CUs (M) is shown. It is seen that increasing the SINR threshold leads to decreasing sum rates, D2D rates,

and success rates since it limits the chances for D2D groups to find CU partners. It can be also observed that the total D2D throughput improves slightly with increasing number of CUs since there are more potential candidates for D2D groups to reuse.

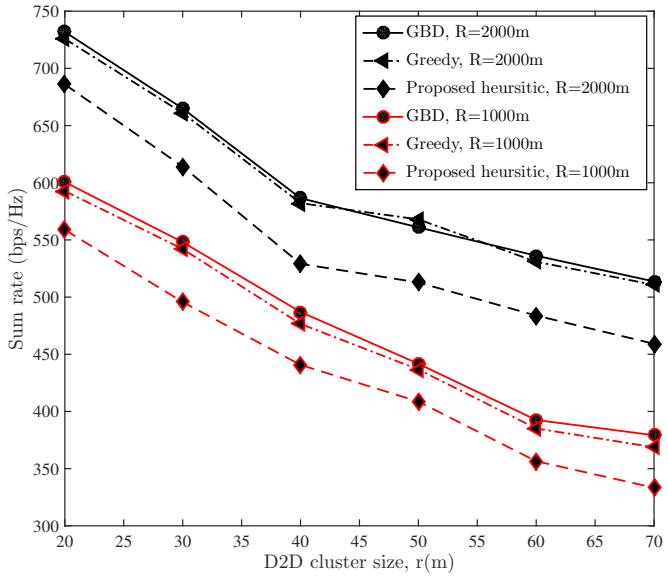

(a) $C_1 = 4, C_2 = 3$

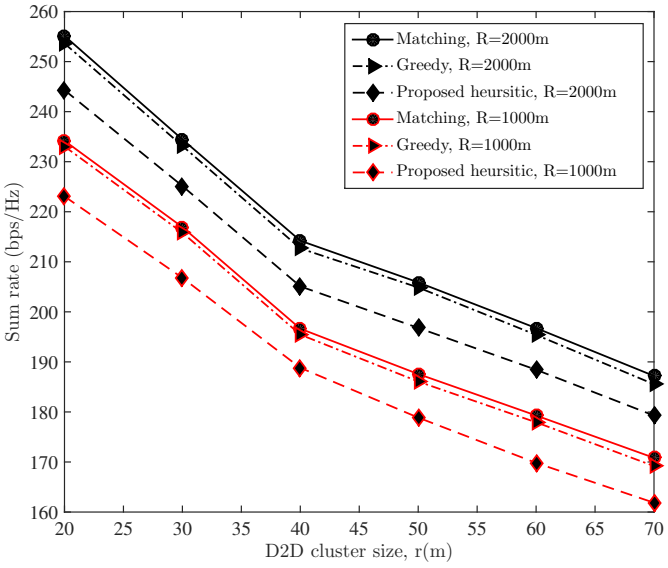

(b) $C_1 = 1, C_2 = 1$

Figure 5.5: Average sum throughput versus D2D cluster radius for different cell radii (R), $M = 10, K = 4$

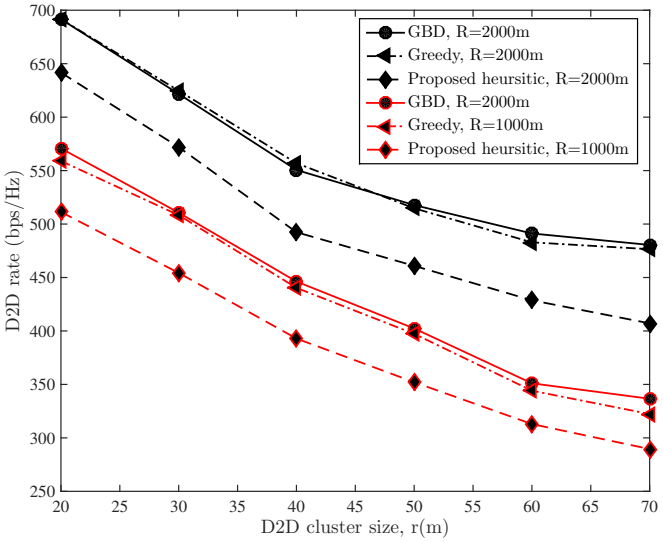

(a) $C_1 = 4, C_2 = 3$

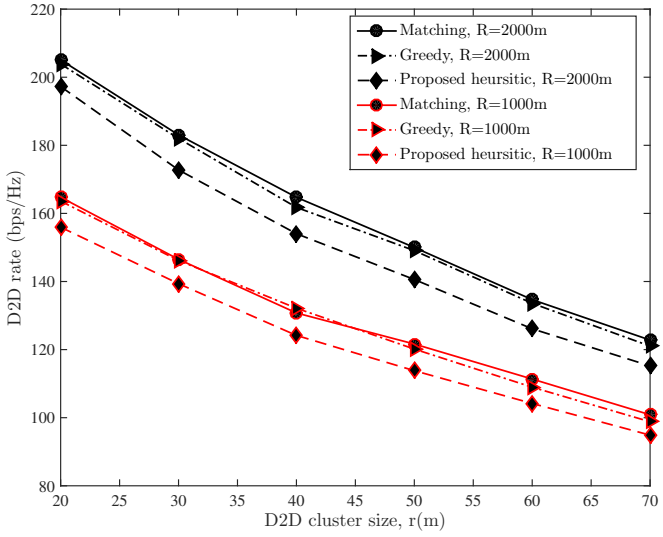

(b) $C_1 = 1, C_2 = 1$

Figure 5.6: Average D2D throughput versus D2D cluster radius for different cell radii (R), $M = 10, K = 4$

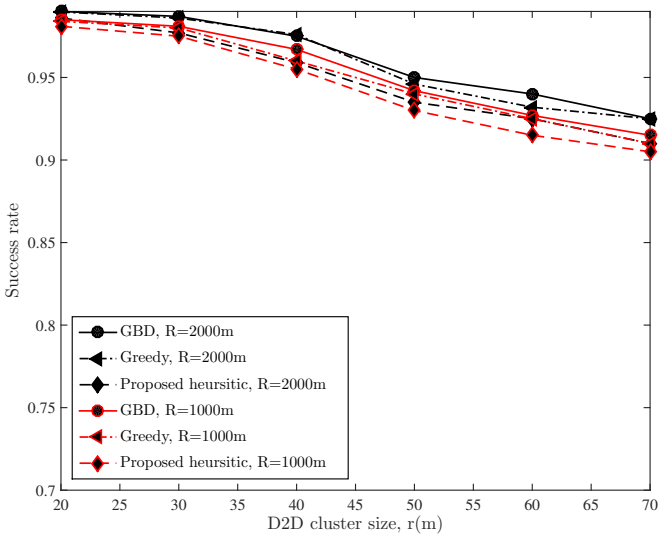

(a) $C_1 = 4, C_2 = 3$

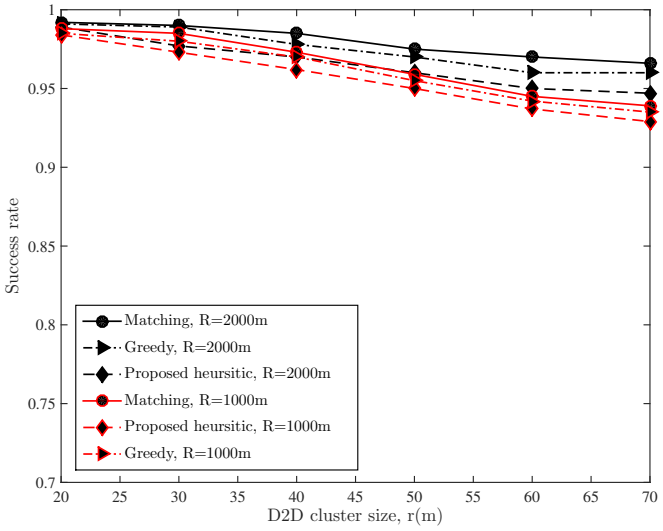

(b) $C_1 = 1, C_2 = 1$

Figure 5.7: Average D2D success rate versus D2D cluster radius for different cell radii (R), $M = 10, K = 4$

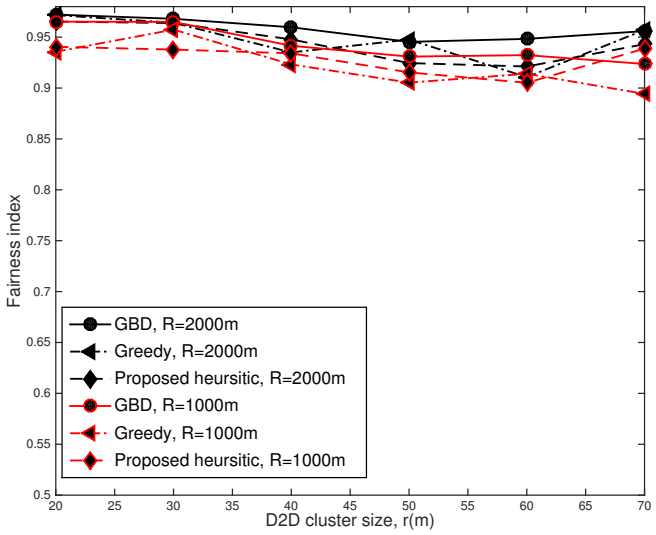

(a) $C_1 = 4, C_2 = 3$

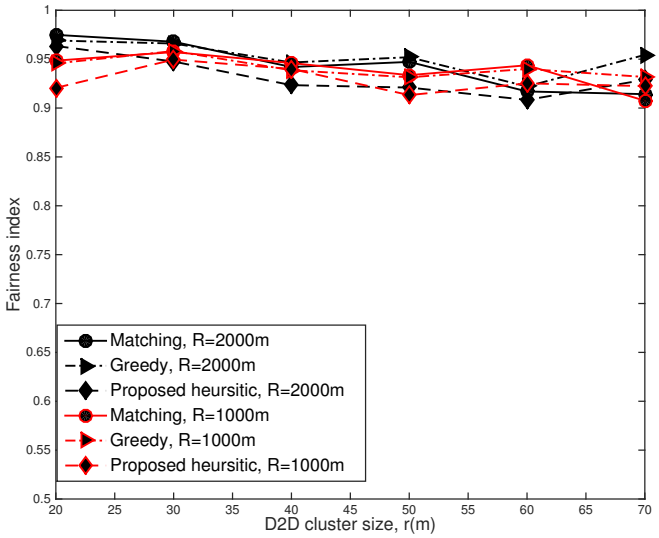

(b) $C_1 = 1, C_2 = 1$

Figure 5.8: Average fairness index versus D2D cluster radius for different cell radii (R), $M = 10, K = 4$

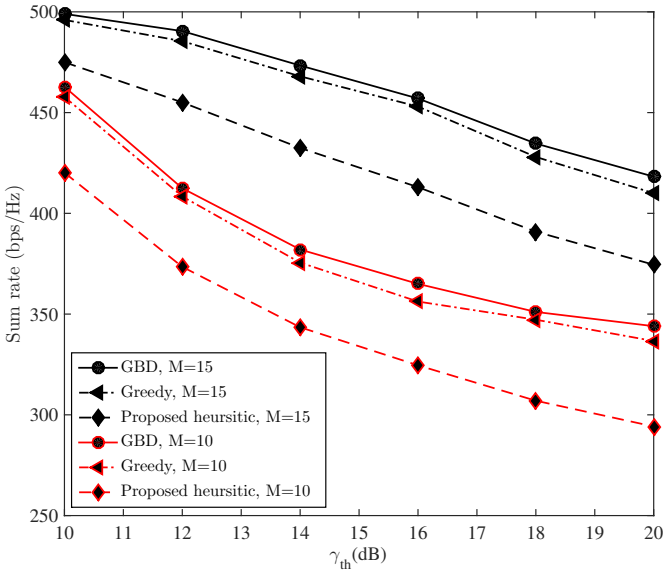

(a) $C_1 = 4, C_2 = 3$

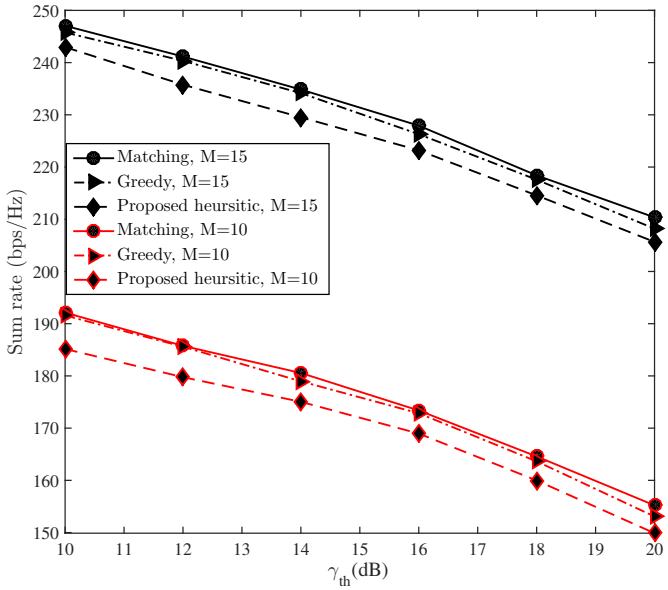

(b) $C_1 = 1, C_2 = 1$

Figure 5.9: Average sum throughput versus γ_{th} for different number of cellular users (M), $R = 1000$ m, $K = 4$

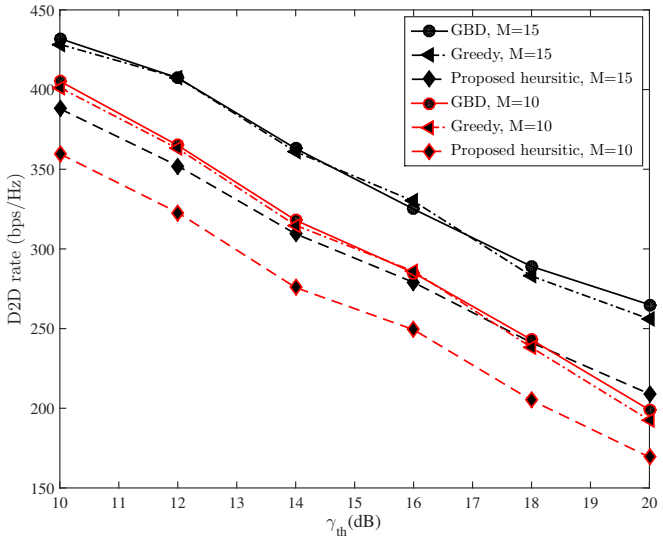

(a) $C_1 = 4, C_2 = 3$

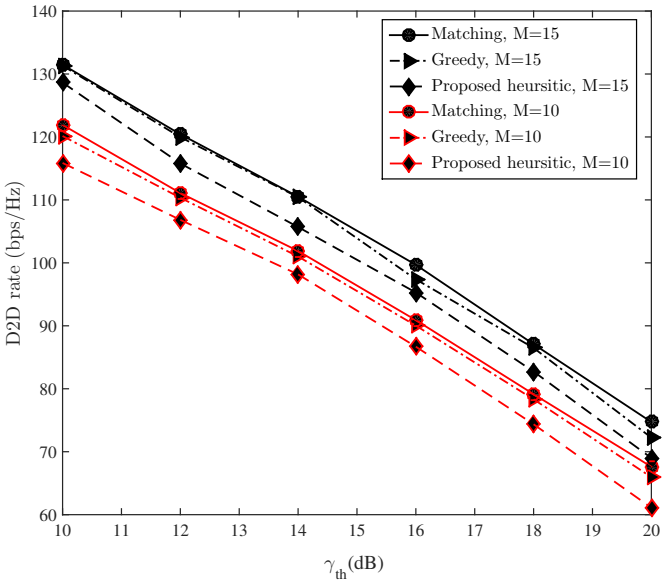

(b) $C_1 = 1, C_2 = 1$

Figure 5.10: Average D2D throughput versus γ_{th} for different number of cellular users (M), $R = 1000$ m, $K = 4$

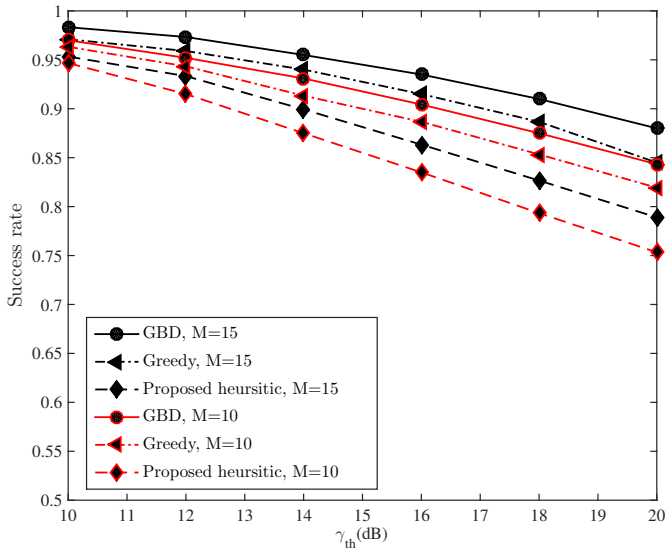

(a) $C_1 = 4, C_2 = 3$

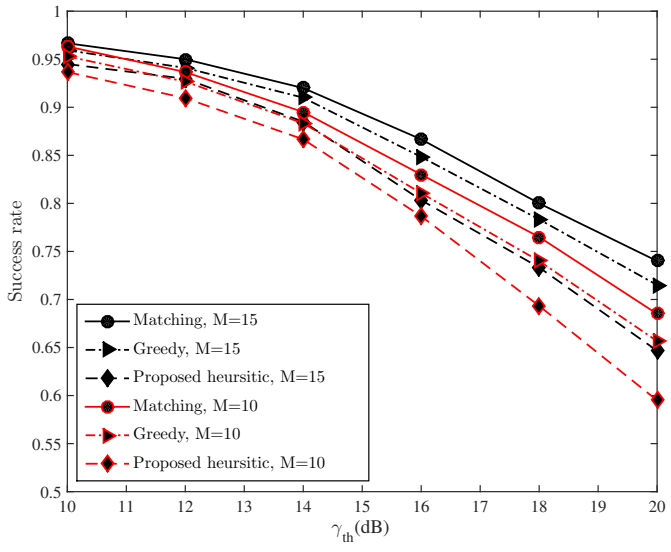

(b) $C_1 = 1, C_2 = 1$

Figure 5.11: Average D2D success rate versus γ_{th} for different number of cellular users (M), $R = 1000$ m, $K = 4$

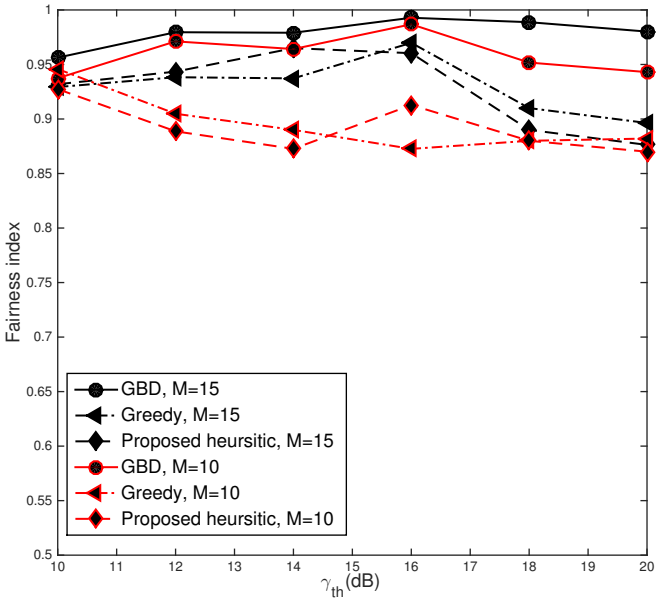

(a) $C_1 = 4, C_2 = 3$

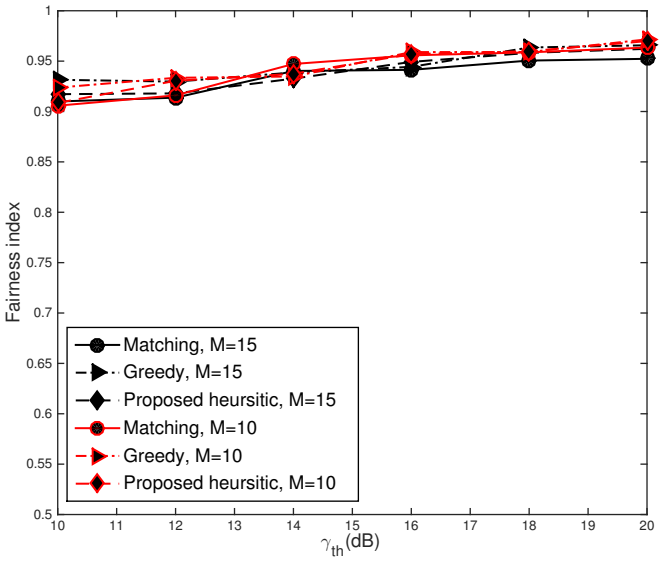

(b) $C_1 = 1, C_2 = 1$

Figure 5.12: Average fairness index versus γ_{th} for different number of cellular users (M), $R = 1000$ m, $K = 4$

5.7 Summary

In this chapter, we considered joint power and channel allocation for multicast D2D communications sharing uplink resource in a fully loaded cellular network. To maximize the overall throughput while guaranteeing the QoS requirements of both CUs and D2D groups, we formulated the optimization problem and found the optimal solution using GBD. Then, we solved a special case when each D2D group can reuse the channels of at most one CU and each CU can share their channels with at most one D2D group, using the maximum weight bipartite matching algorithm. Finally, a greedy algorithm and a low-complexity heuristic algorithm were also proposed. We performed extensive simulations with different parameters such as SINR threshold, cell size, D2D cluster size, and the number of CUs. Results showed that the greedy algorithm has close-to-optimal performance. In comparison, our proposed heuristic algorithm has good performance (but worse than that of the greedy) with lower computational complexity.

Chapter 6

Conclusions and Future Works

In this thesis, we have studied radio resource management issues related to multicast/broadcast feature in wireless networks. For unicast communications, the broadcast nature of wireless transmissions can be utilized opportunistically in traffic scheduling and transmission power allocations. In particular, this feature allows the relay node to decide whether or not multiple packets should be forwarded in one transmission by using network coding. For a network of bidirectional relaying communication links, optimum and heuristic cross-layer scheduling schemes have been proposed for different objectives, and results have shown that the proposed solutions can indeed increase radio resource utilization of the network and improve quality of service performance provided to users.

We have also studied resource management for D2D multicast groups underlaying cellular networks and proposed algorithms for channel assignments and power allocations. Even though the existence of multiple D2D multicast groups underlaying cellular communication results in very complicated interference conditions, our results indicate that with careful channel and power allocations, high throughput can

be achieved for D2D multicast communication groups with very minor throughput degradation to cellular users. Moreover, the overall throughput of D2D and cellular communications is much higher than that of the cellular communications without D2D groups.

The research conducted in this thesis can be extended in a number of directions:

- In the resource management for bidirectional relaying networks, we assumed that there was only one relay node shared by all the links. Further extending the work to networks with more complicated scenarios can be interesting. One example is the relay-assisted cellular networks, where a transmitter is assisted with multiple candidate relay nodes that are distributed in its coverage area. Each link can dynamically select the best relay node depending on channel and interference conditions, traffic load variations, and other network conditions. In such a network with multiple bidirectional relaying links, studying the radio resource management jointly with relay station selection may further improve the data transmission performance and radio resource utilization.

- In this thesis, the use of network coding is limited to networks with bidirectional relaying links. The resource management problem can become more complicated when network coding is applied in networks with different topologies. One example is wireless mesh networks, where using network coding can potentially simplify traffic scheduling, improve data transmission throughput, etc. In order to take good advantage of network coding, individual relay nodes should consider not only routing and resource allocations (such as transmission power and buffer space), but also specific coding strategies (e.g., how to mix the received packets before forwarding).

- Traffic was assumed to be Bernoulli distributed in the first part of the work. Future work can be done to consider more accurate traffic models, such as the hidden Markov model, and design the traffic scheduling policies.

- In the work on D2D multicast, we considered single-rate multicast transmissions. That is, all the receivers in each group receive messages at the same rate, which is limited by the receiver with the worst receiving condition. Next, we can extend the work so that receivers in a multicast group can receive at different rates. This can be achieved, for example, by using rateless coding [104, 105]. Resource management in such a scenario is an interesting issue so that the rateless setting can help achieve better transmission reliability to combat mobility and poor channel conditions.

- Another important and practical application for D2D multicast is mission critical public safety services, in which delay guarantee is important. D2D communications serve as a technology component for providing public protection, disaster relief, security and public safety service. The service can underlay cellular spectrum so that no additional network infrastructure is required for the public safety services, and the resource availability and communication quality for these services remain to be controlled by the cellular base stations. Studying radio resource management in D2D multicast underlaying cellular communications will be an interesting issue in such a scenario. In addition to channel selection and transmission power allocations, admission control will be more important in order to guarantee the time critical services.

Bibliography

[1] Z. Wang, *Internet QoS: architectures and mechanisms for quality of service*. Morgan Kaufmann, 2001.

[2] X. Liu, E. K. Chong, and N. B. Shroff, "A framework for opportunistic scheduling in wireless networks," *Computer Networks*, vol. 41, no. 4, pp. 451–474, 2003.

[3] M. Médard and A. Sprintson, *Network coding: fundamentals and applications*. Academic Press, 2012.

[4] G. J. Foschini and Z. Miljanic, "A simple distributed autonomous power control algorithm and its convergence," *IEEE Transactions on Vehicular Technology*, vol. 42, no. 4, pp. 641–646, 1993.

[5] R. D. Yates, "A framework for uplink power control in cellular radio systems," *IEEE Journal on Selected Areas in Communications*, vol. 13, no. 7, pp. 1341–1347, 1995.

[6] M. Chiang, P. Hande, T. Lan, and C. W. Tan, "Power control in wireless cellular networks," *Foundations and Trends in Networking*, vol. 2, no. 4, pp. 381–533, 2008.

[7] F. Zhang, T. D. Todd, D. Zhao, and V. Kezys, "Power saving access points for ieee 802-11 wireless network infrastructure," *IEEE Transactions on Mobile Computing*, vol. 5, no. 2, pp. 144–156, 2006.

[8] G. Miao, N. Himayat, Y. Li, and A. Swami, "Cross-layer optimization for energy-efficient wireless communications: a survey," *Wireless Communications and Mobile Computing*, vol. 9, no. 4, pp. 529–542, 2009.

[9] Q. Wu, W. Chen, M. Tao, J. Li, H. Tang, and J. Wu, "Resource allocation for joint transmitter and receiver energy efficiency maximization in downlink ofdma systems," *IEEE Transactions on Communications*, vol. 63, no. 2, pp. 416–430, 2015.

[10] F. Meshkati, H. V. Poor, and S. C. Schwartz, "Energy-efficient resource allocation in wireless networks," *IEEE Signal Processing Magazine*, vol. 24, no. 3, pp. 58–68, 2007.

[11] X. Xiao, X. Tao, and J. Lu, "Energy-efficient resource allocation in LTE-based mimo-ofdma systems with user rate constraints," *IEEE Transactions on Vehicular Technology*, vol. 64, no. 1, pp. 185–197, 2015.

[12] G. Y. Li, Z. Xu, C. Xiong, C. Yang, S. Zhang, Y. Chen, and S. Xu, "Energy-efficient wireless communications: tutorial, survey, and open issues," *IEEE Wireless Communication*, vol. 18, no. 6, pp. 28–35, 2011.

[13] E. Liu and K. K. Leung, "Proportional fair scheduling: analytical insight under rayleigh fading environment," in *IEEE Wireless Communications and Networking Conference (WCNC)*, 2008, pp. 1883–1888.

[14] A. Asadi and V. Mancuso, "A survey on opportunistic scheduling in wireless communications," *IEEE Communications Surveys & Tutorials*, vol. 15, no. 4, pp. 1671–1688, 2013.

[15] S. Andreev, O. Galinina, and A. Vinel, "Cross-layer channel-aware approaches for modern wireless networks," in *Multiple Access Communications*. Springer, 2010, pp. 163–179.

[16] X. Lin, N. B. Shroff, and R. Srikant, "A tutorial on cross-layer optimization in wireless networks," *IEEE Journal on Selected Areas in Communications*, vol. 24, no. 8, pp. 1452–1463, 2006.

[17] R. Knopp and P. A. Humblet, "Information capacity and power control in single-cell multiuser communications," in *IEEE International Conference on Communications (ICC)*, vol. 1, 1995, pp. 331–335.

[18] L. Badia, A. Baiocchi, A. Todini, S. Merlin, S. Pupolin, A. Zanella, and M. Zorzi, "On the impact of physical layer awareness on scheduling and resource allocation in broadband multicellular ieee 802.16 systems [radio resource management and protocol engineering for ieee 802.16]," *IEEE Wireless Communications*, vol. 14, no. 1, pp. 36–43, 2007.

[19] A. Asadi and T. S. Wei, "An enhanced cross layer downlink scheduling algorithm for ieee 802.16 networks," in *IEEE International Conference on Information Networking (ICOIN)*, 2011, pp. 212–217.

[20] K. Khalil, M. Karaca, O. Ercetin, and E. Ekici, "Optimal scheduling in

cooperate-to-join cognitive radio networks," in *Proceedings IEEE INFOCOM*, April 2011, pp. 3002–3010.

[21] H. Al-Zubaidy, I. Lambadaris, and J. Talim, "Optimal scheduling in high-speed downlink packet access networks," *ACM Transactions on Modeling and Computer Simulation (TOMACS)*, vol. 21, no. 1, p. 3, 2010.

[22] L. Tassiulas, "Scheduling and performance limits of networks with constantly changing topology," *IEEE Transactions on Information Theory*, vol. 43, no. 3, pp. 1067–1073, 1997.

[23] M. J. Neely, E. Modiano, and C. E. Rohrs, "Dynamic power allocation and routing for time-varying wireless networks," *IEEE Journal on Selected Areas in Communications*, vol. 23, no. 1, pp. 89–103, 2005.

[24] P. Chaporkar, A. Proutiere, H. Asnani, and A. Karandikar, "Scheduling with limited information in wireless systems," in *Proceedings of the tenth ACM international symposium on Mobile ad hoc networking and computing*, 2009, pp. 75–84.

[25] P. Jacko, "Value of information in optimal flow-level scheduling of users with markovian time-varying channels," *Performance Evaluation*, vol. 68, no. 11, pp. 1022–1036, 2011.

[26] H. Kim and G. De Veciana, "Losing opportunism: evaluating service integration in an opportunistic wireless system," in *26th IEEE International Conference on Computer Communications.*, 2007, pp. 982–990.

[27] B. Sadiq, S. J. Baek, and G. De Veciana, "Delay-optimal opportunistic scheduling and approximations: The log rule," *IEEE/ACM Transactions on Networking (TON)*, vol. 19, no. 2, pp. 405–418, 2011.

[28] M. J. Neely, "Opportunistic scheduling with worst case delay guarantees in single and multi-hop networks," in *Proceedings IEEE INFOCOM*, April 2011, pp. 1728–1736.

[29] K. W. Choi, W. S. Jeon, and D. G. Jeong, "Resource allocation in ofdma wireless communications systems supporting multimedia services," *IEEE/ACM Transactions on Networking*, vol. 17, no. 3, pp. 926–935, 2009.

[30] R. K. Beidokhti, M. H. Y. Moghaddam, and J. Chitizadeh, "Adaptive qos scheduling in wireless cellular networks," *Wireless Networks*, vol. 17, no. 3, pp. 701–716, 2011.

[31] M. L. Puterman, *Markov decision processes: discrete stochastic dynamic programming*. John Wiley & Sons, 2014.

[32] F. Hartung, U. Horn, J. Huschke, M. Kampmann, T. Lohmar, and M. Lundevall, "Delivery of broadcast services in 3g networks," *IEEE Transactions on Broadcasting*, vol. 53, no. 1, pp. 188–199, 2007.

[33] U. Varshney, "Multicast support in mobile commerce applications," *Computer*, vol. 35, no. 2, pp. 115–117, 2002.

[34] J. Xu, S.-J. Lee, W.-S. Kang, and J.-S. Seo, "Adaptive resource allocation for mimo-ofdm based wireless multicast systems," *IEEE Transactions on Broadcasting*, vol. 56, no. 1, pp. 98–102, 2010.

[35] R. Ahlswede, N. Cai, S.-Y. Li, and R. Yeung, "Network information flow," *IEEE Transactions on Information Theory*, vol. 46, no. 4, pp. 1204–1216, 2000.

[36] S. Zhang, S. C. Liew, and P. P. Lam, "Hot topic: physical-layer network coding," in *Proceedings of the ACM 12th annual international conference on Mobile computing and networking*, 2006, pp. 358–365.

[37] Y. E. Sagduyu and A. Ephremides, "On joint mac and network coding in wireless ad hoc networks," *IEEE Transactions on Information Theory*, vol. 53, no. 10, pp. 3697–3713, 2007.

[38] Y. Yan, B. Zhang, Z. Zhao, X. Shen, and J. Ma, "Mechanism for maximizing area-centric coding gains in wireless multihop networks," in *IEEE International Conference on Communications (ICC)*, 2009, pp. 1–5.

[39] S. Deb, M. Effros, T. Ho, D. R. Karger, R. Koetter, D. S. Lun, M. Médard, and N. Ratnakar, "Network coding for wireless applications: a brief tutorial." IWWAN, 2005.

[40] J. Liu, D. Goeckel, and D. Towsley, "Bounds on the throughput gain of network coding in unicast and multicast wireless networks," *IEEE Journal on Selected Areas in Communications*, vol. 27, no. 5, pp. 582–592, 2009.

[41] H. Su and X. Zhang, "Modeling throughput gain of network coding in multi-channel multi-radio wireless ad hoc networks," *IEEE Journal on Selected Areas in Communications*, vol. 27, no. 5, pp. 593–605, 2009.

[42] Y. E. Sagduyu and A. Ephremides, "Some optimization trade-offs in wireless

network coding," in *40th IEEE Annual Conference on Information Sciences and Systems*, 2006, pp. 6–11.

[43] P. Fan, C. Zhi, C. Wei, and K. Ben Letaief, "Reliable relay assisted wireless multicast using network coding," *IEEE Journal on Selected Areas in Communications*, vol. 27, no. 5, pp. 749–762, 2009.

[44] T. Tran, D. Nguyen, T. Nguyen, and D. Tran, "Joint network coding and power control for cellular radio networks," in *Second IEEE International Conference on Communications and Electronics (ICCE)*, 2008, pp. 109–114.

[45] J. Zhang, P. Fan, and K. Ben Letaief, "Network coding for efficient multicast routing in wireless ad-hoc networks," *IEEE Transactions on Communications*, vol. 56, no. 4, pp. 598–607, 2008.

[46] J. Yuan, Z. Li, W. Yu, and B. Li, "A cross-layer optimization framework for multihop multicast in wireless mesh networks," *IEEE Journal on Selected Areas in Communications*, vol. 24, no. 11, pp. 2092–2103, 2006.

[47] Y. Yan, Z. Zhao, B. Zhang, H. T. Mouftah, and J. Ma, "Rate-adaptive coding-aware multiple path routing for wireless mesh networks," in *IEEE Global Telecommunications Conference (GLOBECOM)*, 2008, pp. 1–5.

[48] C. Zhang, X. Zhu, and Y. Fang, "On the improvement of scaling laws for large-scale manets with network coding," *IEEE Journal on Selected Areas in Communications*, vol. 27, no. 5, pp. 662–672, 2009.

[49] T. Ho, R. Koetter, M. Medard, D. Karger, and M. Effros, "The benefits of coding over routing in a randomized setting," in *Proceedings of IEEE International Symposium on Information Theory*, June 2003, pp. 442–446.

[50] J.-S. Park, M. Gerla, D. S. Lun, Y. Yi, and M. Médard, "Codecast: a network-coding-based ad hoc multicast protocol," *IEEE Wireless Communications*, vol. 13, no. 5, pp. 76–81, 2006.

[51] S. K. D. K. W. Hu and H. R. M. Médard, "The importance of being opportunistic: Practical network coding for wireless environments," *Newsletter ACM SIGCOMM Computer Communication Review*, vol. 36, no. 4, 2006.

[52] H. Yomo and P. Popovski, "Opportunistic scheduling for wireless network coding," in *IEEE International Conference on Communications (ICC)*, June 2007, pp. 5610–5615.

[53] A. Eryilmaz, A. Ozdaglar, M. Médard, and E. Ahmed, "On the delay and throughput gains of coding in unreliable networks," *IEEE Transactions on Information Theory*, vol. 54, no. 12, pp. 5511–5524, 2008.

[54] K. Rajawat, N. Gatsis, and G. B. Giannakis, "Cross-layer designs in coded wireless fading networks with multicast," *IEEE/ACM Transactions on Networking*, vol. 19, no. 5, pp. 1276–1289, 2011.

[55] H. Yomo and P. Popovski, "Opportunistic scheduling for wireless network coding," *IEEE Transactions on Wireless Communications*, vol. 8, no. 6, pp. 2766–2770, June 2009.

[56] P. Tarasak, U. Sethakaset, and S. Sun, "Capacity analysis of two-user opportunistic scheduling for wireless network coding," in *IEEE International Symposium on Information Theory (ISIT)*, June 2009, pp. 2572–2576.

[57] ——, "Analysis of opportunistic scheduling for wireless network coding: non-identical two-user case," in *Proceedings of the 28th IEEE conference on Global telecommunications*, 2009, pp. 2659–2664.

[58] W. Chen, K. B. Letaief, and Z. Cao, "Buffer-aware network coding for wireless networks," *IEEE/ACM Transactions on Networking*, vol. 20, no. 5, pp. 1389–1401, 2012.

[59] P. Parag and J. Chamberland, "Queueing analysis of a butterfly network for comparing network coding to classical routing," *IEEE Transactions on Information Theory*, vol. 56, no. 4, pp. 1890–1908, 2010.

[60] B.-G. Kim and J.-W. Lee, "Opportunistic resource scheduling for ofdma networks with network coding at relay stations," *IEEE Transactions on Wireless Communications*, vol. 11, no. 1, pp. 210–221, 2012.

[61] B. Han, M. Peng, Z. Zhao, and W. Wang, "A multidimensional resource-allocation optimization algorithm for the network-coding-based multiple-access relay channels in ofdm systems," *IEEE Transactions on Vehicular Technology*, vol. 62, no. 8, pp. 4069–4078, 2013.

[62] Y. E. Sagduyu, R. A. Berry, and D. Guo, "Throughput and stability for relay-assisted wireless broadcast with network coding," *IEEE Journal on Selected Areas in Communications*, vol. 31, no. 8, pp. 1506–1516, 2013.

[63] S. Wang, Q. Song, X. Wang, and A. Jamalipour, "Distributed mac protocol supporting physical-layer network coding," *IEEE Transactions on Mobile Computing*, vol. 12, no. 5, pp. 1023–1036, 2013.

[64] S. Chieochan, E. Hossain, T. Issariyakul, and D. Niyato, "Opportunistic network coding and dynamic buffer allocation in a wireless butterfly network," in *IEEE Global Telecommunications Conference (GLOBECOM)*, 2009, pp. 1–6.

[65] Y. Wu, P. A. Chou, S.-Y. Kung *et al.*, "Information exchange in wireless networks with network coding and physical-layer broadcast," MSR-TR-2004, Tech. Rep., 2005.

[66] Z. Chen, T. J. Lim, and M. Motani, "Energy efficiency and queue stability in a two-way relay network," in *IEEE International Conference on Communication Systems (ICCS)*, 2012, pp. 36–40.

[67] D. M. Kim and S.-L. Kim, "Network coded rate scheduling for two-way relay networks," in *11th European Wireless Conference-Sustainable Wireless Technologies*. VDE, 2011, pp. 1–6.

[68] M. Mohseni and D. Zhao, "Transmission scheduling in a multi-channel wireless network with bidirectional relaying links," *Wireless Communications and Mobile Computing*, 2015.

[69] Z. Lin and B. Vucetic, "Power and rate adaptation for wireless network coding with opportunistic scheduling," in *IEEE International Symposium on Information Theory (ISIT)*, 2008, pp. 21–25.

[70] S. Tang, H. Yomo, M. N. Shirazi, T. Ueda, R. Miura, and S. Obana, "Exploiting network coding for pseudo bidirectional relay in wireless lan," in *IEEE 20th International Symposium on Personal, Indoor and Mobile Radio Communications*, 2009, pp. 706–711.

[71] X. Zhang, M. Peng, Z. Ding, and W. Wang, "Multi-user scheduling for network coded two-way relay channel in cellular systems," *IEEE Transactions on Wireless Communications*, vol. 11, no. 7, pp. 2542–2551, 2012.

[72] Y. Jeon, Y.-T. Kim, M. Park, and I. Lee, "Opportunistic scheduling for multi-user two-way relay systems with physical network coding," *IEEE Transactions on Wireless Communications*, vol. 11, no. 4, pp. 1290–1294, 2012.

[73] M. L. Littman, T. L. Dean, and L. P. Kaelbling, "On the complexity of solving markov decision problems," in *Proceedings of the Eleventh conference on Uncertainty in artificial intelligence*. Morgan Kaufmann Publishers Inc., 1995, pp. 394–402.

[74] H. S. Wang and N. Moayeri, "Finite-state markov channel - a useful model for radio communication channels," *IEEE Transactions on Vehicular Technology*, vol. 44, no. 1, pp. 163–171, 1995.

[75] M. Hassan, M. M. Krunz, and I. Matta, "Markov-based channel characterization for tractable performance analysis in wireless packet networks," *IEEE Transactions on Wireless Communications*, vol. 3, no. 3, pp. 821–831, 2004.

[76] D. P. Bertsekas, "Approximate dynamic programming," 2011.

[77] H. S. Chang, J. Hu, M. C. Fu, and S. I. Marcus, *Simulation-based algorithms for Markov decision processes*. Springer Science & Business Media, 2013.

[78] J. Wu, Y. Bao, G. Miao, S. Zhou, and Z. Niu, "Base station sleeping control and power matching for energy-delay tradeoffs with bursty traffic," *Accepted for publication in the IEEE Transactions on Vehicular Technology*, vol. http://arxiv.org/abs/1407.2322, 2015.

[79] F. Moety, S. Lahoud, K. Khawam, and B. Cousin, "Joint power-delay minimization in green wireless access networks," in *IEEE 24th International Symposium on Personal Indoor and Mobile Radio Communications (PIMRC)*, 2013, pp. 2819–2824.

[80] R. A. Berry, "Power and delay trade-offs in fading channels," Ph.D. dissertation, Massachusetts Institute of Technology, 2000.

[81] I. Kamitsos, L. Andrew, H. Kim, S. Ha, and M. Chiang, "Better energy-delay tradeoff via server resource pooling," in *IEEE International Conference on Computing, Networking and Communications (ICNC)*, 2012, pp. 611–616.

[82] V0.4.1, "3rd generation partnership project; technical specification group SA; study on architecture enhancements to support proximity services (prose) (release 12)," June 2013.

[83] X. Lin, J. Andrews, A. Ghosh, and R. Ratasuk, "An overview of 3gpp device-to-device proximity services," *IEEE Communications Magazine*, vol. 52, no. 4, pp. 40–48, April 2014.

[84] L. Lei, Z. Zhong, C. Lin, and X. Shen, "Operator controlled device-to-device communications in LTE-advanced networks," *IEEE Wireless Communications*, vol. 19, no. 3, pp. 96–104, June 2012.

[85] K. Doppler, M. Rinne, C. Wijting, C. Ribeiro, and K. Hugl, "Device-to-device communication as an underlay to LTE-advanced networks," *IEEE Communications Magazine*, vol. 47, no. 12, pp. 42–49, Dec 2009.

[86] A. Asadi, Q. Wang, and V. Mancuso, "A survey on device-to-device communication in cellular networks," *IEEE Communications Surveys Tutorials*, vol. 16, no. 4, pp. 1801–1819, 2014.

[87] T. Peng, Q. Lu, H. Wang, S. Xu, and W. Wang, "Interference avoidance mechanisms in the hybrid cellular and device-to-device systems," in *IEEE 20th International Symposium on Personal, Indoor and Mobile Radio Communications*, Sept 2009, pp. 617–621.

[88] P. Janis, V. Koivunen, C. Ribeiro, J. Korhonen, K. Doppler, and K. Hugl, "Interference-aware resource allocation for device-to-device radio underlaying cellular networks," in *IEEE 69th Vehicular Technology Conference, (VTC)*, April 2009, pp. 1–5.

[89] Y. Pei and Y.-C. Liang, "Resource allocation for device-to-device communications overlaying two-way cellular networks," *IEEE Transactions on Wireless Communications*, vol. 12, no. 7, pp. 3611–3621, July 2013.

[90] A. Asadi and V. Mancuso, "WiFi direct and LTE D2D in action," in *IFIP Wireless Days (WD)*, Nov 2013, pp. 1–8.

[91] G. Fodor, E. Dahlman, G. Mildh, S. Parkvall, N. Reider, G. Miklós, and Z. Turányi, "Design aspects of network assisted device-to-device communications," *IEEE Communications Magazine*, vol. 50, no. 3, pp. 170–177, March 2012.

[92] H. Min, W. Seo, J. Lee, S. Park, and D. Hong, "Reliability improvement using receive mode selection in the device-to-device uplink period underlaying cellular networks," *IEEE Transactions on Wireless Communications*, vol. 10, no. 2, pp. 413–418, February 2011.

[93] C.-H. Yu, K. Doppler, C. Ribeiro, and O. Tirkkonen, "Resource sharing optimization for device-to-device communication underlaying cellular networks," *IEEE Transactions on Wireless Communications*, vol. 10, no. 8, pp. 2752–2763, August 2011.

[94] M. Zulhasnine, C. Huang, and A. Srinivasan, "Efficient resource allocation for device-to-device communication underlaying LTE network," in *IEEE 6th International Conference on Wireless and Mobile Computing, Networking and Communications (WiMob)*, Oct 2010, pp. 368–375.

[95] D. Feng, L. Lu, Y. Yuan-Wu, G. Li, G. Feng, and S. Li, "Device-to-device communications underlaying cellular networks," *IEEE Transactions on Communications*, vol. 61, no. 8, pp. 3541–3551, August 2013.

[96] R. Afolabi, A. Dadlani, and K. Kim, "Multicast scheduling and resource allocation algorithms for ofdma-based systems: a survey," *IEEE Communications Surveys Tutorials*, vol. 15, no. 1, pp. 240–254, Jan 2013.

[97] K. Doppler, M. P. Rinne, P. Janis, C. Ribeiro, and K. Hugl, "Device-to-device communications; functional prospects for LTE-advanced networks," in *IEEE International Conference on Communications Workshops*, 2009, pp. 1–6.

[98] A. M. Geoffrion, "Generalized benders decomposition," *Journal of Optimization Theory and Applications*, vol. 10, no. 4, pp. 237–260, 1972.

[99] C. Hua and R. Zheng, "Robust topology engineering in multiradio multichannel wireless networks," *IEEE Transactions on Mobile Computing*, vol. 11, no. 3, pp. 492–503, 2012.

[100] M. Chiang, "Geometric programming for communication systems," *Communications and Information Theory*, vol. 2, no. 1/2, pp. 1–154, 2005.

[101] H. W. Kuhn, "The hungarian method for the assignment problem," *Naval Research Logistics Quarterly*, vol. 2, no. 1-2, pp. 83–97, 1955.

[102] M. Grant, S. Boyd, and Y. Ye, "cvx users' guide," Technical Report Build 711, Citeseer. Available at: http://citeseerx. ist. psu. edu/viewdoc/download, Tech. Rep., 2009.

[103] B. Kaufman and B. Aazhang, "Cellular networks with an overlaid device to device network," in *42nd IEEE Asilomar Conference on Signals, Systems and Computers*, 2008, pp. 1537–1541.

[104] D. J. C. MacKay, "Fountain codes," *IEE Proceedings - Communications*, vol. 152, no. 6, pp. 1062–1068, 2005.

[105] O. Etesami and A. Shokrollahi, "Raptor codes on binary memoryless symmetric

channels," *IEEE Transactions on Information Theory*, vol. 52, no. 5, pp. 2033–2051, 2006.